THE UNIVERSITY OF MICHIGAN

INDUSTRY PROGRAM OF THE COLLEGE OF ENGINEERING

THERMAL EFFECTS IN JOURNAL BEARINGS

Elsayed Morsi Aly Afify

April, 1959

IP-366

Doctoral Committee:

Professor Frank L. Schwartz, Chairman
Professor Jack R. Britton, University of Colorado
Professor Ruel V. Churchill
Professor Stuart W. Churchill
Professor Arnet B. Epple
Professor Rune L. Evaldson

ACKNOWLEDGMENTS

The writer wishes to express his gratitude to Professor F. L. Schwartz, Chairman of the Doctoral Committee for his advice, guidance and encouragement throughout this investigation.

The writer also expresses his appreciation to the members of the committee, Professor R. V. Churchill, Professor S. W. Churchill, Professor A. B. Epple and Professor R. L. Evaldson for their interest and cooperation.

The valuable help of Mr. W. G. Huizinga, Mr. M. W. Kaufman, and W. K. Salva during the construction of the experimental apparatus is appreciated.

The patience and devotion of the writer's wife during this period is greatly appreciated.

Last of all, the writer is indebted to the Industry Program of the College of Engineering for the typing and the printing of the dissertation.

TABLE OF CONTENTS

TABLE OF CONTENTS (CONT'D)

LIST OF TABLES

LIST OF FIGURES

LIST OF FIGURES (CONT'D)

LIST OF FIGURES (CONT'D)

NOMENCLATURE

a	Empirical constant.	$\frac{BTU}{hr(°F)^m ft^2}$
c	Radial clearance.	inches
c_d	Diametral clearance.	inches
c_h	Average specific heat of oil.	$\frac{BTU}{lb\ °F}$
d	Nominal diameter of the bearing.	inches
e	Eccentricity.	inches
F	Frictional force.	lbs
h	Oil film thickness.	inches
H_c	Rate of heat dissipation through the bearing.	BTU/hr
H_e	Rate of heat addition by the heater.	BTU/hr
H_J	Rate of heat generation.	BTU/hr
H_o	Rate of heat carried away by the oil.	BTU/hr
H_p	Rate of heat generation at no-load.	BTU/hr
H_w	Rate of heat carried away by the cooling water.	BTU/hr
J	The mechanical equivalent of heat = 778.	ft lb/BTU
k	Average coefficient of thermal conductivity of oil.	$\frac{BTU}{hr\ ft\ °F}$
ℓ	Bearing length.	inches
L	Nondimensional bearing length = ℓ/c.	
m	Empirical constant.	
M_J	Journal friction torque.	
n	Eccentricity ratio.	
N	Speed of rotation.	rpm
N'	Speed of rotation.	rps
p	Unit pressure on projected area	psi

q	Oil flow rate.	in^3/hr
Q	Oil flow rate.	in^3/hr
r	Bearing radius.	inches
R	Nondimensional radius E r/c.	
S	Sommerfeld number = $\mu N'/p\ (d/c_d)^2$.	
1/S	Load Number.	
T	Temperature at any point in the oil film.	°F
T_a	Average oil film temperature.	°F
T_B	Temperature of the oil film at bearing inner surface.	°F
T_J	Temperature of the oil film at journal surface.	°F
T_1	Oil inlet temperature.	°F
T_2	Oil outlet temperature.	°F
ΔT	Average oil film temperature - ambient temperature.	°F
u	Linear velocity at any point in the x-direction.	in/sec
v	Linear velocity at any point in the y-direction.	in/sec
V	Linear velocity at the journal surface.	in/sec
w	Linear velocity at any point in the z-direction.	in/sec
W	Load.	lbs
μ	Oil viscosity.	Reyns.
μ_B	Oil viscosity at the bearing at the bearing temperature.	Reyns.
μ_o	Oil viscosity at an arbitrary constant temperature.	Reyns.
α	Angle.	degrees
β	Viscosity exponent index.	1/°F
β'	Nondimensional index = $\beta(T_J-T_B)$.	
γ	Attitude Angle	degrees

τ	Shear stress.	psi
ρ	Average density of the oil.	lb/ft^3
ν	Kinematic viscosity.	in^2/sec
Θ	Nondimensional temperature $= \frac{T - T_B}{T_J - T_B}$.	

I. INTRODUCTION

To determine the temperature at which a bearing will run, the removal of frictional heat has to be studied first.

The question of the removal of heat from journal bearings has been the subject of experimental and analytical investigations. Two approaches have been used in analyzing the problem. One approach considers that the heat generated in the oil film is removed only be conduction. The other approach treats the problem from the point of adiabtic flow, that is, all the heat generated by friction remains in the oil, raising its temperature and is carried away by convection.

In practice, the heat generated is by no means confined within the clearance space, neither is it entirely carried away by the oil. It is partly carried away in the film itself and partly by conduction, at first from the interior of the film to the inner bearing surface and then through the bearing to the atmosphere.

The present investigation explored some of the aspects not discussed by most of the previous investigators. Both the heat conducted through the bearing and that convected by the oil flow were considered in the study of the effect of speed, load and external heating on the average oil film temperature, oil flow and correspondingly the heat balance of journal bearings.

Most of the early investigators based their work on the assumption that the heat generated by the internal viscous shear stresses was entirely dissipated from the bearing by conduction; and the oil flow through the bearing played no part.

In 1903, Lasche[11] represented the first detailed investigation of thermal effects in bearings. He measured the friction loss in bearings running at peripheral speeds up to 80 fps, and considered the heat dissipation characteristics of the bearing. He found out that the heat dissipation was proportional to the 1.3 power of the temperature difference between the bearing and the surroundings.

Muskat and Morgan[12] carried out tests at low peripheral speeds up to 10 fps on a lightly loaded bearing to determine the correlation between the classical petroff formula for heat generation in journal bearings and their experimental results. This was accomplished by measuring the bearing friction torque, and comparing the results with those calculated using the Petroff formula. The close correspondence of their results and the theory is noteworthy. They included in their work the effect of speed on the transient temperature of the bearing and the heat balance.

Hagg[10] conducted an analytical and experimental investigation on the heat conduction effects in concentric bearings. He derived an equation for the temperature distribution across the oil film in terms of velocity and viscosity variations.

McKee[13], working on his four bearing friction machine, proposed an empirical method to determine the safe operating load for journal bearings taking into consideration the maximum allowable bearing temperature and the minimum Hersey number ($\mu N'/p$).

However, in 1941 Christopherson[5] extended the hydrodynamic theory of lubrication to include thermal effects using the method of relaxation. His solution was obtained under two restricted assumptions:

1. The heat generated by friction remained in the oil for film and no heat was lost to the surroundings.
2. The temperature distribution across the oil film was constant.

Pinkus and Sternlicht[18], using the same assumptions, derived mathematically an expression for the circumferential temperature distribution in journal bearings based on the Sommerfeld infinitely wide journal bearing theory.

Analogous investigation was made by Purvis, Meyer, and Benton[19] using the narrow bearing approximation theory which was suggested by Michell[14] and developed by Ocvirk and DuBois.[17]

Clayton and Wilkie[6] carried out tests with speeds up to 35 fps to measure the temperature distribution in journal bearings. Their work was largely of an exploratory nature.

Boyd and Robertson[3] were the first to consider both the heat conducted through the bearing and that convected by oil flow in their analysis. Their work was restricted to the study of the effect of speed and oil inlet pressure on lightly loaded journal bearings.

Cameron[4] carried out a preliminary investigation on journal bearings with oil pockets to determine the equilibrium temperature of the bearing, considering the overall heat balance. He found out that more detailed investigation had to be made on the heat conduction part and also on the effect of oil pocketing in deciding the partition of the amount of heat between convection and conduction.

For this investigation, a simple journal bearing was constructed with means to measure the journal and bearing temperatures as well as the

oil flow rate. A slip-ring and brush arrangement was used in the measurement of the journal temperature. Devices for loading the bearing and varying the speed of rotation were provided. A method of detecting metal-to-metal contact between the journal and the bearing was used.

As a result of this investigation, a better understanding of the effect of load, speed, and external heating on the heat dissipation through the bearing and that convected by the oil flow was achieved. The hydrodynamic effect on the average oil film temperature was also established. A mathematical treatment of the unloaded bearing was derived, while experimental correlations from the test results were obtained to calculate the heat convected by the oil flow, the heat conducted through the bearing, and the oil flow rate. A method, for estimating the average temperature of the bearing, was also presented.

II. THEORETICAL INVESTIGATION

The fundamental starting point for the analysis will be the general energy equation for an element of lubricant(7)

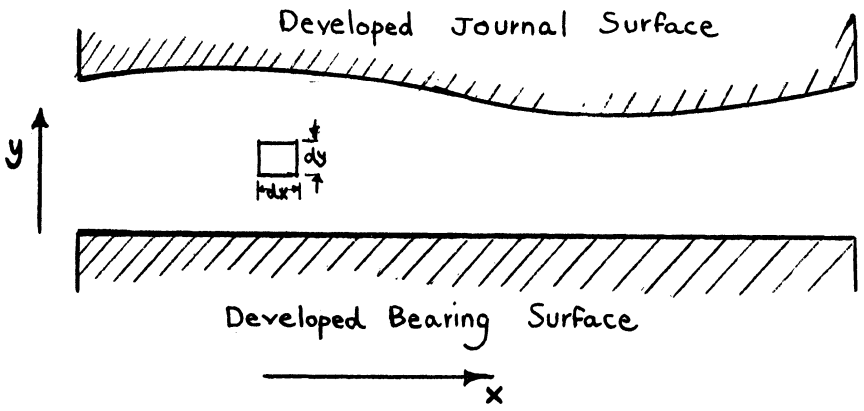

Figure 1. Lubricant Element and Co-ordinate System.

between the boundaries shown in Figure 1, namely,

$$\rho c_h u \frac{\partial T}{\partial x} + \rho c_h v \frac{\partial T}{\partial y} + \rho c_h w \frac{\partial T}{\partial z} = \frac{\partial}{\partial x}\left(k \frac{\partial T}{\partial x}\right) + \frac{\partial}{\partial y}\left(k \frac{\partial T}{\partial y}\right) + \frac{\partial}{\partial z}\left(k \frac{\partial T}{\partial z}\right)$$

$$+ \mu \phi \ . \ . \ . \qquad (2.1)$$

where ϕ is the dissipation function.

$$\phi = 2\left[\left(\frac{\partial u}{\partial x}\right)^2 + \left(\frac{\partial v}{\partial y}\right)^2 + \left(\frac{\partial w}{\partial z}\right)^2\right] + \left(\frac{\partial v}{\partial x} + \frac{\partial u}{\partial y}\right)^2 + \left(\frac{\partial w}{\partial y} + \frac{\partial v}{\partial z}\right)^2$$

$$+\left(\frac{\partial u}{\partial z} + \frac{\partial v}{\partial x}\right)^2 - \frac{2}{3}\left(\frac{\partial u}{\partial x} + \frac{\partial v}{\partial y} + \frac{\partial w}{\partial z}\right)^2 .$$

The first group of terms in Equation (2.1) represents the rate of change of internal energy; the second the rate at which heat is conducted away; and the third the rate at which energy is being dissipated through the action of viscosity.

The following assumptions are introduced in order to simplify the mathematical analysis:

1. The change of the coefficient of thermal conductivity with temperature of ordinary lubricants is small and will be considered negligible.
2. The flow is considered laminar in view of the small dimensions of the clearance and the high viscosity of the oil. In Appendix C a numerical analysis for the validity of this assumption is given in detail.
3. The lubricant is Newtonian, that is, the shear stress is proportional to the rate of shear.
4. The change of the density of the oil with temperature is neglected. The specific gravity of the oil used changes

very little with temperature, as can be seen from the properties of the oil given in Appendix B .

5. The heat conducted in the x and z directions can be neglected with respect to the heat conducted in the y direction.
6. The velocity v in the y direction can be neglected when compared to the velocity u in the x direction.
7. The velocity gradients across the film are much more important than velocity gradients parallel to it. That is, it is assumed that

$$\frac{\partial u}{\partial y} \gg \frac{\partial u}{\partial x}$$

When the above assumptions have been applied to the fundamental Equation (2.1), one gets:

$$\rho c_h u \frac{\partial T}{\partial x} + \rho c_h w \frac{\partial T}{\partial z} = k \frac{\partial^2 T}{\partial y^2} + \mu[(\frac{\partial u}{\partial y})^2 + (\frac{\partial w}{\partial y})^2] \qquad (2.2)$$

There are two desired solutions for the above equation. These are:

1. The unloaded bearing solution.
2. The loaded bearing solution.

The Unloaded Bearing Solution

When the bearing is not loaded, the journal will run concentrically with respect to the bearing. The following assumptions will be made in connection with this case:

1. The oil film is so thin that the curvature of the bearing surface may be ignored, that is, the distinction between

the polar and rectangular coordinates can be neglected and the problem can be considered as equivalent to that of the flow between parallel plates.

2. The viscosity of the oil is dependent on its temperature. It is sufficiently accurate for our purpose to use Reynolds empirical formula:

$$\mu = \mu_o e^{-\beta T} \tag{2.3}$$

3. As the parabolic velocity distribution, due to the pressure gradient, is small compared to the velocity distribution due to the journal motion, the flow of the lubricant in the clearance space will be considered as a Couette flow, that is, the velocity distribution will be linear. The velocity distribution will be expressed as follows:

$$u = U \frac{y}{h} \tag{2.4}$$

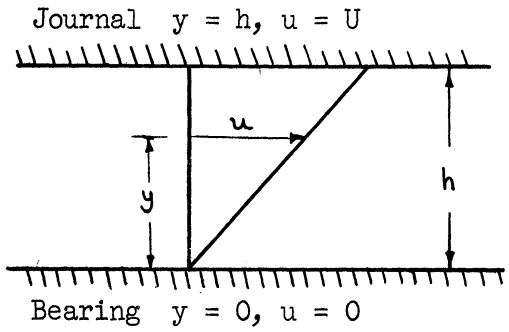

Figure 2. The Velocity Distribution.

4. The oil supply pressure adopted for the experimental investigation is low. This will justify the negligence of the velocity w in the z direction.

5. The temperature gradient $\partial T/\partial x$ will be neglected for the following reasons:

   a. The journal runs concentrically in the bearing and the problem can be considered symmetrical.

   b. As the thermal coefficient of conductivity of the bearing material is high, thermal recirculation in the bearing will tend to smooth out the small variations in the oil film temperature.

When the above assumptions have been applied to Equation (2.2), it becomes

$$k \frac{d^2T}{dy^2} = -\mu_o e^{-\beta T} \frac{U^2}{h^2} \tag{2.5}$$

To represent Equation (2.5) in a dimensionless form let:

$$\Theta = \frac{T - T_B}{T_J - T_B}$$

$$\beta' = \beta(T_J - T_B)$$

$$Y = \frac{y}{h}$$

$$\text{Prandtl Number} = Pr. = \frac{c_h \mu_B}{k}$$

$$\text{Eckert Number} = E. = \frac{U^2}{c_h(T_J - T_B)}$$

Substituting the above values in Equation (2.5) gives:

$$\frac{d^2\Theta}{dY^2} = - Pr.E.e^{-\beta'\Theta}$$

or

$$e^{\beta'\Theta} \frac{d^2\Theta}{dY^2} = - Pr.E. \tag{2.6}$$

This is a nonlinear second order differential equation. To linearize the above equation, the following substitution is introduced.[9]

$$\Phi = e^{\beta'\Theta} - 1$$

$$\therefore \frac{d\Phi}{dY} = \beta' e^{\beta'\Theta} \frac{d\Theta}{dY} \tag{2.7}$$

$$\frac{d^2\Phi}{dY^2} = \beta' e^{\beta'\Theta} \left\{ \frac{d^2\Theta}{dY^2} + \beta' e^{\beta'\Theta} \left(\frac{d\Theta}{dY}\right)^2 \right\}$$

The last term in the above equation can be neglected compared to the second by the order of magnitude analysis. The above equation, then becomes:

$$\frac{d^2\Phi}{dY^2} = \beta' e^{\beta'\Theta} \frac{d^2\Theta}{dY^2}$$

Substituting in Equation (2.6) gives:

$$\frac{d^2\Phi}{dY^2} = - \beta' \text{Pr.E.} \tag{2.8}$$

Integrating Equation (2.8) with respect to Y twice one gets:

$$\Phi = \frac{- \beta' \text{Pr.E. } Y^2}{2} + c_o Y + c_1 \tag{2.9}$$

In order to evaluate the constants of integration c_o and c_1, the boundary conditions have to be specified.

Boundary Conditions

Two cases will be considered in the choice of the boundary conditions:

a. The no heating case.

b. The external heating case.

The No Heating Case.--In this case the boundary conditions can be described as follows:

1. at $Y = 0$, $\Theta = 0$, $\Phi = 0$ (2.10)

2. at $Y = 1$, $\frac{d\Theta}{dY} = 0$, $\frac{d\Phi}{dY} = 0$ (2.11)

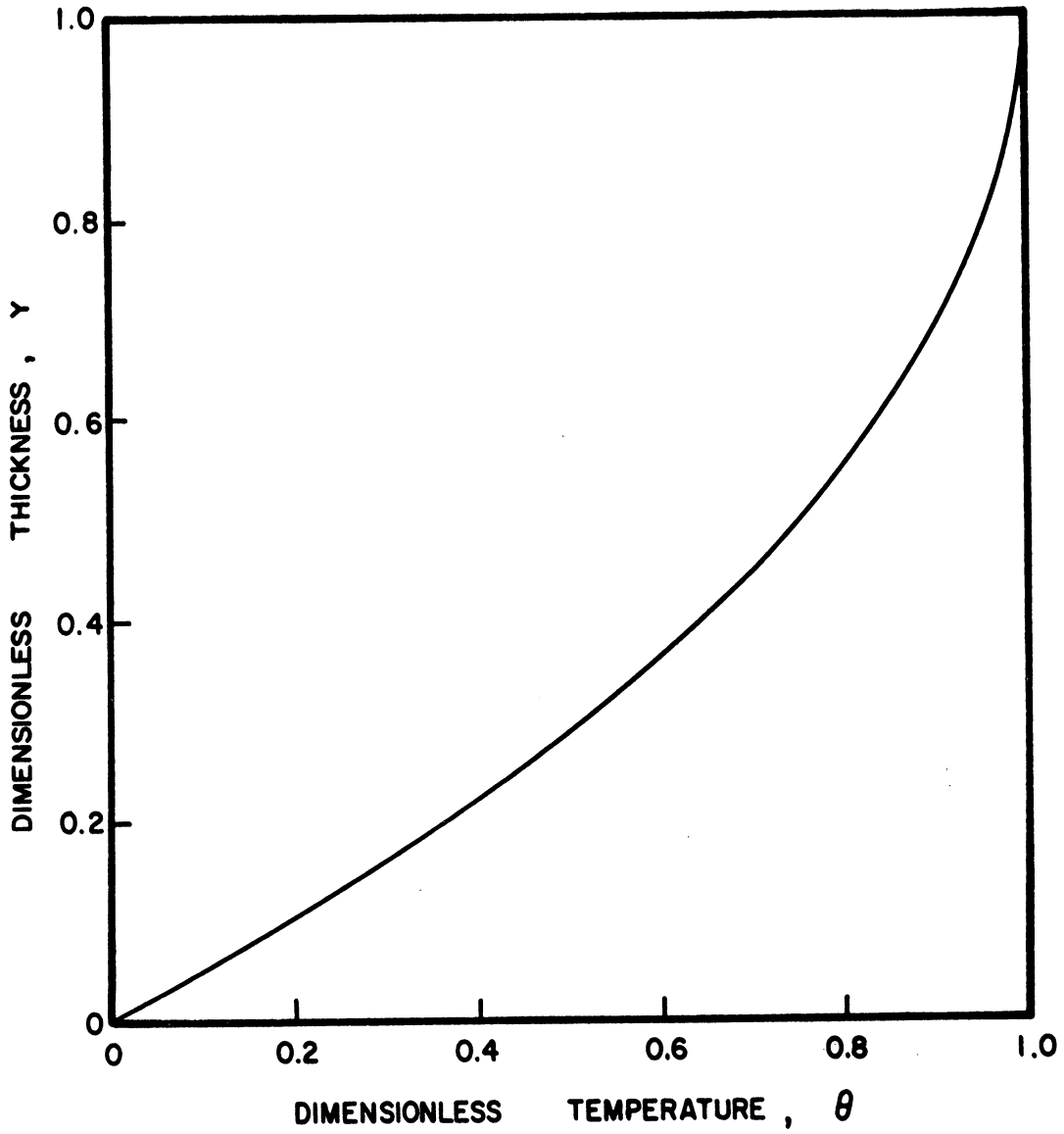

Figure 3. Temperature Distribution Across the Oil Film.

The first boundary condition is based on assumption number (5) in the analysis.

The second boundary condition is established from the consideration that, as the steady condition is reached, the journal can be regarded as virtually insulated since the rate of loss of heat from the journal is relatively very small.

Solution of the No Heating Case.-Applying the first boundary condition to Equation (2.9) gives:

$$C_1 = 0$$

Applying the second boundary condition gives:

$$C_o = \beta' \text{ Pr.E.}$$

$$\therefore \quad \Phi = \frac{\beta' \text{ Pr.E. } Y^2}{2} + \beta' \text{ Pr.E.Y.}$$

But

$$\Theta = \frac{1}{\beta'} \ell n(\Phi + 1)$$

$$\therefore \quad \Theta = \frac{1}{\beta'} \ell n \left[\beta' \text{ Pr.E.}\left(Y - \frac{Y^2}{2}\right) + 1\right] \qquad (2.12)$$

This is the temperature distribution across the oil film, expressing the temperature as a function of the film thickness. Figure 3 gives the form the temperature distribution across the oil film will take, according to Equation (2.12). In Appendix I an exact solution for Equation (2.6) is carried out and an evaluation of the experimental results shown in Figure 4 and the theoretical result is given.

The External Heating Case.--In this case the boundary conditions can be expressed as follows:

1. at $Y = 0$, $\Theta = 0$, $\Phi = 0$ (2.10)

2. at $Y = 1$, $\Theta = 1$, $\Phi = e^{\beta'} - 1$ (2.13)

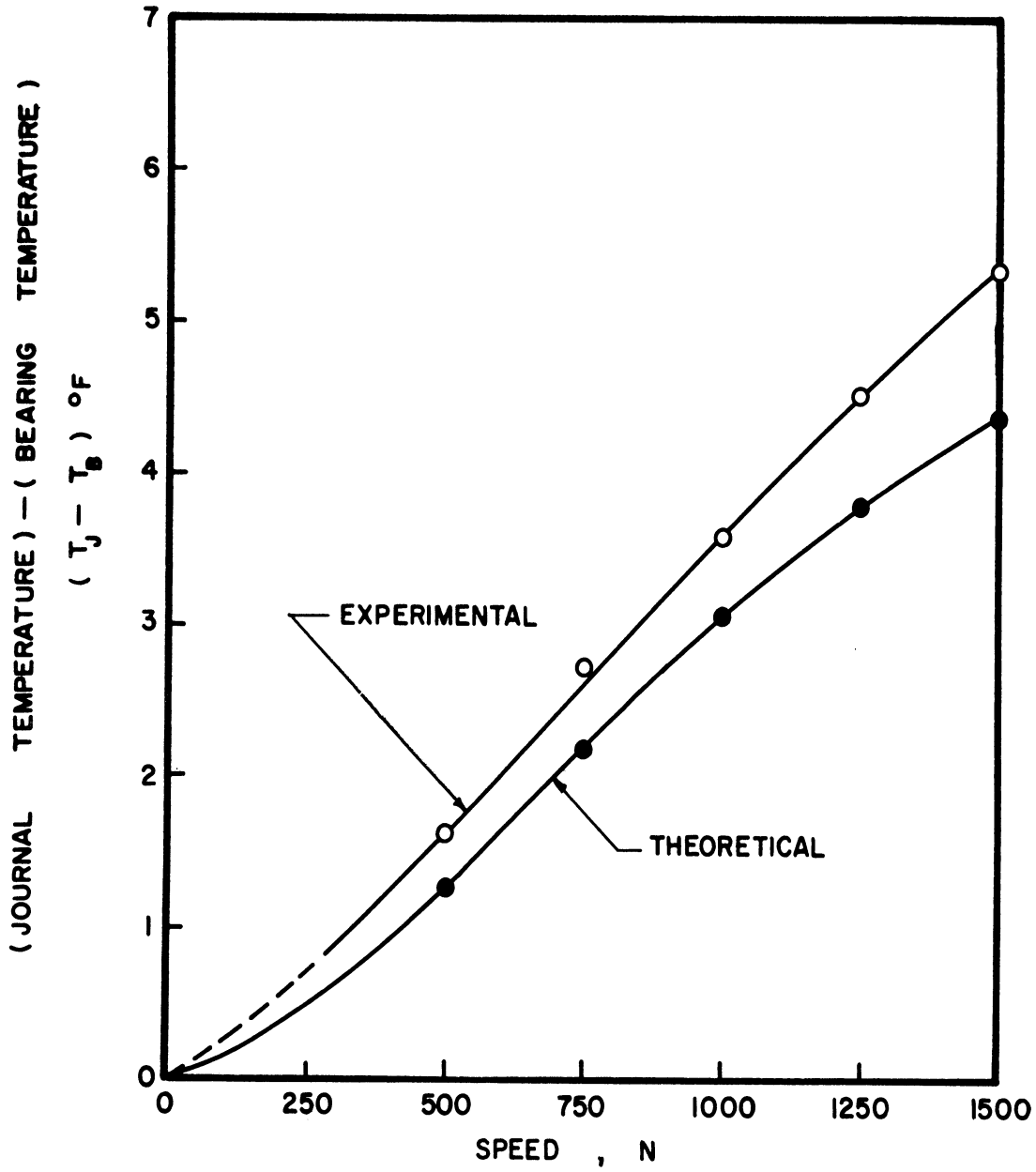

Figure 4. Comparison Between the Theoretical and Experimental (Journal Temperature-Bearing Temperature) at Different Speeds - N.

Applying the above boundary conditions to Equation (2.9) gives:

$$C_1 = 0$$

$$C_o = \left(\frac{\beta' \text{ Pr.E.}}{2} + e\beta' - 1\right)$$

substituting the values of the constants in Equation (2.9) one gets:

$$\Phi = \frac{\beta' \text{ Pr.E.}}{2} \cdot Y^2 + \left(\frac{\beta' \text{ Pr.E.}}{2} + e\beta' - 1\right) Y$$

But

$$\Theta = \frac{1}{\beta'} \ln (\Phi + 1) \qquad (2.14)$$

$$\therefore \quad \Theta = \frac{1}{\beta'} \ln \left[1 - \beta' \frac{\text{Pr.E.}}{2} Y^2 + \left(\beta' \frac{\text{Pr.E.}}{2} + e\beta' - 1\right) Y\right]$$

This is the temperature distribution across the film for the external heating case which is presented in Figure 5 for different values of E.Pr.

Constant Viscosity Theory

If the viscosity of the oil is not appreciably affected by the temperature differences within the film, the following simplified equations for the temperature distribution across the film for both cases can be written as follows:

a. The no heating case:

$$\Theta = \text{Pr.E.} \left(Y - \frac{Y^2}{2}\right) \qquad (2.15)$$

b. The external heating case:

$$\Theta = Y + \frac{\text{Pr.E.}}{2} (Y - Y^2) \qquad (2.16)$$

The above equations are derived using the same analysis as above except for the variable viscosity assumption.

It is worthy of mention that the temperature distribution for the external heating case, Equation (2.16), consists of a linear term which

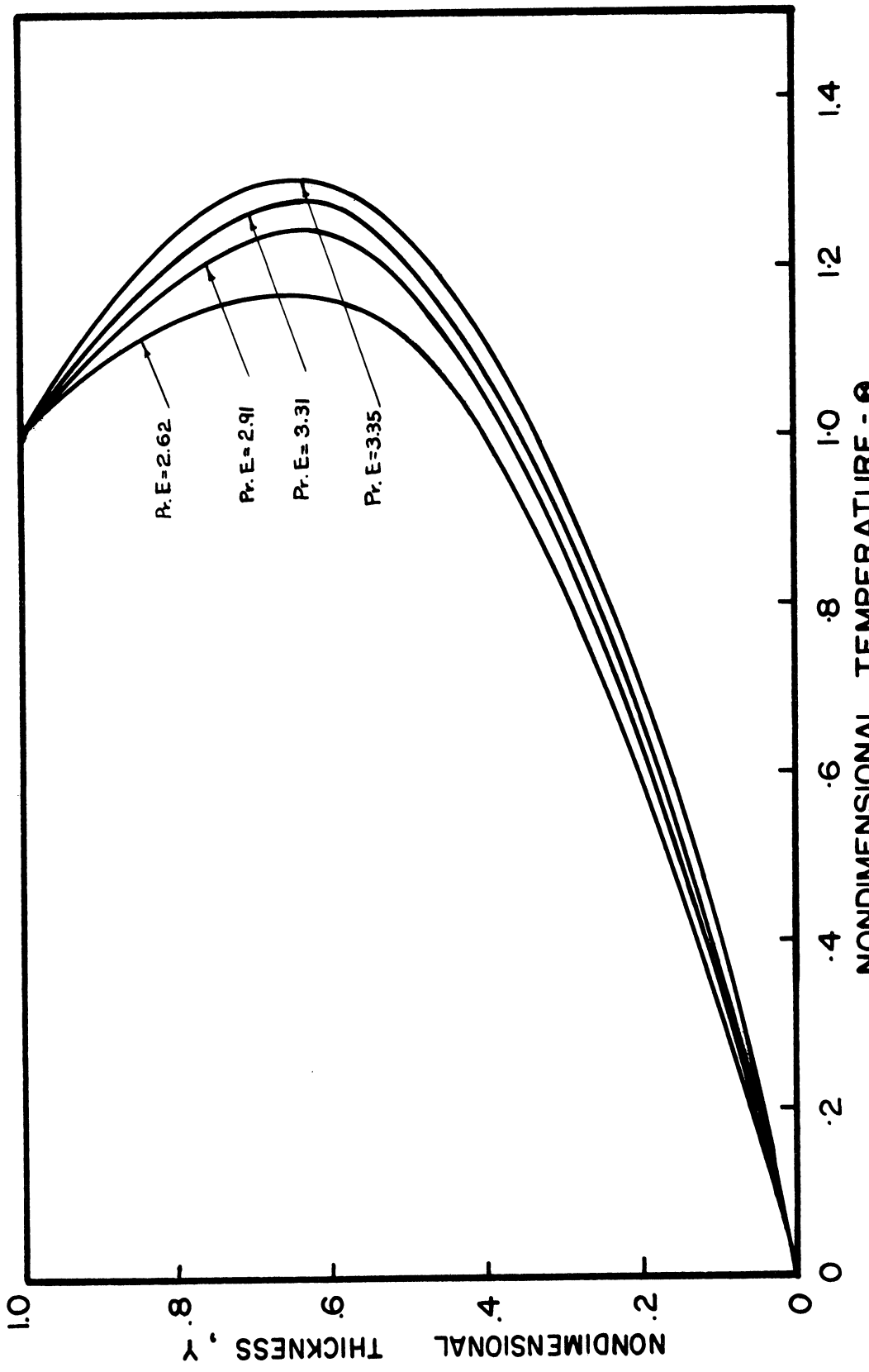

Figure 5. Temperature Distribution Across the Oil Film for the External Heating Case at Different Products of Pr.E.

is the same as in the case of mere conduction with no frictional heat generation. Superimposed on this is a parabolic distribution, represented by the last term in the equation, which is due to the heat generation by friction.

The Loaded Bearing Solution

In this case, the journal will run eccentrically with respect to the bearing as shown in Figure 6. The simplified general energy

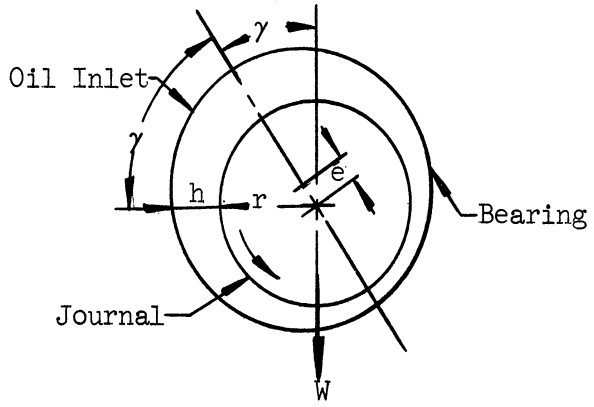

Figure 6. Position of Journal Under Load.

Equation (2.2) will describe to a good approximation the heat effects in the lubricating film. For mathematical simplicity, the following assumptions are made:

1. The velocity distribution across the oil film is linear, that is

$$u = U\frac{y}{h} \tag{2.4}$$

2. As the velocity u in the x-direction is greater than the velocity w in the z-direction, the term $(\partial w/\partial y)^2$ can be neglected with respect to the term $(\partial u/\partial y)^2$.

Substituting for the value of w, h, and dx by:

$$w = \frac{1}{2\mu} y(y-h) \frac{\partial p}{\partial z}$$

$$h = c(1+n \cos \alpha)$$

$$dx = r \, d \, \alpha$$

in Equation (2.2) one gets:

$$\rho c_h \frac{U y}{c(1+n \cos \alpha) r} \frac{\partial T}{\partial \alpha} + \rho c_n \frac{y[y-c(1+n \cos \alpha)] \partial p/\partial z}{2\mu} \frac{\partial T}{\partial z} = \frac{\partial^2 T}{\partial y^2}$$

$$+ \mu \frac{U^2}{c^2(1+n \cos \alpha)^2} \qquad (2.17)$$

assuming a linear pressure gradient in the z-direction and dividing the above equation by $\rho c_h U/c$ on gets:

$$\frac{y}{r(1+n \cos \alpha)} \frac{\partial T}{\partial \alpha} + \frac{cy[y-c(1+n \cos \alpha)]p}{2\mu \, U \, \ell} \frac{\partial T}{\partial z} = \frac{kc}{\rho c_h U} \frac{\partial^2 T}{\partial y^2}$$

$$+ \frac{\mu \, U}{\rho c_h c(1+n \cos \alpha)^2} \qquad (2.18)$$

At this point, it is convenient to introduce dimensionless variables. Let

$$\Theta = \frac{T - T_B}{T_J - T_B} \quad , \qquad \frac{z}{c} = Z$$

$$Y = \frac{y}{c}$$

$$R = \frac{r}{c}$$

$$\mu = \mu_B e^{-\beta' \Theta} \quad , \qquad \frac{\ell}{c} = L$$

also let

$$R_e = \frac{\rho \, U \, c}{\mu_B} \quad , \qquad G = \frac{pc}{\mu_B U}$$

$$E = \frac{U^2}{c_h(T_J - T_B)}$$

$$P_r = \frac{c_h \mu B}{k}$$

$$P_e = \frac{\rho c_h U c}{k}$$

Substitution in Equation (3.18) gives:

$$\frac{Y}{R(1+n\cos\alpha)} \frac{\partial\Theta}{\partial\alpha} + \frac{Y[Y - (1+n\cos\alpha)]}{2 L e^{-\beta'\Theta}} G \frac{\partial\Theta}{\partial Z} = \frac{1}{P_e} \frac{\partial^2\Theta}{\partial Y^2} + \frac{E e^{-\beta'\Theta}}{R_e(1+n\cos\alpha)^2}$$

multiplying the above equation by $e^{\beta\Theta'}$ yields:

$$\frac{e^{\beta'\Theta} Y}{R(1+n\cos\alpha)} \frac{\partial\Theta}{\partial\alpha} + \frac{Y e^{2\beta'\Theta}[Y - (1+n\cos\alpha)]}{2 L} G \frac{\partial\Theta}{\partial Z}$$

$$= \frac{e^{\beta'\Theta}}{p_e} \frac{\partial^2\Theta}{\partial Y^2} \frac{E}{R_e(1+n\cos\alpha)^2} \qquad (2.19)$$

After trying a few practical relationships, the writer was unsuccessful in proceeding with the solution. The reason for this difficulty is that Equation (2.19) is a non-linear non-homogeneous differential equation, added to that the difficulty in expressing the boundary conditions for the problem. For the above reasons, an empirical method is adopted for this case.

The Empirical Solution

The heat generated due to the viscous resistance of the lubricant film to the rotation of the shaft is carried away, after thermal equilibrium has been reached, partly in the oil film itself to the outlet end of the bearing, and partly by conduction, at first from the oil film to the bearing and then through the bearing to the atmosphere.

The heat balance can be expressed by:

$$H = H_c + H_o \qquad (2.20)$$

where H is the rate of heat generation in the film,

H_c is the rate of heat dissipation through the bearing and surroundings and

H_o is the rate at which heat is carried away by the oil flow.

From Appendix E the rate of heat generation is given by:

$$H = 300 \left[\frac{8}{J} \frac{\pi^3 r^3 \ell}{c} \frac{\mu N'^2}{(1-n^2)^{1/2}} + \left(\frac{W e \sin \gamma}{2J} \right) 2\pi N' \right] \tag{2.21}$$

The rate of heat dissipation H_c can be described by a power of the temperature elevation of the oil film over the ambient,

$$H_c = a(2\pi r \ell)(\Delta T)^m \tag{2.22}$$

where a and m are empirical constants, depending upon the type of housing and surroundings.

The rate at which heat is carried away by the oil flow can be written as:

$$H_o = \rho q c_h (T_2 - T_1) \tag{2.23}$$

Substituting Equations (2.21), (2.22), and (2.23) in Equation (2.20) yields:

$$300 \left[\frac{8}{J} \frac{\pi^3 r^3 \ell}{c} \frac{\mu N'^2}{(1-n^2)^{1/2}} + \left(\frac{W e \sin \gamma}{2J} \right) 2\pi N' \right] = a(2\pi r \ell)(\Delta T)^m + \rho q c_h (T_2 - T_1) \tag{2.24}$$

This is the general heat balance equation for the loaded bearing. The numerical values for the empirical constants a and m will be determined experimentally.

For the external heating case the heat balance equation can be written as:

$$H_e + 300\left[\frac{8}{J}\,\frac{\pi^3 r^3 \ell}{c}\,\frac{\mu N'}{(1-n^2)^{1/2}} + \left(\frac{W\, e \sin\gamma}{2\,J}\right) 2\pi N'\right] = a'(2\pi r\ell)(\Delta T)^{m'} + \rho q c_h (T_2 - T_1) \qquad (2.25)$$

where H_e is the external heat applied.

For the unloaded bearing, the heat balance equation can be obtained from Equation (2.24) and (2.25) when substituting zero for the value of e.

For the no heating case:

$$\frac{2400}{J}\,\frac{\pi^3 r^3 \ell}{c}\,\mu N'^2 = a(2\pi r\ell)(\Delta T)^m + \rho q c_h (T_2 - T_1) \qquad (2.26)$$

For the external heating case:

$$H_e + \frac{2400}{J}\,\frac{\pi^3 r^3 \ell}{c}\,\mu N'^2 = a(2\pi r\ell)(\Delta T)^m + \rho q c_h (T_2 - T_1) \qquad (2.27)$$

III. EXPERIMENTAL APPARATUS

General Description of the Apparatus

The test apparatus consisted mainly of the equipment shown in Figures 7 through 9.

The heart of the apparatus is the test journal and bearing as indicated in Figure 10.

Figure 13 illustrates diagrammatically the loading device and the means for collecting the oil flowing through the test bearing.

The temperature measuring circuit is shown in Figure 20. The slip-ring and brush assembly used in the measurement of the journal surface temperature is sketched in Figure 19.

In addition, Figure 14 illustrates the equipment used in detecting film breakdown.

In the following paragraphs, the details of the various systems are described.

Driving Mechanism

The journal was driven by a 3/4 horsepower variable speed hydraulic transmission unit which was connected to a one horsepower, 1725 rpm, three phase electric motor. The motor and the speed reducer were mounted on a separate frame to prevent the vibration from being transmitted to the test bearing unit. The frame can be raised or lowered for leveling purposes by means of four screws located at the corners.

Test Journal and Bearing

The test journal and bearing are shown in Figure 10. The journal was made of number 4615 steel. A hole one inch in diameter was

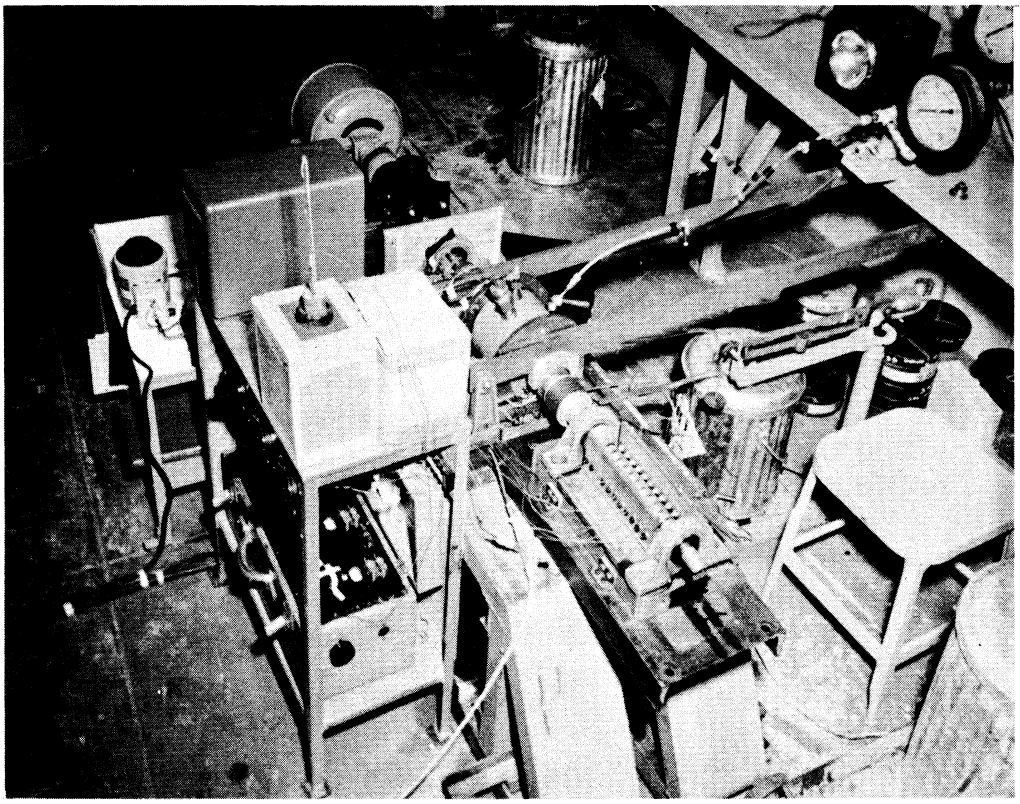

Figure 7. General Layout of the Experimental Apparatus.

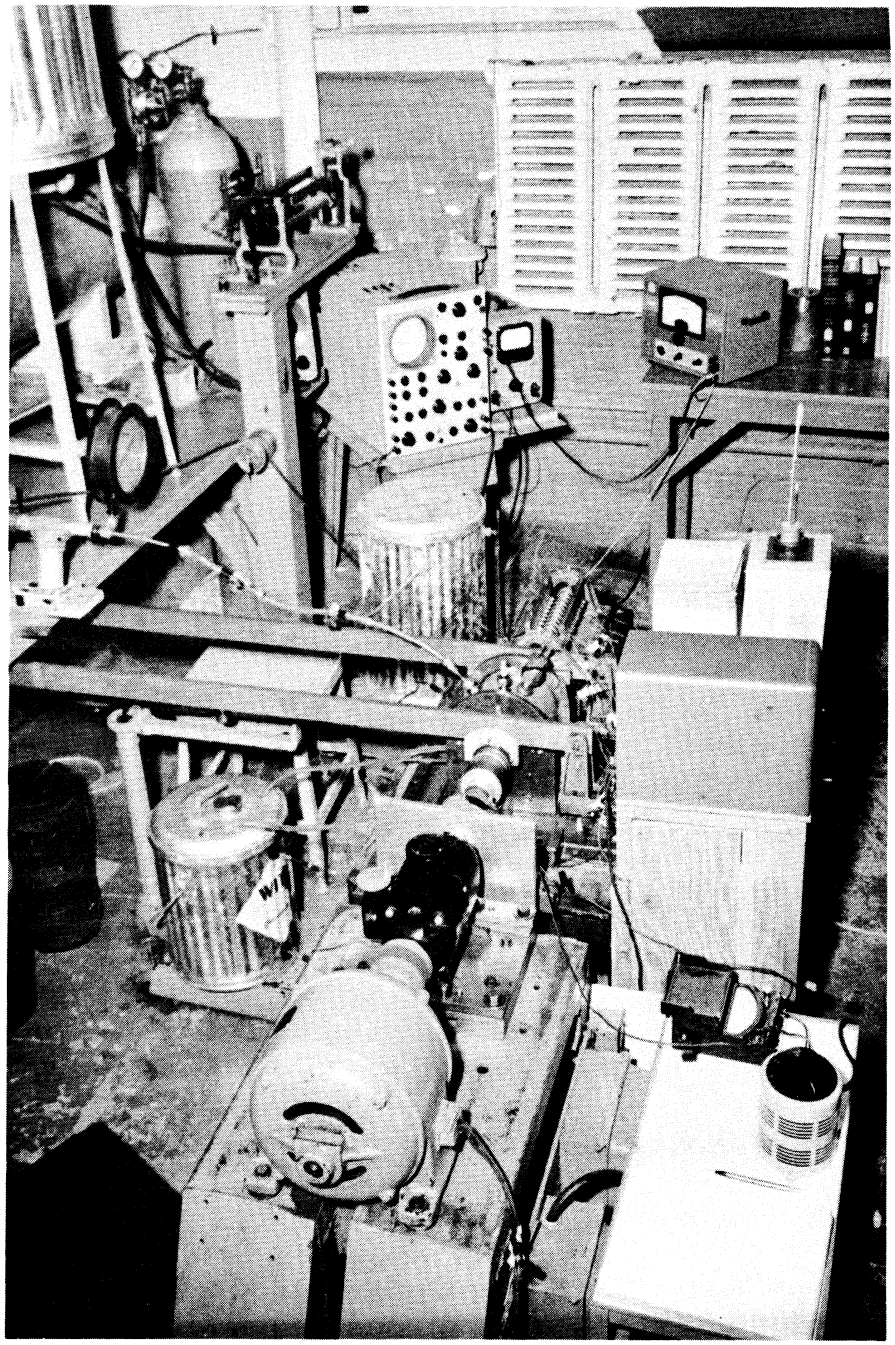

Figure 8. The Experimental Apparatus Showing the Film Breakdown Detection Instrumentation.

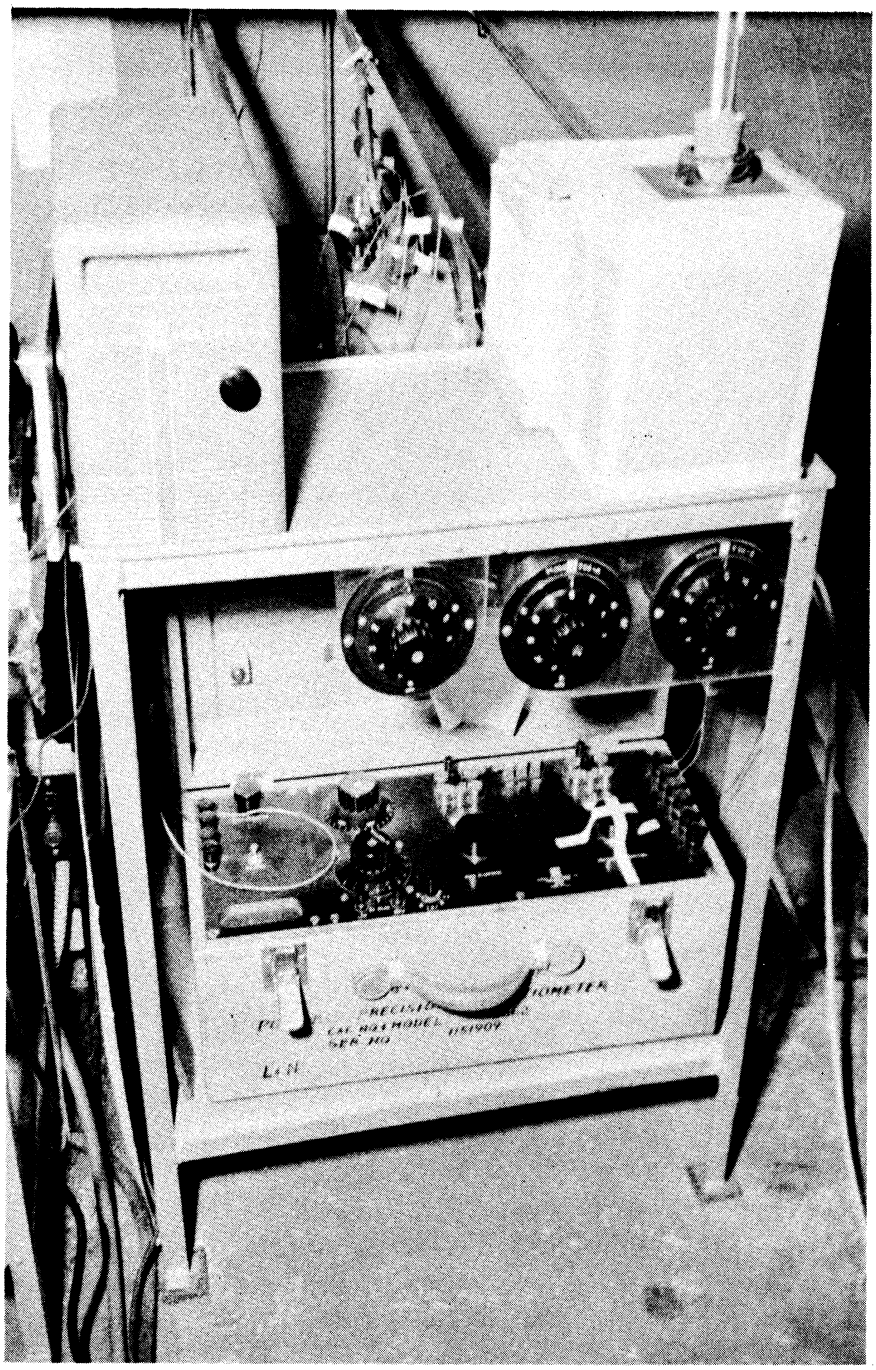

Figure 9. The Temperature Measurement Instrumentation.

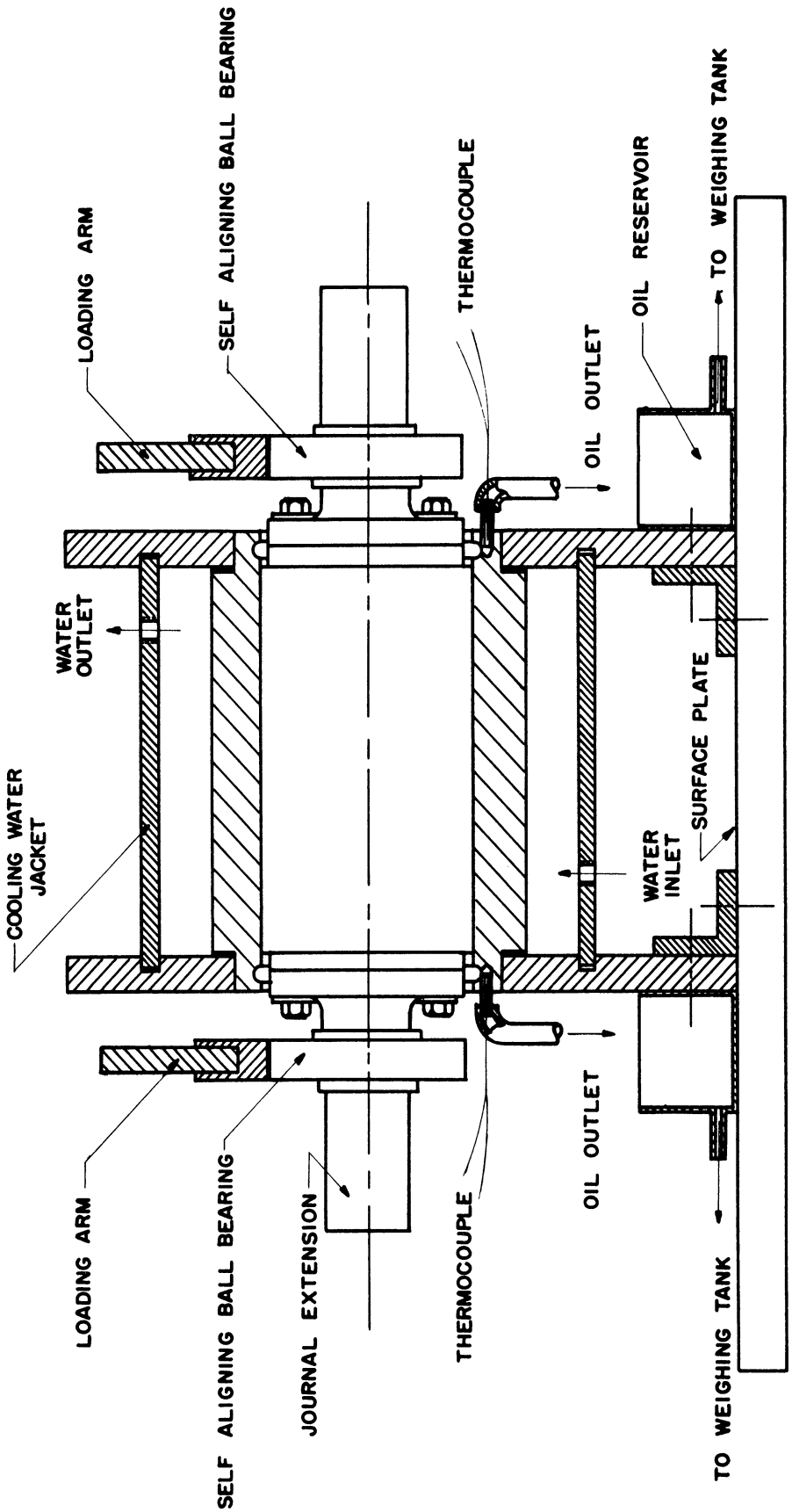

Figure 10. Journal and Bearing Assembly.

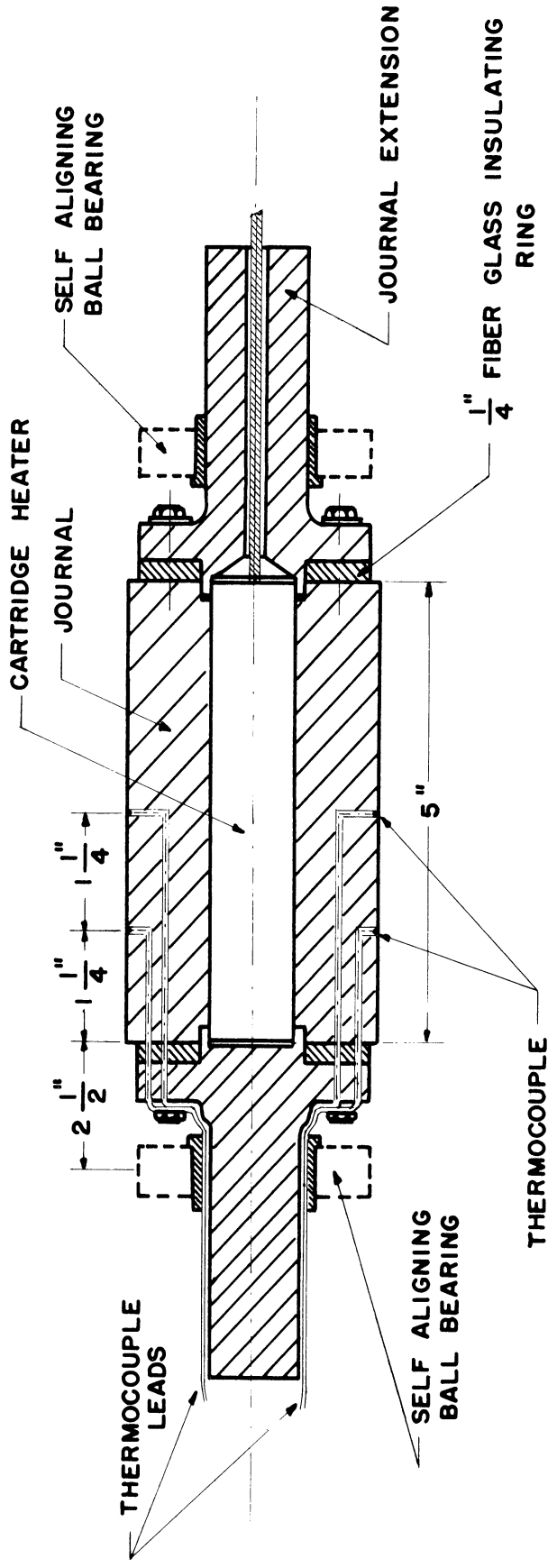

Figure 11. The Test Journal, Showing the Thermocouple Locations, the Heater, and the Self-Aligning Ball Bearings.

bored centrally to provide for a 500 watt cartridge type electric heater to fit snugly, so that metal-to-metal contact is insured over the whole surface of the unit. Four iron-constantan thermocouples were silver soldered to the journal surface, as shown in Figure 11, to measure the temperature at the surface.

In order to reduce the heat conduction in the axial direction, two fiber glass insulating rings of 1/4 inch thickness were placed between the journal and the journal extension at each end of the journal.

After assembly, the journal was ground in a centerless grinder to the required dimensions.

The exact dimensions of the bearing and the journal, and the constructional details are given in Appendix A.

The bearing, shown in Figure 12, was made of Bunting Bronze because of its adequate lubricating properties.

Thermocouples were silver soldered to 12, 1/4 inch diameter, fine thread plugs, which were made of the same material as the bearing. The plugs were then screwed and secured in place in the bearing, such that the final boring would just clear the thermocouple beads.

At both ends of the bearing a groove was made for collecting the oil flowing outwards. A hole at the bottom of each groove was drilled to allow the oil to be collected in a pan.

The bearing was supported at both ends and provision was made for cooling the bearing as shown in Figure 10.

Oil Flow System

As shown in Figure 13, a storage tank of 30 gallons capacity was used to feed the oil to the bearing.

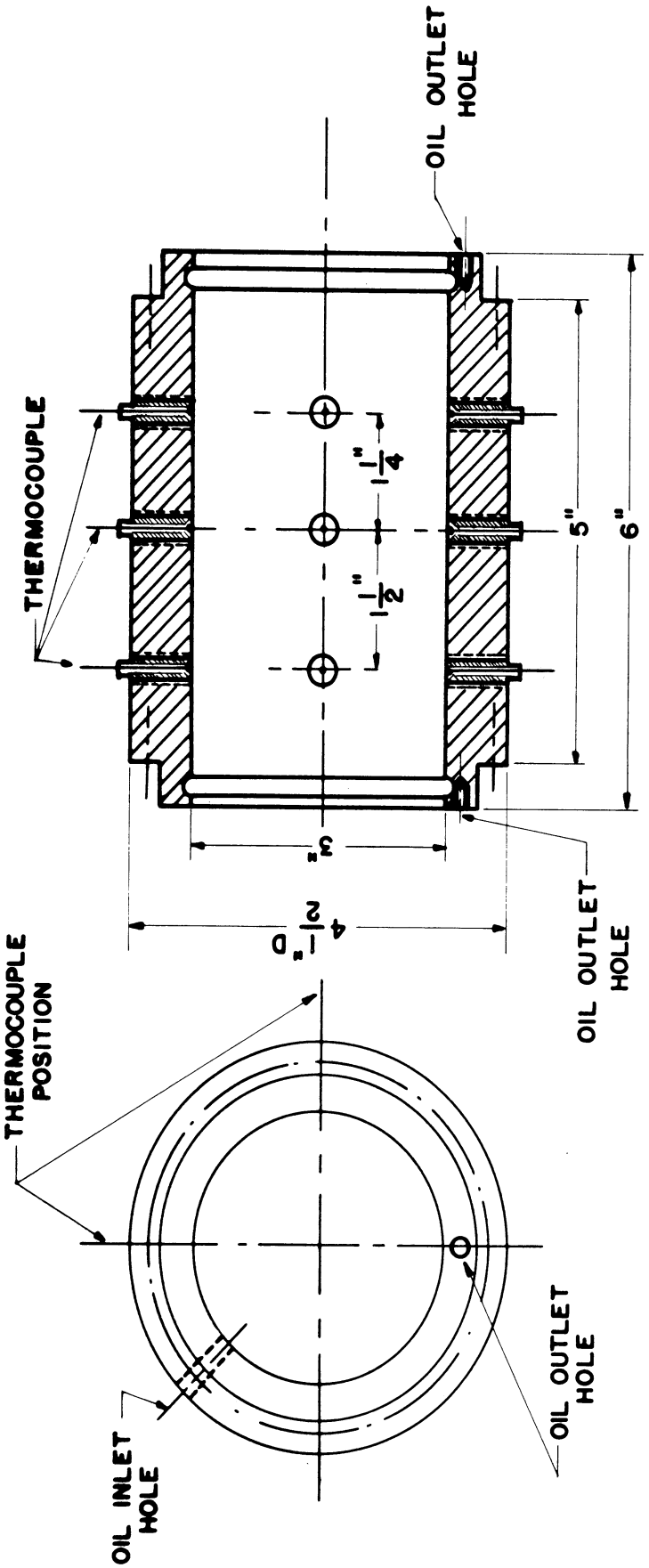

Figure 12. The Bearing, Showing the Thermocouple Locations, Inlet and Outlet Oil Holes.

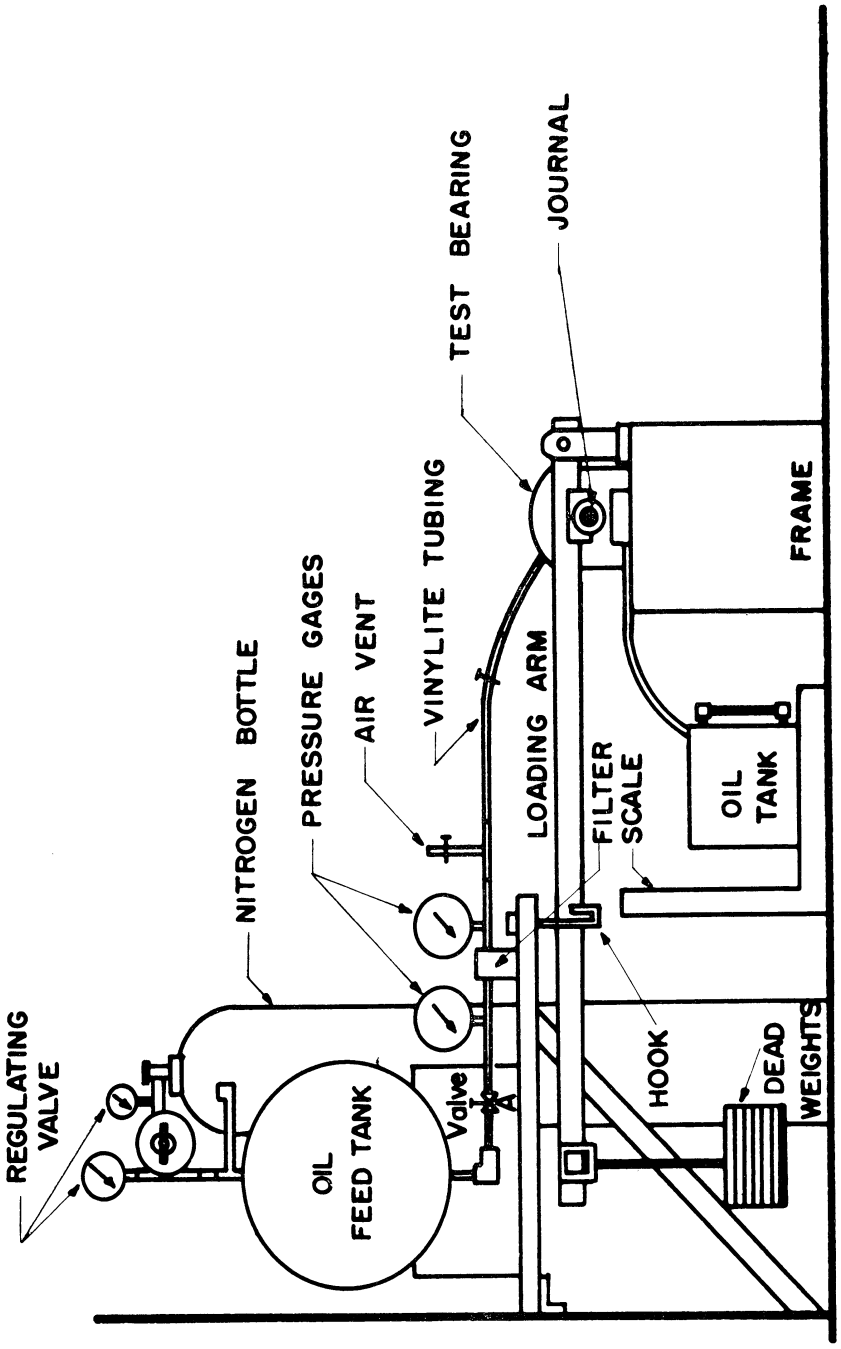

Figure 13. Schematic Sketch of the Oil Supply System and the Loading Device.

A 1700 psi nitrogen cylinder with a pressure regulating valve was connected to the oil tank to raise the pressure of the oil to the desired value. Two filters and a strainer were installed in the line to remove any dirt and contaminants in the oil. Two pressure gauges, placed before and after the filters in the feed line, gave the inlet oil pressure.

After lubricating the bearing, the oil issued through a hole at each end of the bearing and flowed down into a container from which it was collected and weighed on a balance graduated in fiftieths of a pound.

Loading Device

The load was applied at both ends of the journal by means of two levers and dead weights. This arrangement insured a symmetrical loading of the journal ends. The load was transmitted to the journal through two self-aligning ball bearings mounted on the shaft. The levers were pivoted at their front ends, while the dead weights were placed on a pan suspended on a hardened knife-edge at the back ends. The loading arm was chosen to give a 10 to 1 leverage ratio.

As the levers were pivoted at their front ends, the loading system could be raised from the shaft and placed over the hooks, shown in Figure 13, in the case of the no load tests.

Method of Estimating Film Breakdown

It is essential in this investigation that the bearing should be working under hydrodynamic lubrication conditions.

An electric potential was applied between the bearing and the journal to detect any metal-to-metal contact. An audio frequency

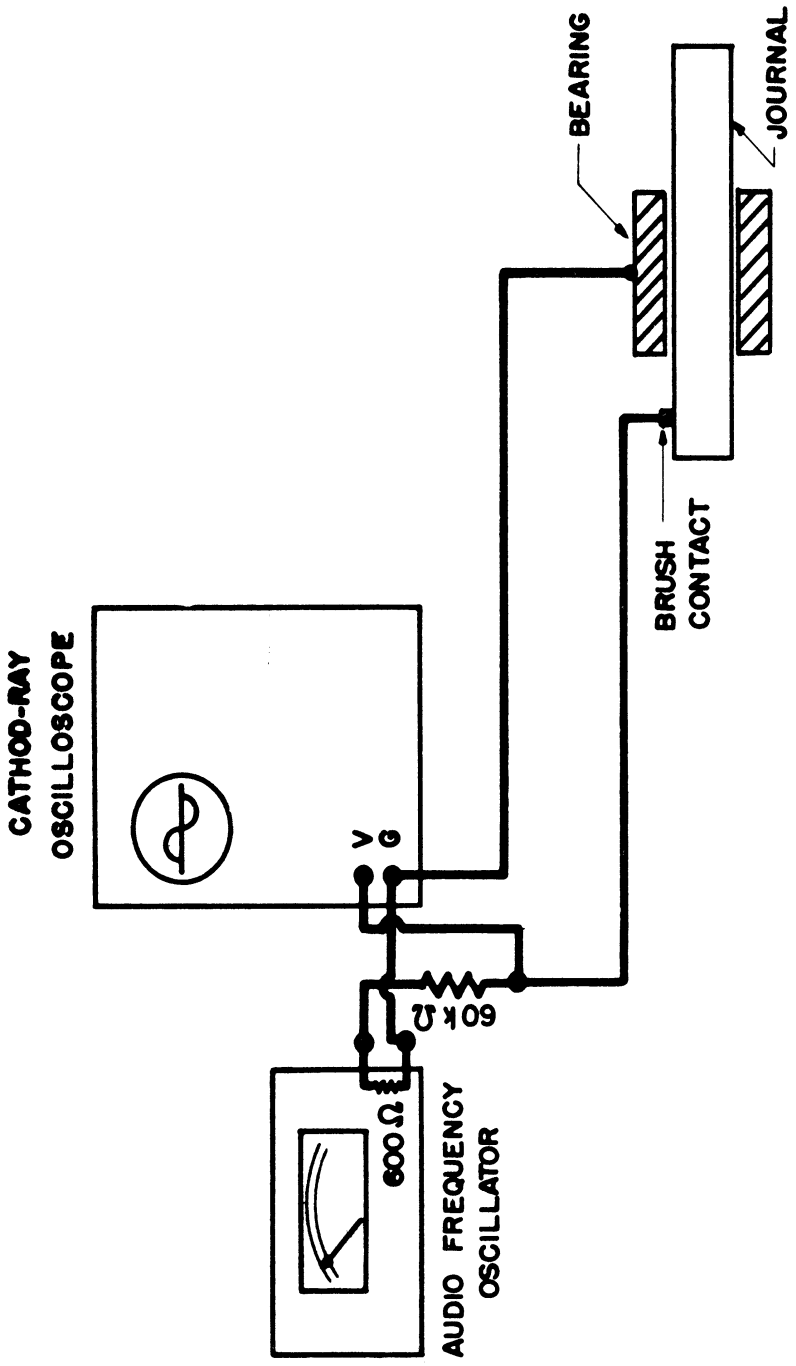

Figure 14. Schematic Sketch of the Electric Circuit for the Estimation of the Film Breakdown.

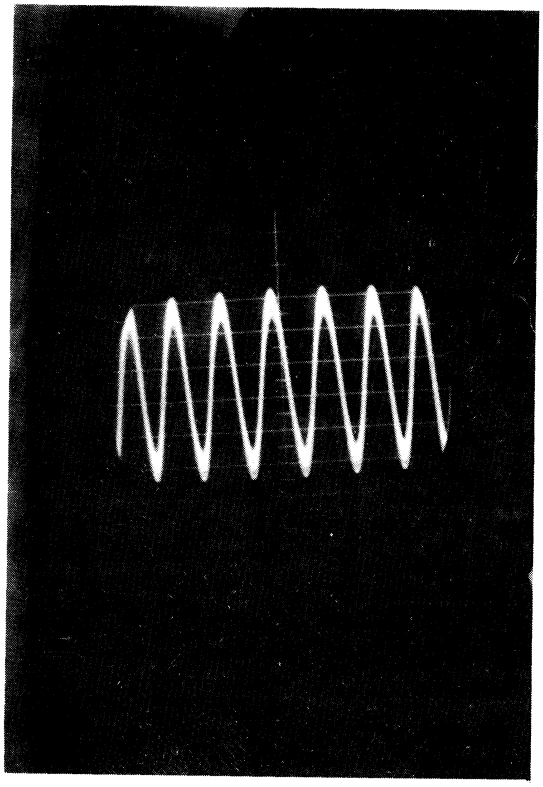

Figure 15. Oscillographic Record for Normal Operation.

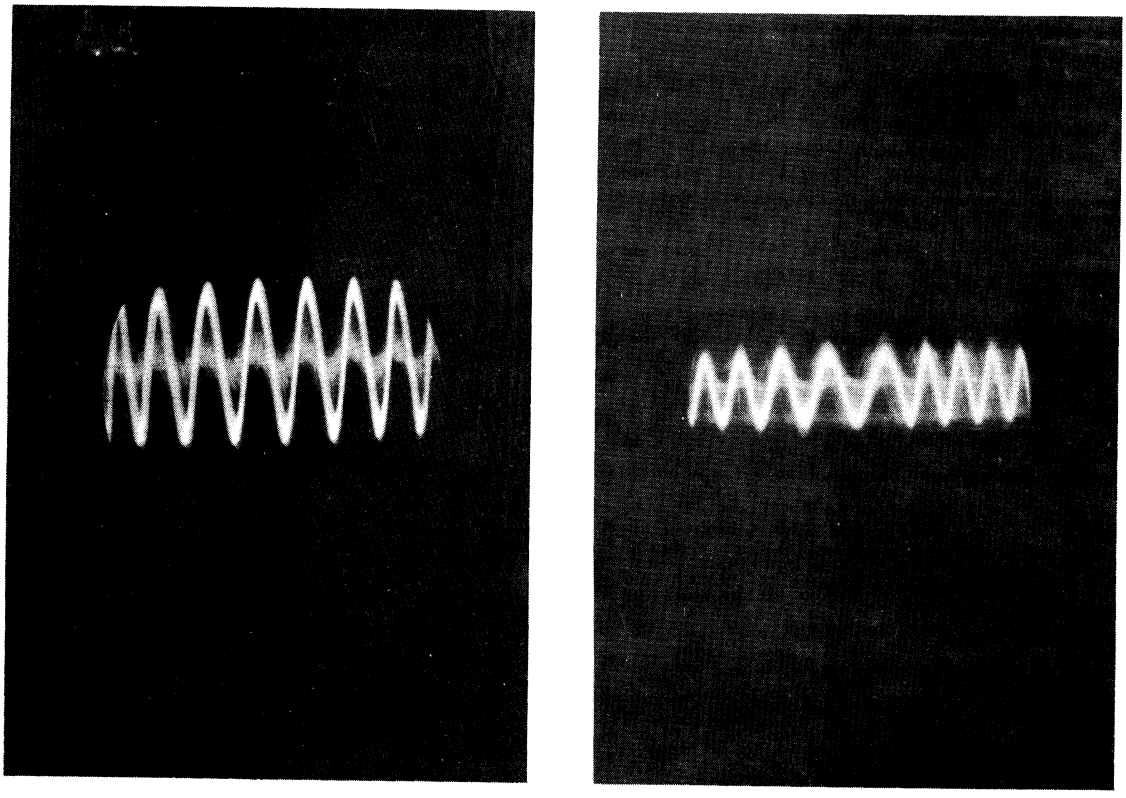

Figure 16. Oscillographic Record for Metal-to-Metal Contact.

oscillator was used as the voltage source. The applied voltage was observed on a cathode-ray oscilloscope screen. A schematic diagram of the electric circuit is illustrated in Figure 14.

The audio frequency oscillator delivered up to 50 volts and was operated at 20,000 cycles.

Figure 15 shows an oscillographic record for normal operation under hydrodynamic conditions. If metal-to-metal contact occurred, the journal was shorted and a picture as illustrated in Figure 16 showed on the cathode-ray oscilloscope screen, indicating film breakdown.

Heating System

The cartridge heater, which was snugly fitted in the journal, was connected to the electric circuit through a slip-ring and brush assumbly.

A variac was used to control the input voltage to the heater. A wattmeter was connected to measure the amount of wattage consumed. Figure 17 shows a schematic diagram of the heating circuit.

Cooling Water System

Water from the supply main was used in cooling the bearing. Two needle valves were installed in the pipe line between the main and the cooling jacket to shut-off and regulate the amount of water flow. After cooling the bearing the water was collected in a 20 gallon tank and weighed on a balance graduated in fiftieths of a pound.

Two thermocouples placed at the inlet and outlet of the cooling jacket registered the temperature of the inlet and outlet water respectively.

Figure 18 shows a schematic sketch of the system.

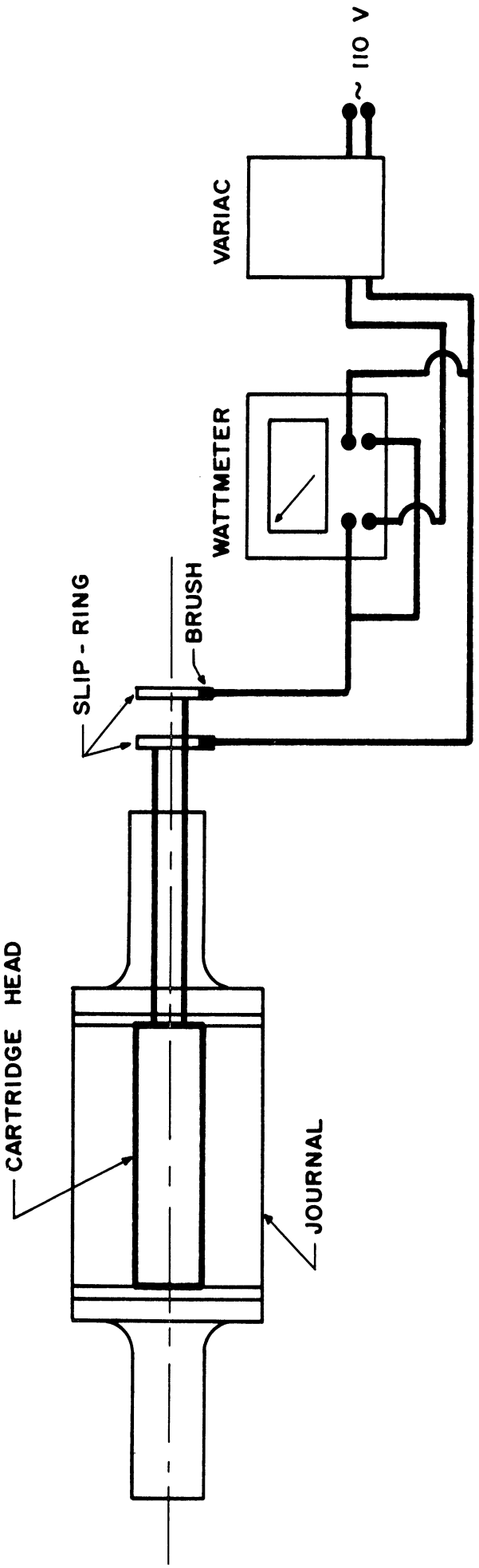

Figure 17. Schematic Diagram of the Heating Circuit.

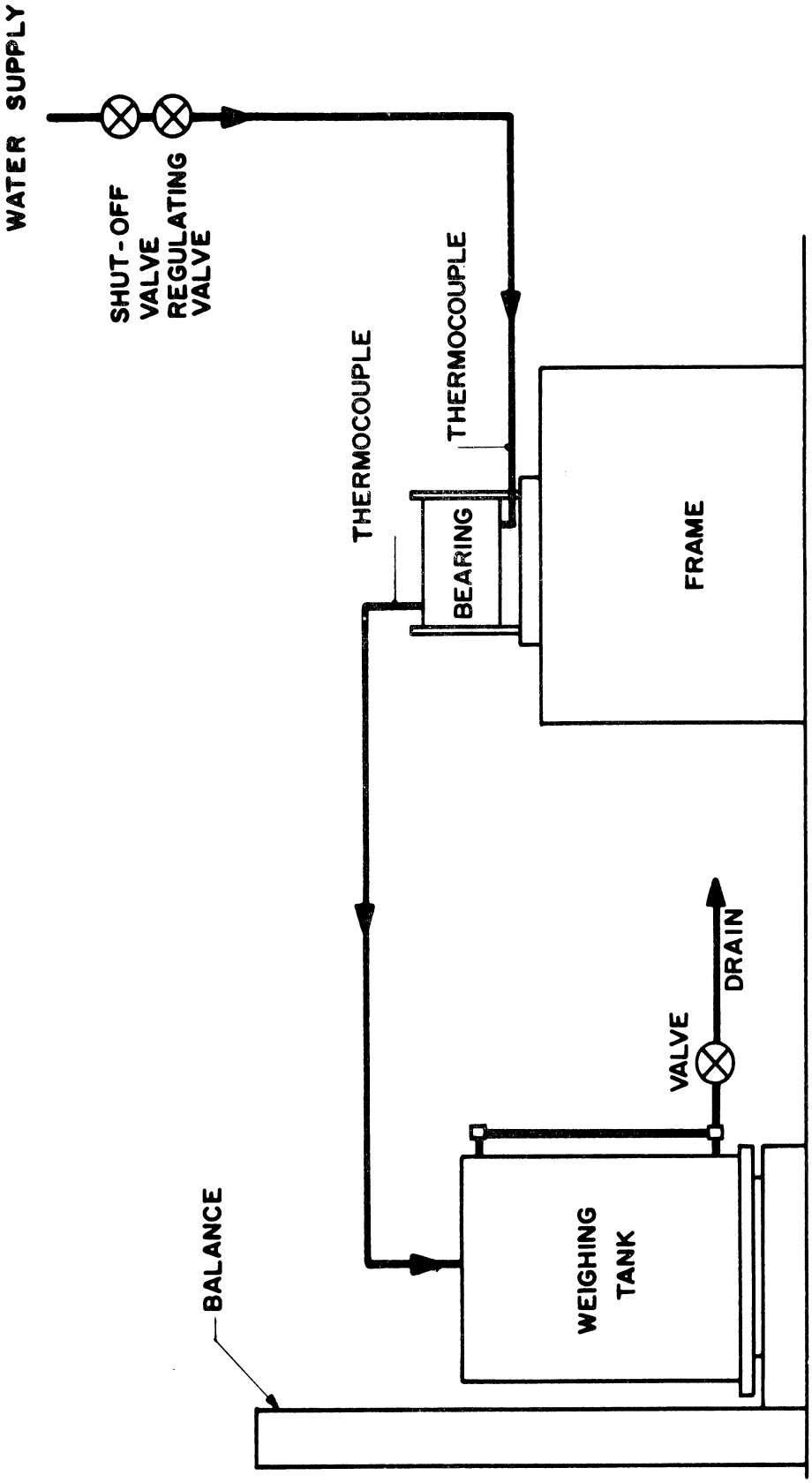

Figure 18. Schematic Diagram of the Cooling System.

Temperature Measurements

Twenty-three thermocouples were used to measure the temperature at various locations in the test apparatus. All the thermocouples used were made from number 24 gauge duplex iron-constantan wire with fiber glass on asbestos insulation, manufactured by the Leeds and Northrup Company.

The temperature of the bearing inner surface was measured by means of 12 thermocouples arranged in four rows placed 90 degrees apart, as shown in Figure 12, to detect any variation in the axial as well as the circumferential temperature distribution.

To measure the temperature of the journal surface while running, the journal thermocouple leads were laid in grooves in the extension journal shaft, and led through the coupling and the bearing to the collector-ring of a slip-ring and brush arrangement. Figure 19 shows a schematic sketch of the unit.

Coin silver slip-rings were used for their durability, low resistivity and excellent dry friction property. Each ring was press-fitted onto an insulating plexiglas ring which in turn was press-fitted on an aluminum shaft. The shaft was mounted at its ends in two self-aligning ball bearings. Thermocouple wires were soldered to the slip-rings and were brought out to the collector-ring through holes equally spaced around the circumference of the insulating ring as shown in Figure 19.

Two brushes, placed 180 degrees apart, were used per slip-ring to insure constant contact. Silver "Graphalloy" brushes were chosen for their excellent performance from the standpoint of low coefficient of friction.

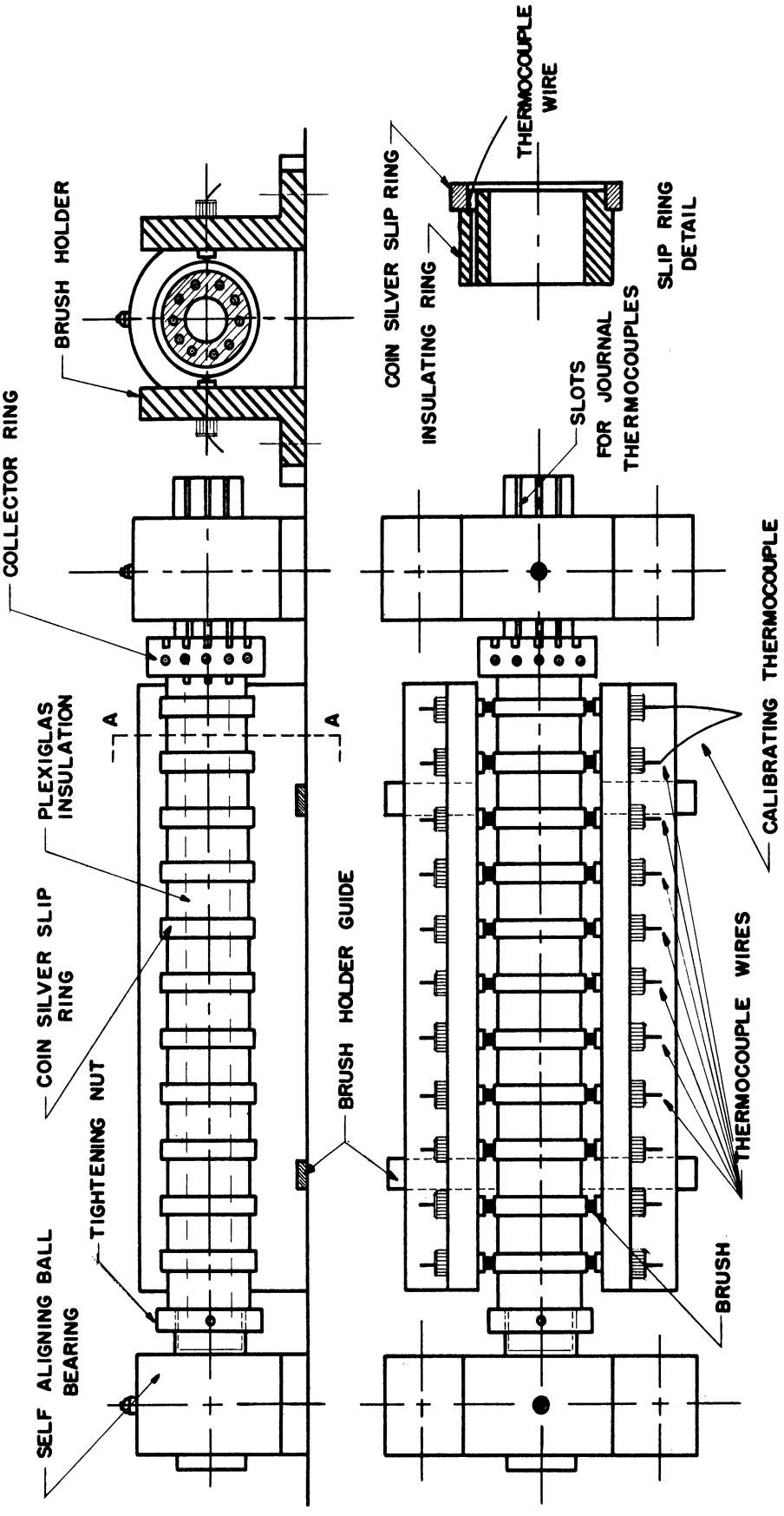

Figure 19. Slip-Ring and Brush Assembly.

Eleven slip-rings were employed, eight of which were used for the journal thermocouple connections. One slip-ring was used to feed the audio oscillator signal to the journal. The remaining two were used for calibrating the system against the extraneous emf generated in the thermocouple circuit due to the frictional heating of the brush and slip-ring at different speeds. This was done by measuring the temperature of the ambient air by means of a thermocouple, connected through the slip-ring and brush arrangement as indicated in Figure 19. The reading was checked against a calibrated thermometer graduated in one-tenth of a degree fahrenheit. The maximum error involved in the thermocouple readings was about .04 millivolt.

The temperature of the inlet oil was measured by a thermocouple inserted in the inlet oil line near the bearing housing. The oil outlet temperature was measured by two thermocouples arranged to contact the oil as it was leaking out as shown in Figure 10.

The temperature of the inlet and outlet cooling water was measured by two thermocouples placed at the inlet and outlet of the cooling jacket respectively.

The temperature of the housing was measured by means of a thermocouple firmly attached to the support four inches from the bearing center.

The leads from the thermocouples were connected to terminal boards from which they were brought to three Leeds and Northrup, 2-pole, 10 position selector switch units. The circuit diagram is shown in Figure 20. This arrangement allowed any thermocouple to be connected into the measuring circuit. The measurement of the thermocouple emf's was made

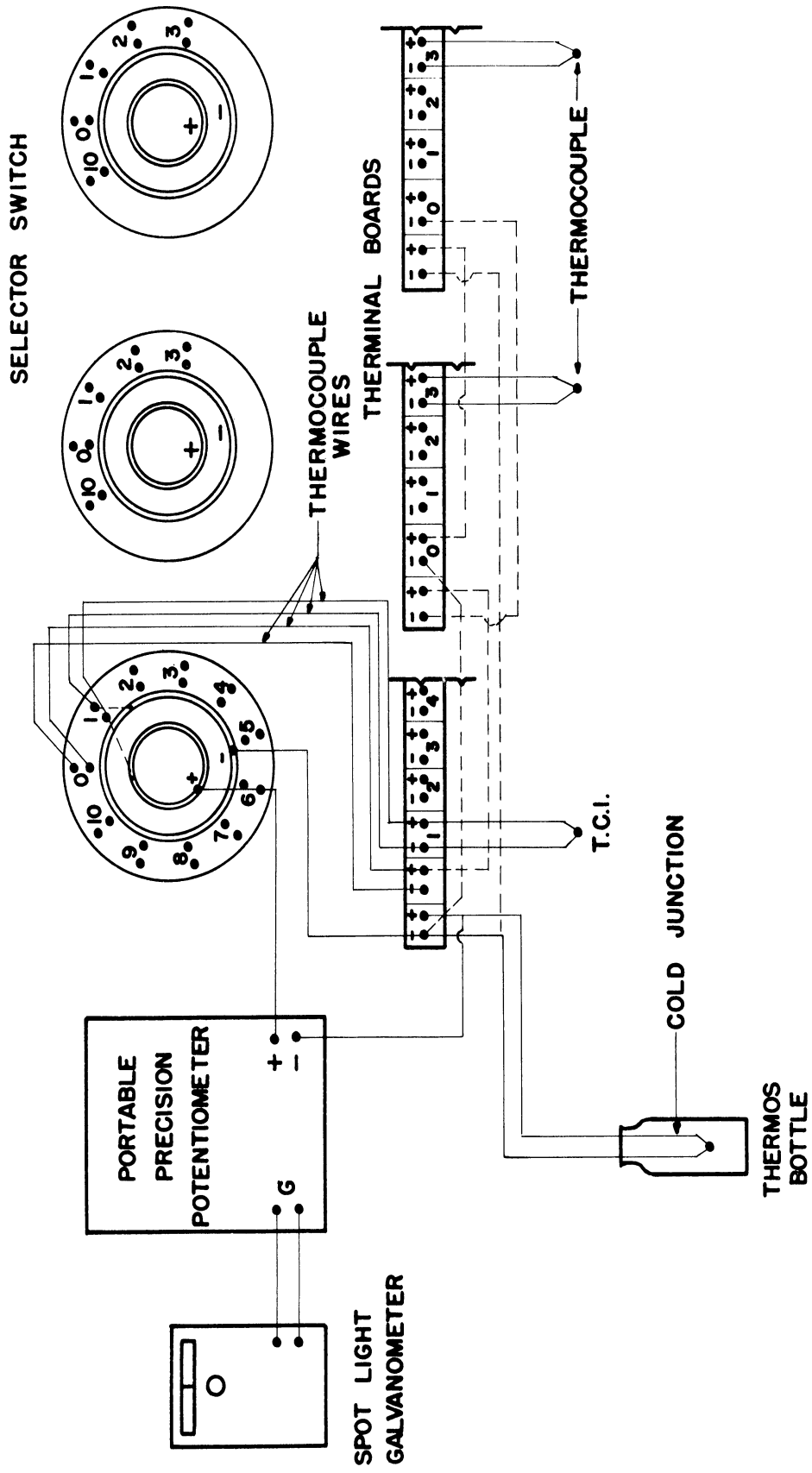

Figure 20. Schematic Diagram of the Temperature Measuring Circuit.

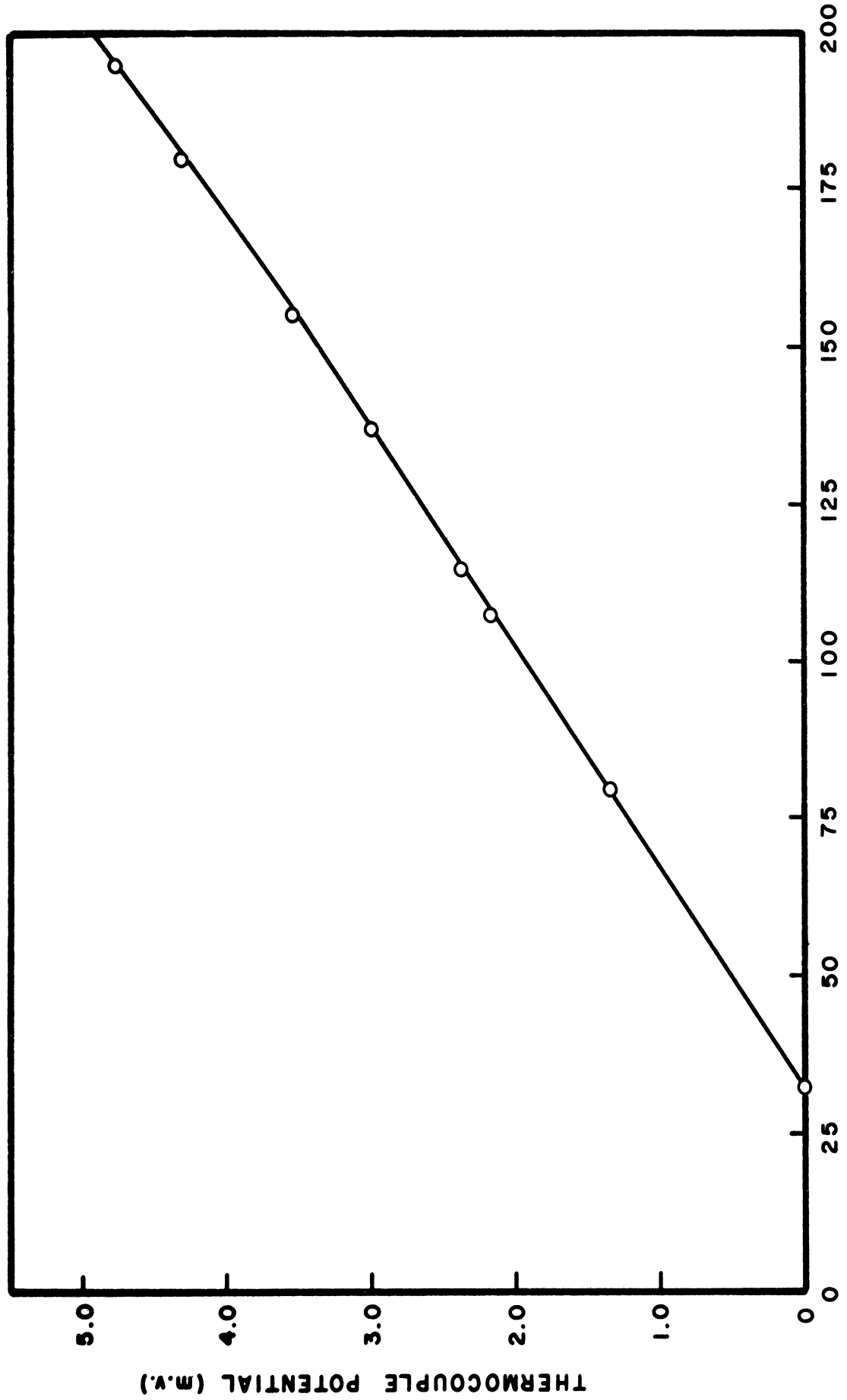

Figure 21. Calibration Curve for Iron-Constantan Thermocouples.

with a manually balanced Leeds and Northrup portable precision potentiometer type 8622, and a spotlight Leeds and Northrup galvanometer as illstrated in Figure 9. The overall sensitivity of the apparatus was estimated about one microvolt.

The melting point of ice was used as the cold junction reference temperature. The cold junction thermocouple was immersed in purified kerosene in a thin glass tube, which was placed six inches deep, side-by-side with a calibrated thermometer in melting ice in a well insulated thermos bottle.

To nullify the effect of introducing dissimilar metals into the circuit, optimum care was taken to keep the temperature measuring equipment at a uniform temperature by placing them in a well insulated cabinet covered from the inside with aluminum lining.

The calibration of the thermocouples were made at the Sohma Laboratory of the Chemical and Metallurgical Engineering Department. The thermocouples were calibrated in a constant temperature both against a thermometer calibrated at the National Bureau of Standards. The thermocouple calibration is shown in Figure 21. It agrees very closely with that given by the Leeds and Northrup Company for their iron-constantan wire.(12)

IV. EXPERIMENTAL PROCEDURE

The procedure used to obtain the data required for determining the effect of speed, load, and external heating on the average oil film temperature and the oil flow rate is described in the following paragraphs. Briefly, three series of experiments were conducted from which the heat convected by the oil flow and the heat dissipated through the bearing and housing could be determined for different combinations of speed and load.

Series A

The external heating was not applied during this series of tests. The heat generated was mainly due to the viscous shear stresses.

Series B

The external heating was applied during this series of tests. The heat generated was due to both the introduction of external heating and that generated due to the viscous shear stresses.

Series C

This series of tests was carried out to check the validity of Petroff's formula. No external heating was applied. The test bearing was running at no load. Cooling water was used to measure the amount of heat conducted through the bearing.

Procedure of Tests

Series A

Before starting the test, the cathode-ray oscilloscope and the audio frequency oscillator were turned on. Oil was then allowed to pass

from the storage tank to the bearing unit by opening valves A and B as shown in Figure 13.

After adjusting the oil inlet pressure to the desired value, the motor was then started with the load completely relieved. This was done by raising the loading levers from the shaft and placing them over the hooks shown in Figure 13.

The speed was then adjusted by means of the speed reducer and checked by a General Radio Strobotac type 631-BL, which has a range of 60 to 14,500 rpm.

To detect the thermal equilibrium condition, the temperature of a thermocouple in the loaded half of the bearing was checked every half-hour until no temperature variation was noticed for two consecutive checks. On the average, the thermal equilibrium was reached in about 5 to 7 hours. This limited the number of runs to one or two runs per day.

After the thermal equilibrium condition was attained, the following data were taken for each run:

1. The ambient temperature.
2. The temperature of the journal.
3. The temperature of the bearing.
4. The temperature of the inlet oil.
5. The temperature of the outlet oil.
6. The temperature of the housing.
7. The oil flow rate.
8. The speed of rotation.

When loading the bearing, the motor was always started at no-load, and the load was then applied. After each loading, the speed was checked and the load was recorded. The same experimental procedure used in the no-loading tests was then followed.

Series B

In all the runs performed in this series the heater was turned on. By means of the variac, the input voltage to the heater was so adjusted that the total wattage, indicated by the wattmeter, was kept constant at 100 watts. The procedure used for this series of tests was similar to that just described for Series A.

Series C

This series of tests was carried out at different constant speeds under no-load condition. Before starting the test, water was allowed to pass through the cooling jacket for about three hours to reach a steady state temperature. It was noticed that the variation in the inlet water temperature during the tests did not exceed 0.2 °F. The motor was then started after following the same experimental procedure adopted in the no-load test series. In addition, the inlet and outlet temperatures of the cooling water and the water flow rate were recorded.

Operating Conditions

For both series of tests A and B, 71 runs were performed. On the average, five different speeds and seven different loads were used for each series of tests. The following ranges and conditions were covered in the experiments:

The speed was varied from 500 to 1500 rpm.

The load applied was varied from 0 up to 3429 lbs.

The inlet oil pressure was kept constant at 1 psig.

The oil used was Gulfpride Motor Oil No. 30.

Its physical properties are given in Appendix B.

The experimental results are given in Appendix F.

V. EXPERIMENTAL RESULTS

This chapter is primarily concerned with the presentation and reduction of the experimental results. Comments and explanations are included wherever necessary, but analysis and discussion are deferred to the next chapter.

The experimental results are presented in a manner which shows the effect of the variables encountered in the investigation on the temperature, oil flow, and correspondingly the heat balance of the test bearing.

Series A

The effect of speed and load on the average oil film temperature is presented in Figures 22 and 23. The average oil film temperature used in this investigation is the average of the journal and bearing thermocouple readings.

In Figure 22, the average oil film temperature is plotted against the calculated eccentricity ratio. The short bearing approximation was adopted for the calculation of the eccentricity ratio. The theory was developed by Michell[14] and Cordullo[8] and was used later by Ocvirk and DuBois[17]. Their extensive experimental work on journal bearing performance was in good agreement with the theory for bearings having ℓ/d ratio up to two.

The effect of speed and load on the circumferential temperature distribution of the oil film is shown in Figures 24 and 25. The temperature, plotted at each of the four positions in these figures, is the

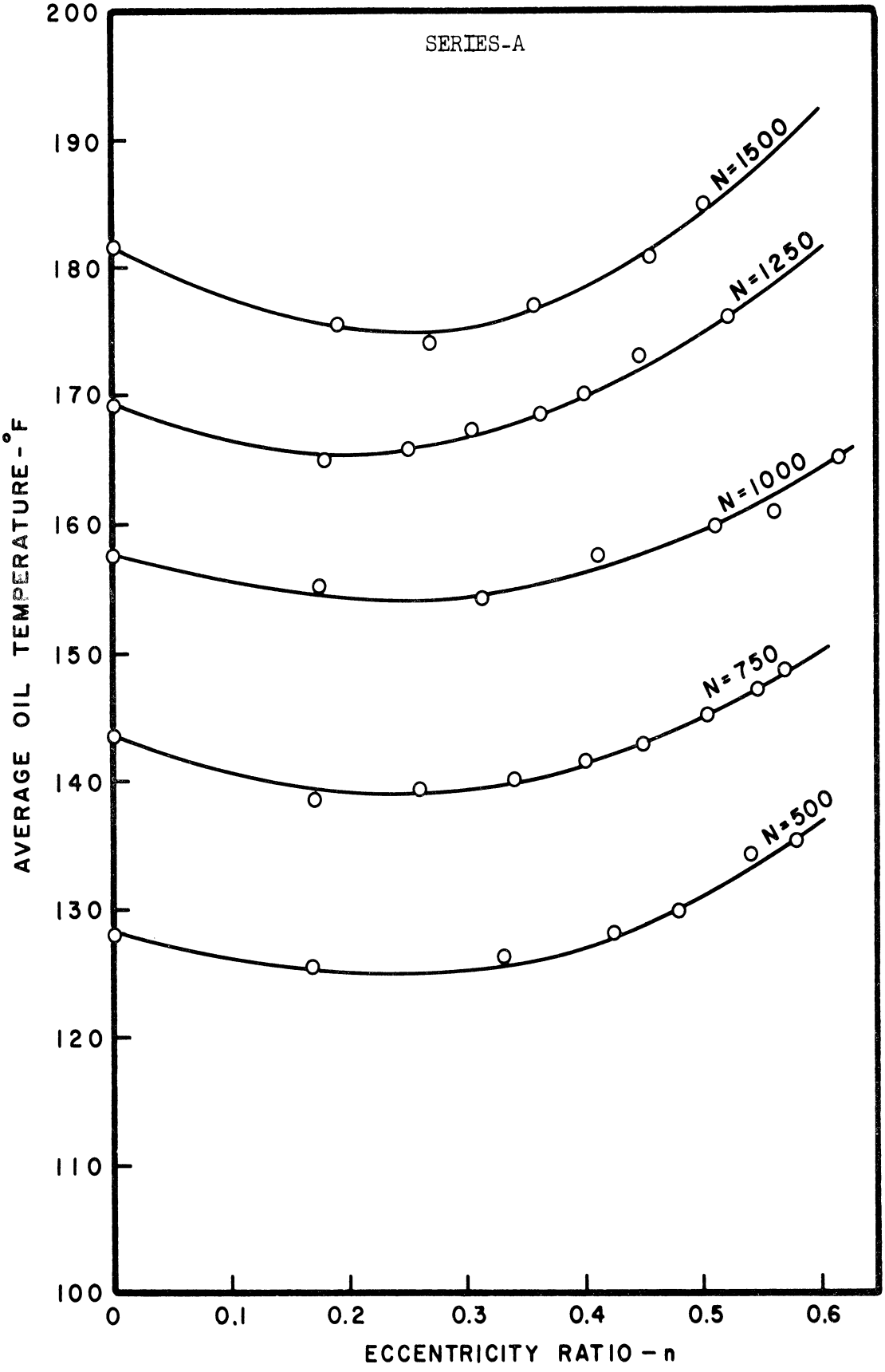

Figure 22. Average Oil Temperature vs. Eccentricity Ratio "n" for Different Speeds.

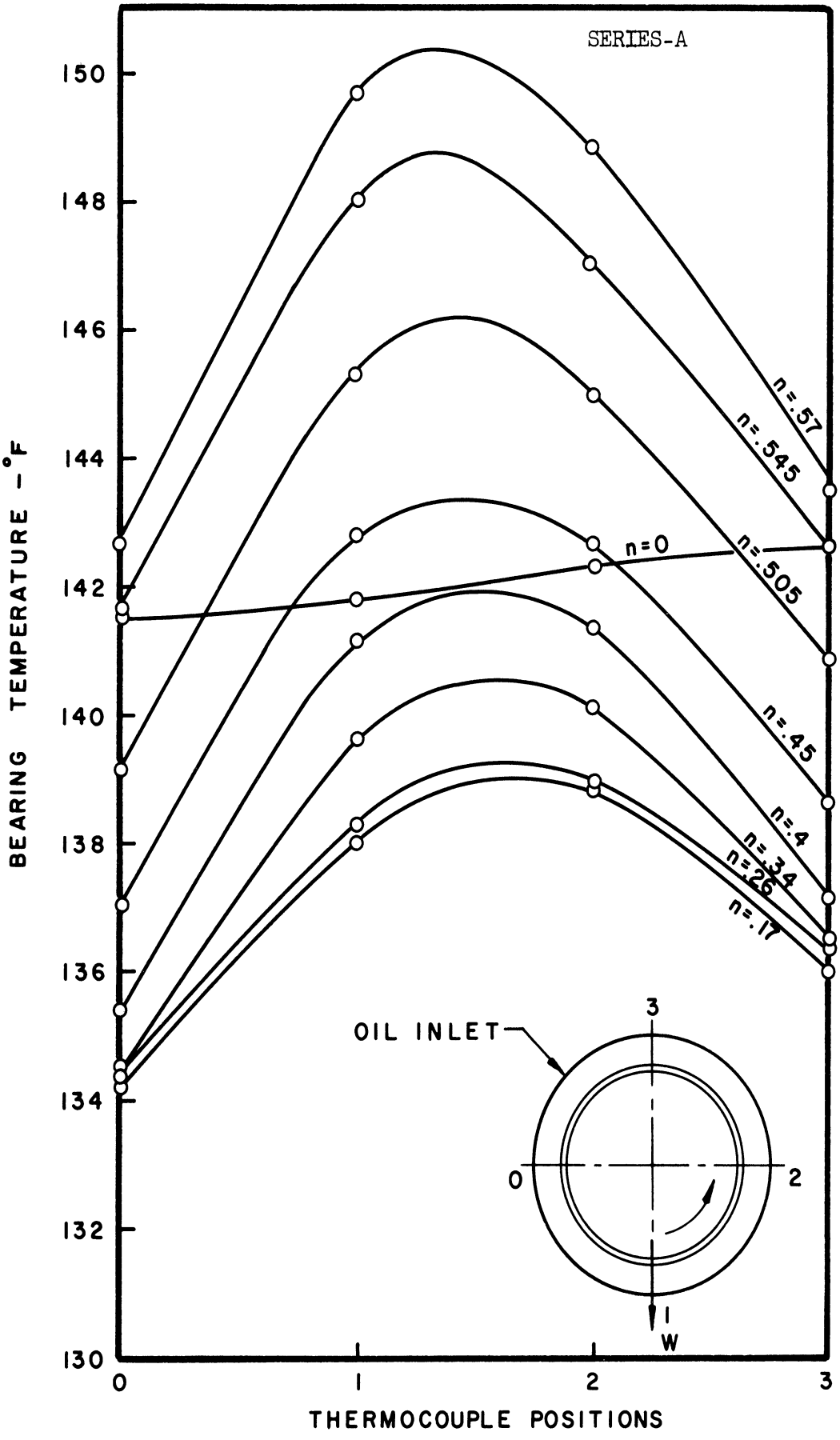

Figure 24. Circumferential Temperature Distribution for Different Eccentricities at 750 rpm.

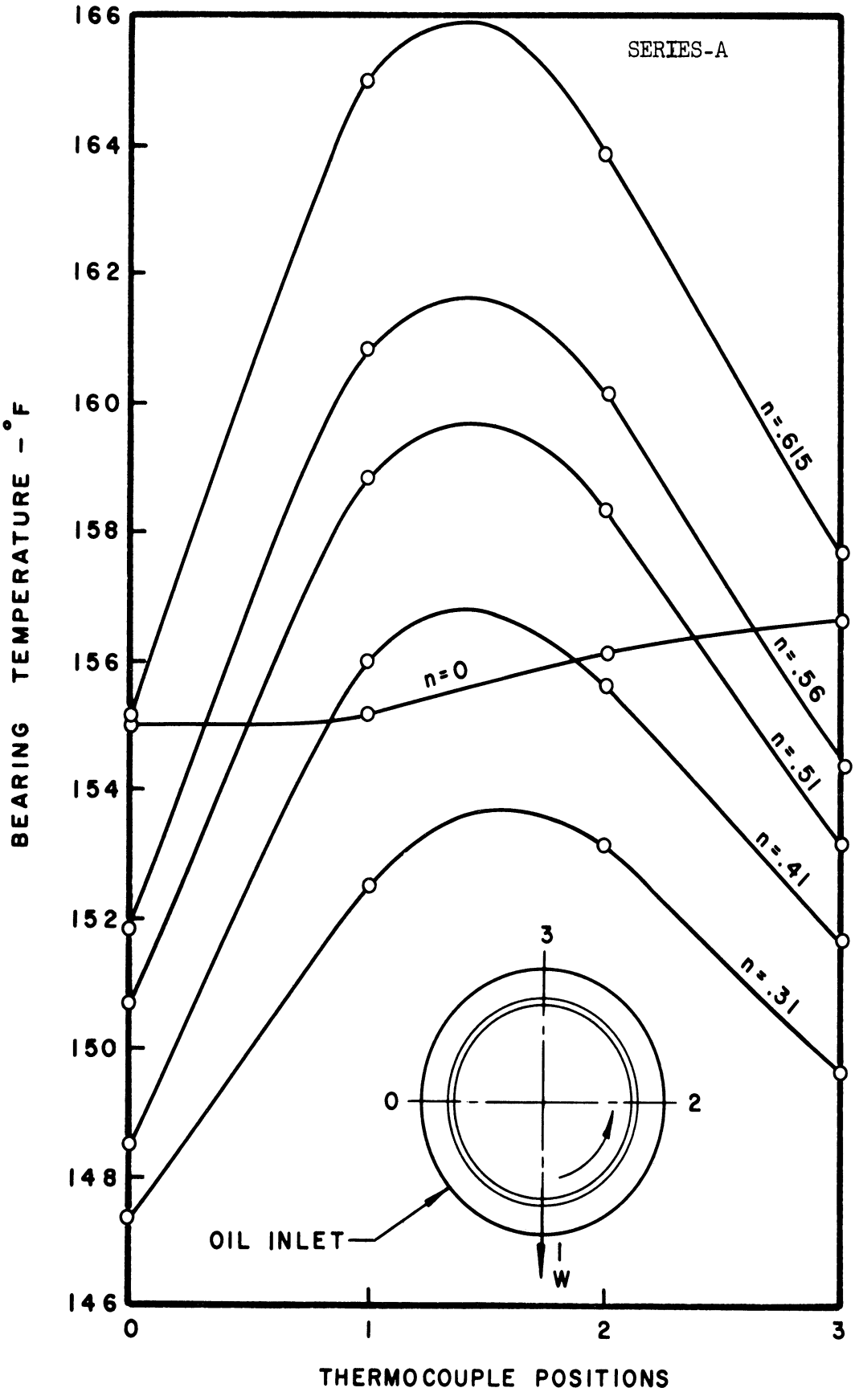

Figure 25. Circumferential Temperature Distribution for Different Eccentricities at 1000 rpm.

average of the axial temperature indicated by three thermocouples placed flush with the bearing inner surface. The load is represented by the eccentricity ratio n. Detailed calculations for the load number and the eccentricity ratio are given in Appendix H, Table V.

The effect of speed and load on the oil flow rate is illustrated in Figures 26, 27, and 28. Figure 26 shows a comparison between the experimental results and the theoretical flow derived by Muskat and Morgan[16] for concentric bearings. In Figure 27 the oil flow rate is given as a function of the calculated eccentricity ratio at different speeds. While in Figure 28 a straight line relationship is correlated when the nondimensional parameter $\frac{\mu Q}{c\,p}\sqrt{\frac{N}{500}}$ is plotted on log paper against the Sommerfeld number S. The equation of the correlating line can be written as:

$$\frac{\mu Q}{c^3 p}\sqrt{\frac{N}{500}} = .375\left[\frac{\mu N'}{p}\left(\frac{d}{cd}\right)^2\right]^{.7679} \qquad (5.1)$$

The method of least square was used in determining the empirical constants. The result of the calculations is given in Table VI.

It is to be noticed that the effect of the change in bearing clearance with temperature was taken into consideration, as the journal and the bearing were of dissimilar metals. The equations derived by Von Gersdorfer[23] were used in calculating the change in clearance. Figure 29 gives the result of the calculations presented in Appendix F. The viscosity of the oil was also considered as a variable. At each load, the viscosity of the oil was determined from the average oil film temperature.

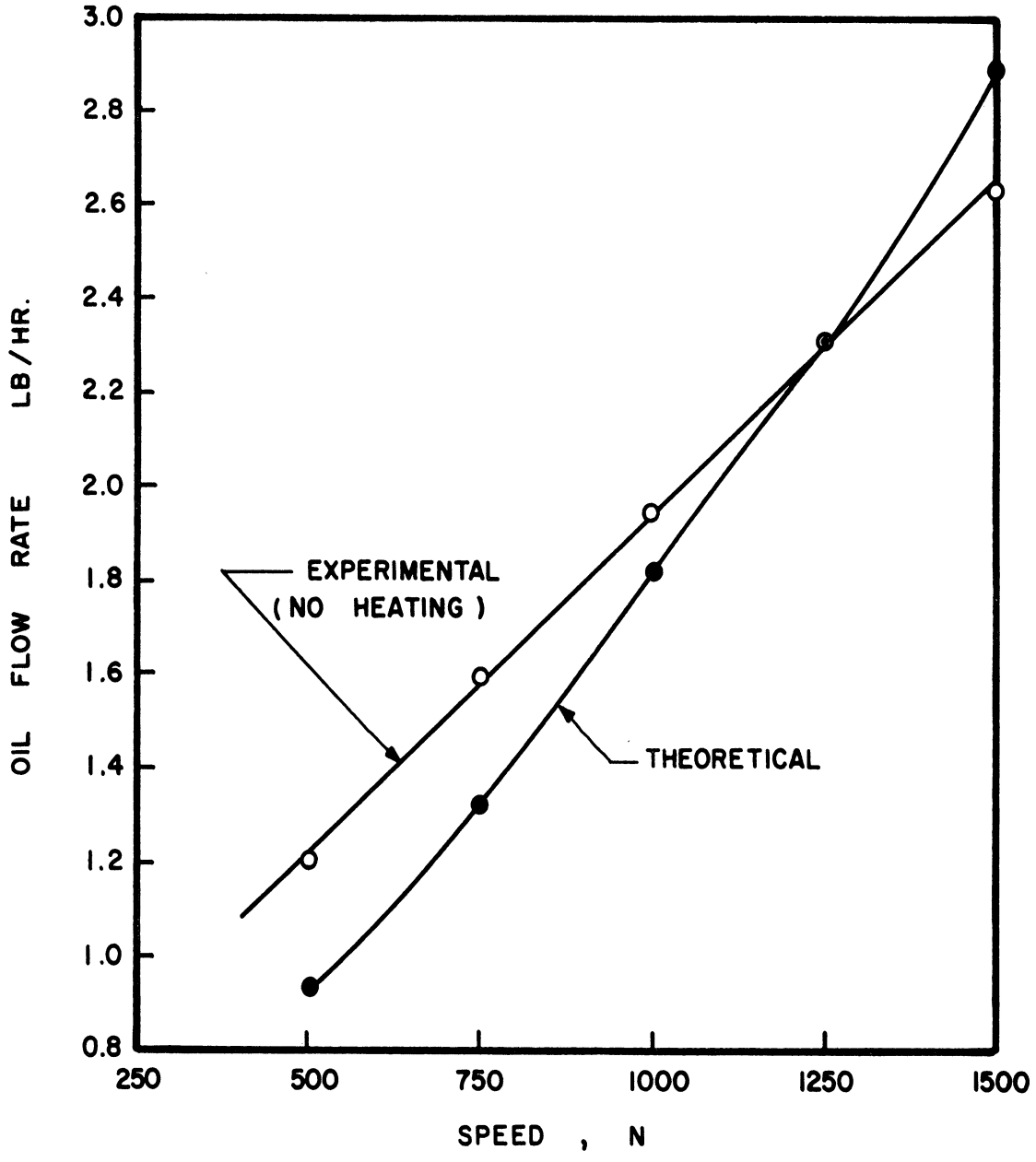

Figure 26. Comparison Between Theoretical and Experimental Oil Flow at No-Load.

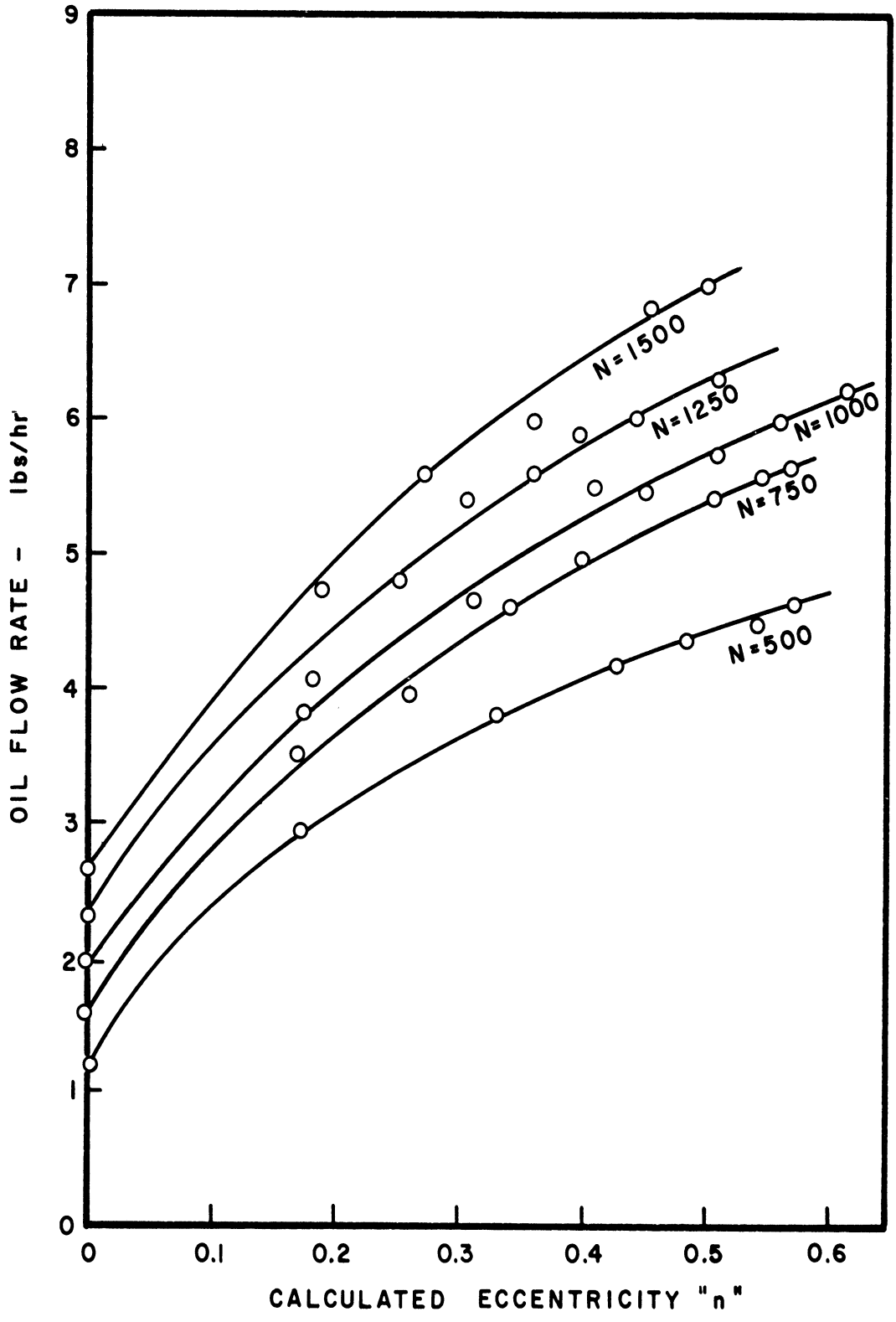

Figure 27. Oil Flow Rate vs. Calculated Eccentricity at Different Speeds.

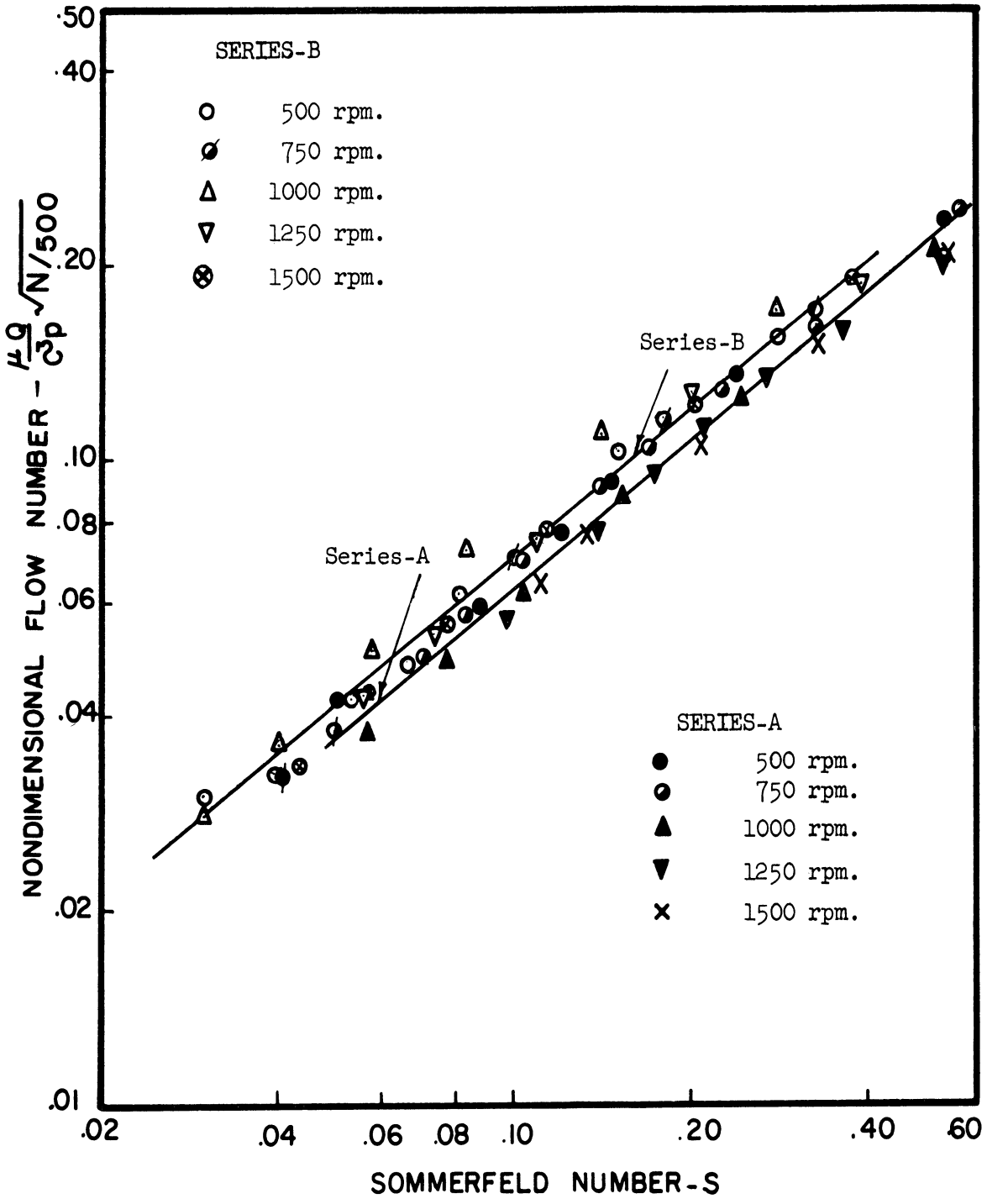

Figure 28. The Nondimensional Flow Number $\frac{\mu Q}{c^3 p}\sqrt{\frac{N}{500}}$ vs. the Sommerfeld Number S.

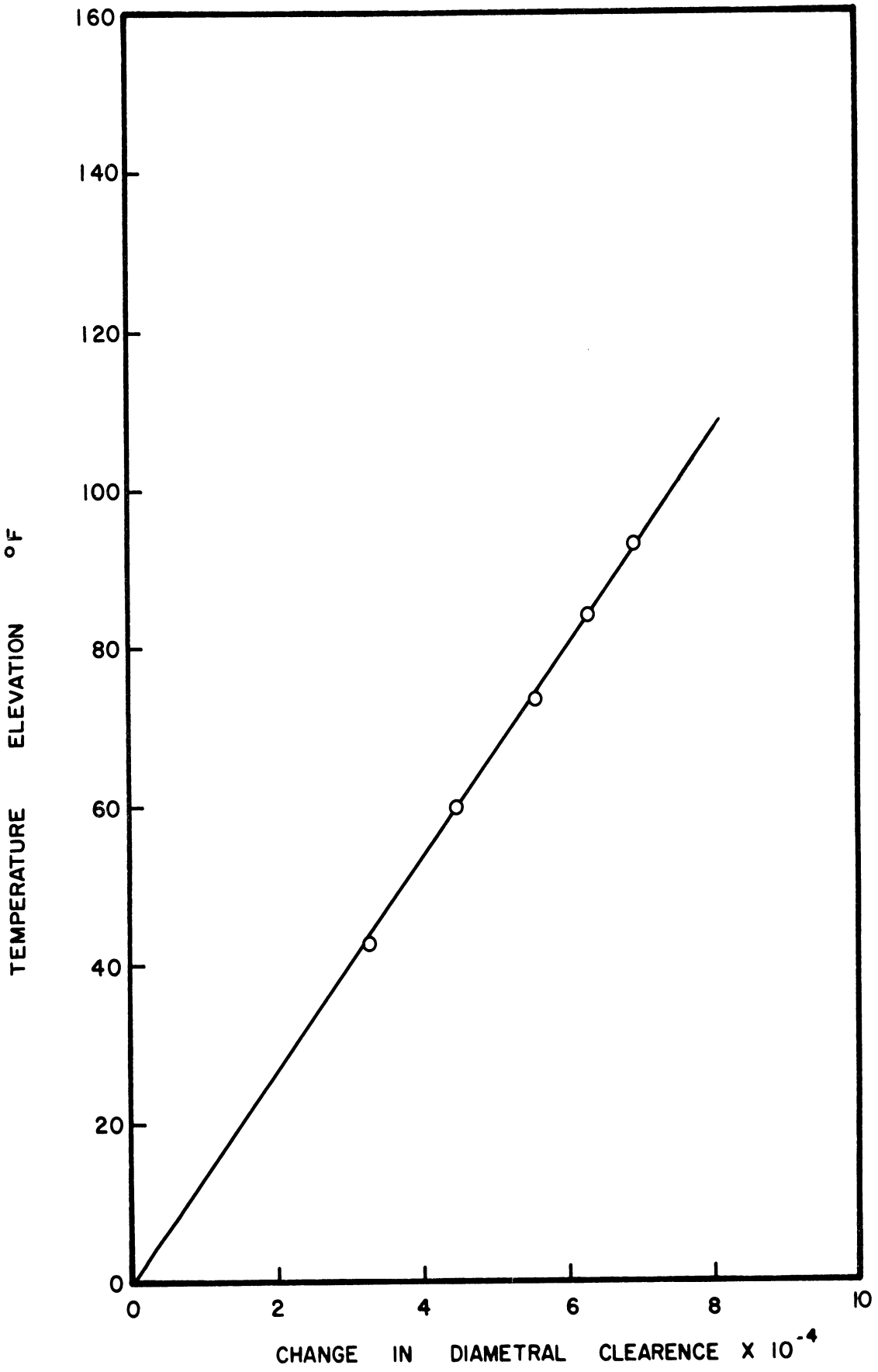

Figure 29. Change in Diametrical Clearance x 10^4 vs. Temperature Elevation - ΔT.

Series B

The combined effect of external heating, speed, and load on the average oil film temperature, circumferential temperature distribution, and oil flow rate is shown in Figures 30 through 33.

Series C

The result of the comparison between the heat generated as calculated by Petroff's formula and the total heat dissipated through the bearing and convected by the oil flow as determined from the experimental data is shown in Figure 34.

Data Reduction for the Heat Balance Analysis

Series A

To determine the heat dissipation characteristics of the bearing and housing, the heat balance Equation (2.26) for the unloaded bearing was used. The heat convected by the oil flow was calculated from the experimental data. The results of the calculations are shown in Table VI. Petroff's formula was used in determining the heat generated.

To determine the empirical constants a and m, the temperature elevation ΔT is plotted against $H_J - H_O$ on log paper as shown in Figure 35. It is noticed that all the data points are well correlated by a single straight line. The method of least square was used in fitting the line and determining the constants a and m. The correlating equation is found to be of the form:

$$H_J - H_O = H_c = 3.26\ (\Delta T)^{1.43} \qquad (5.2)$$

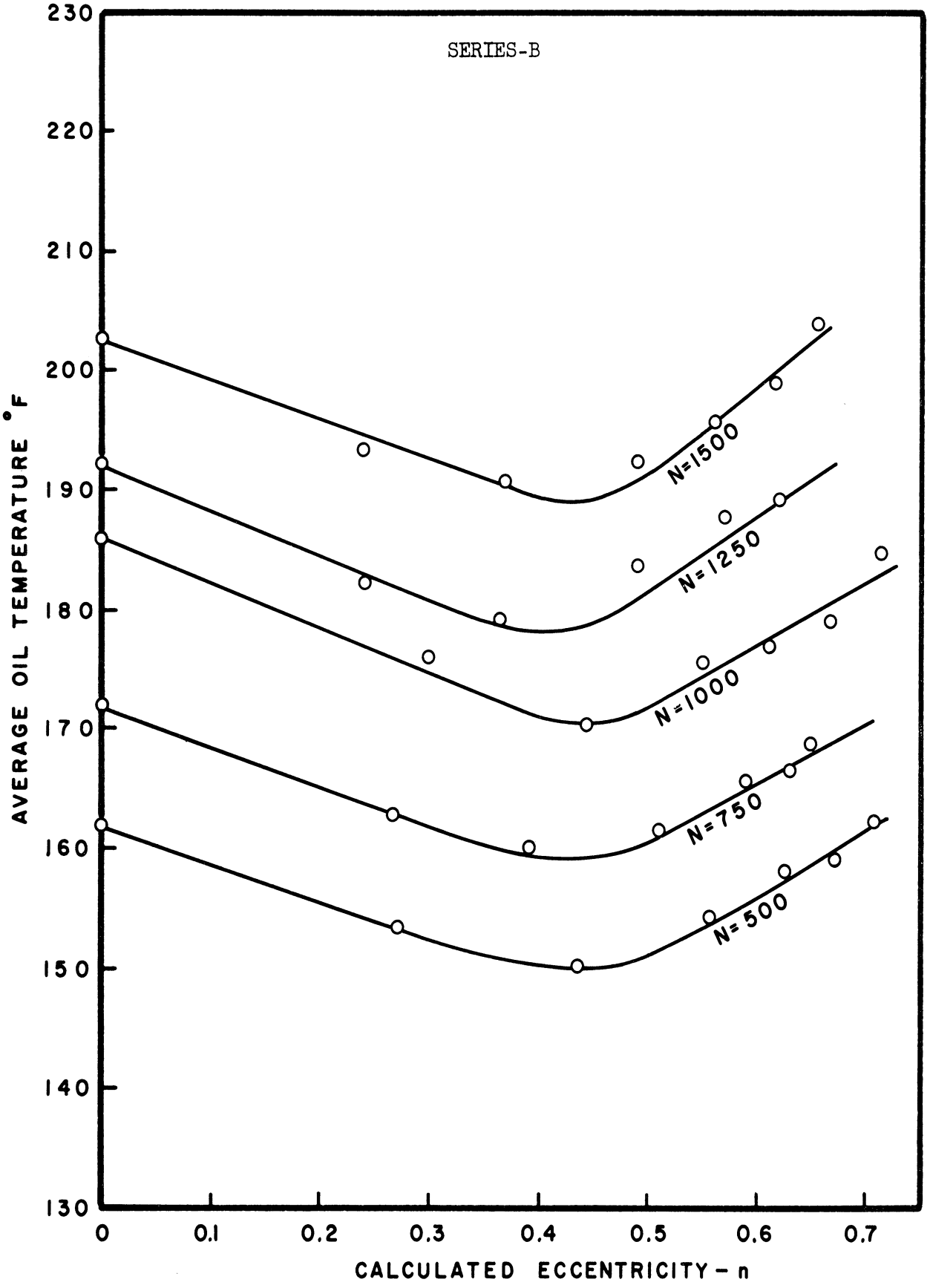

Figure 30. Average Oil Film Temperature vs. Calculated Eccentricity at Different Speeds.

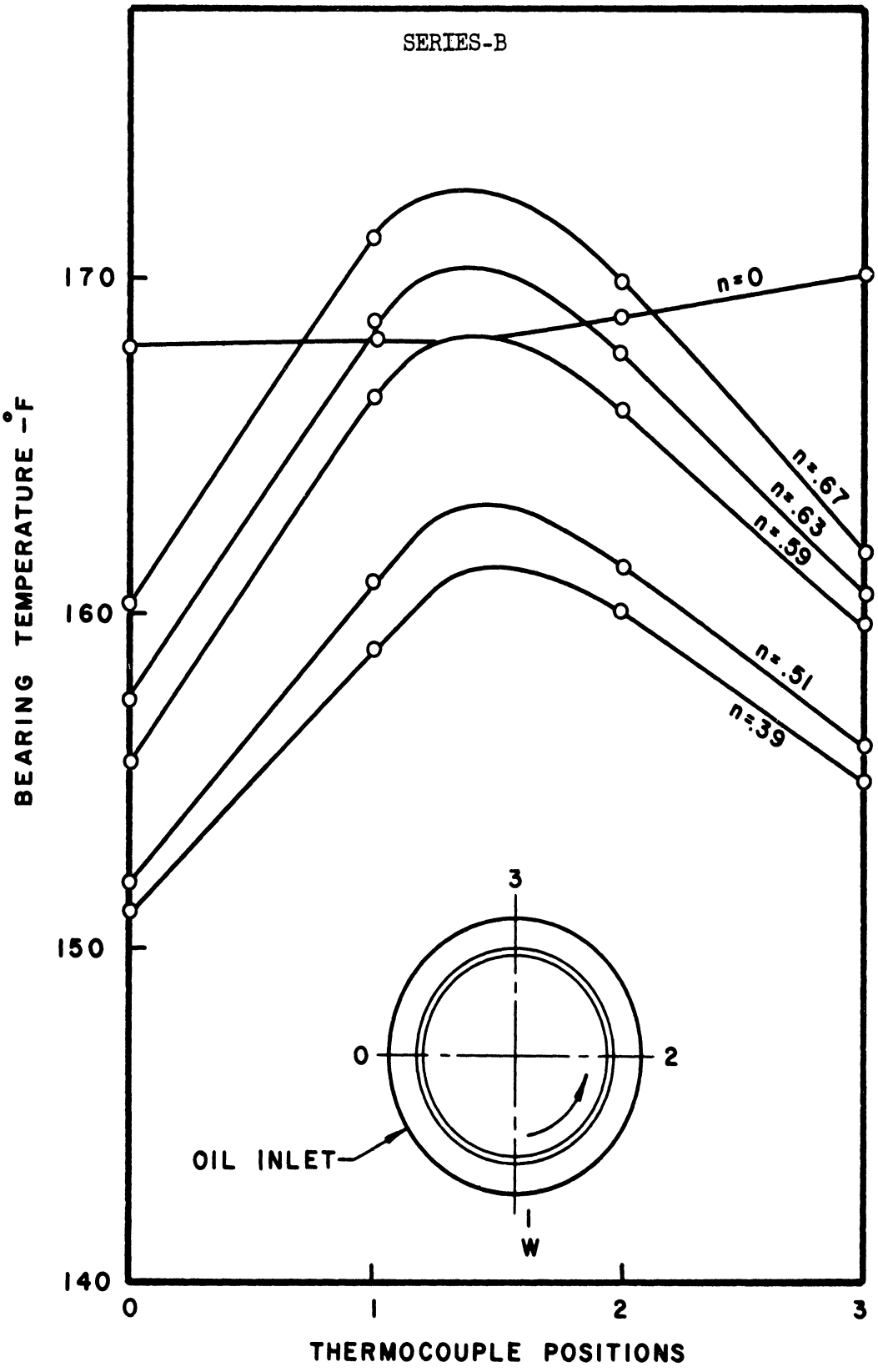

Figure 31. Circumferential Temperature Distribution for Different Eccentricities at 750 rpm.

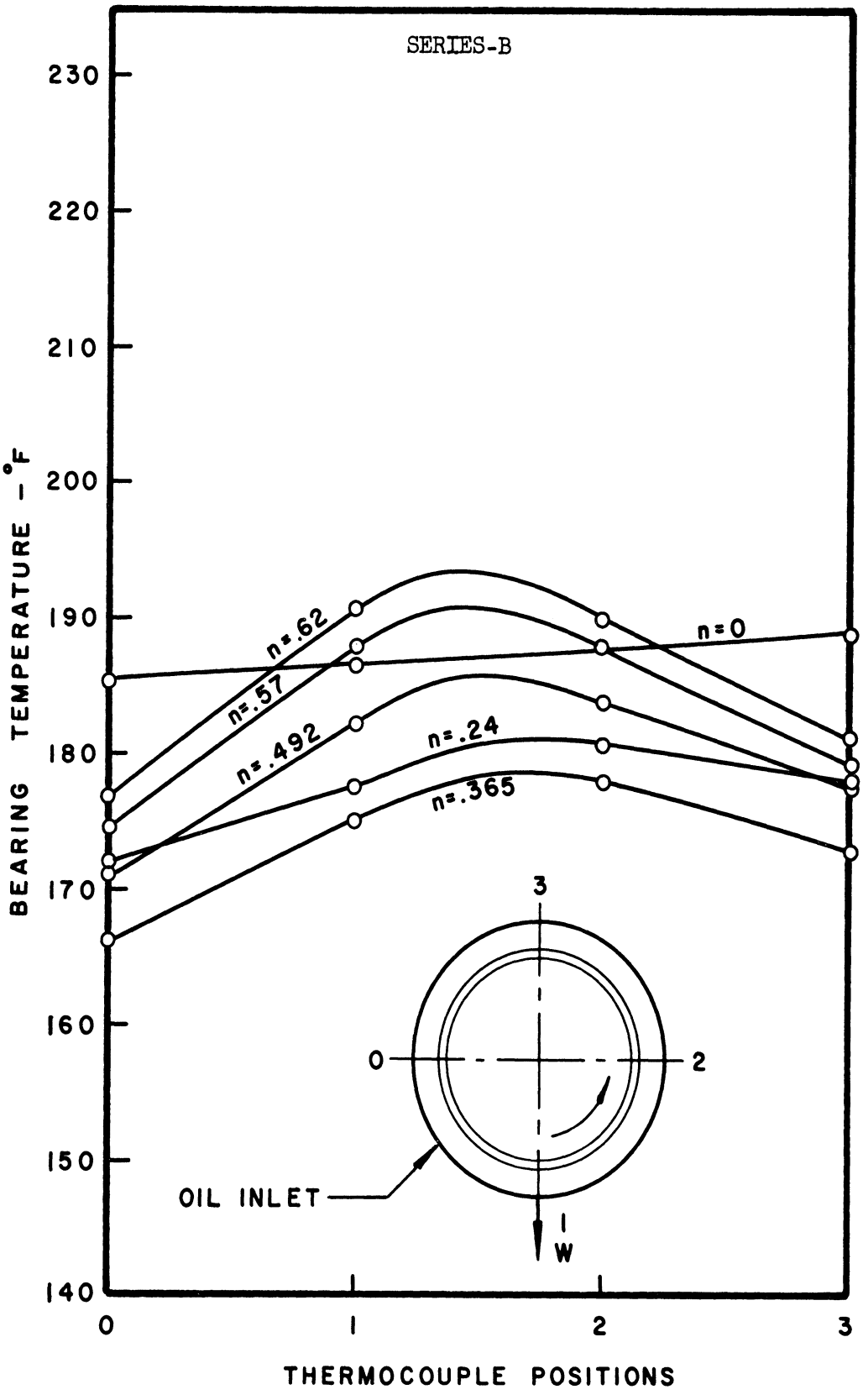

Figure 32. Circumferential Temperature Distribution for Different Eccentricities at 1250 rpm.

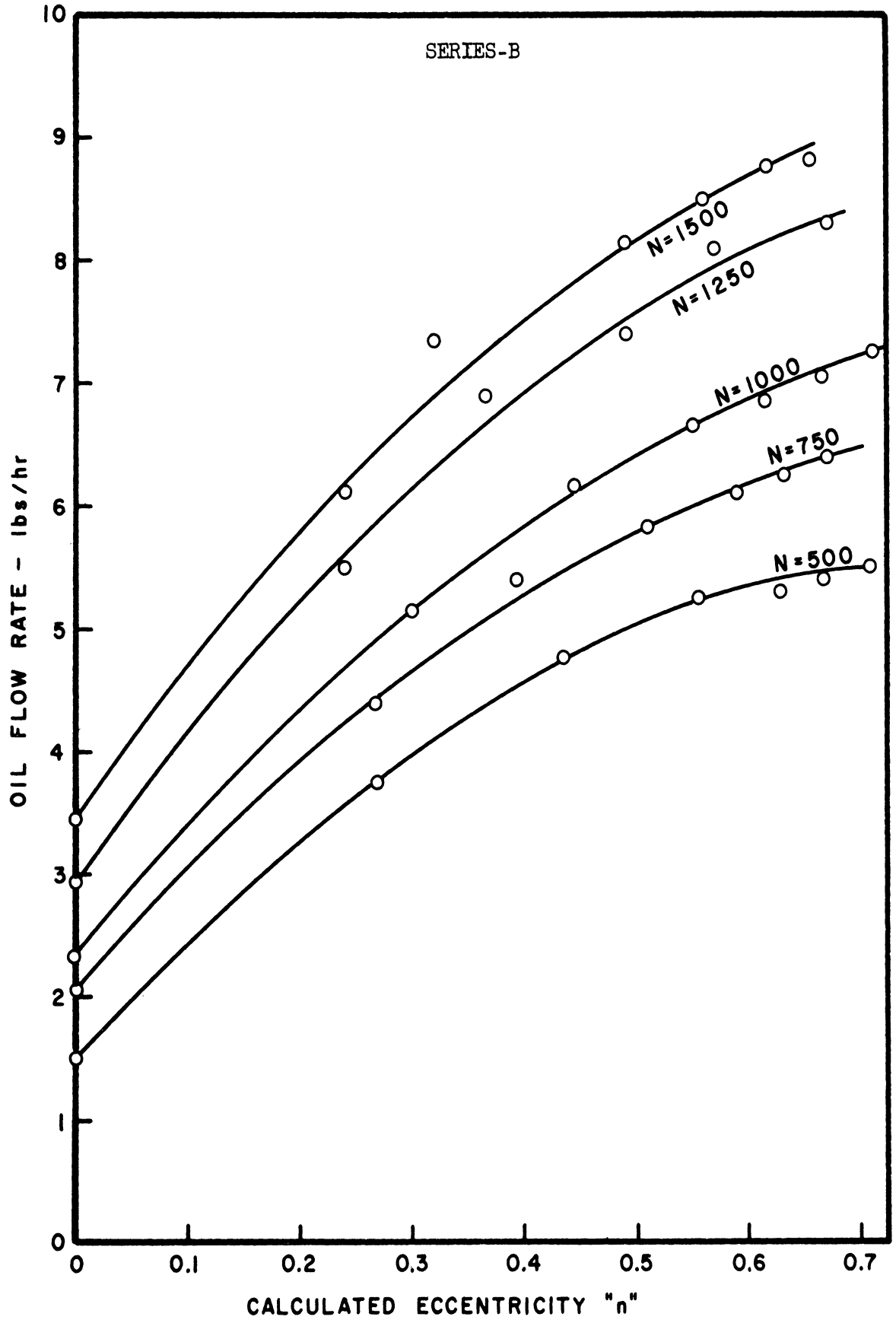

Figure 33. Oil Flow Rate vs. Calculated Eccentricity-n at Different Speeds-N.

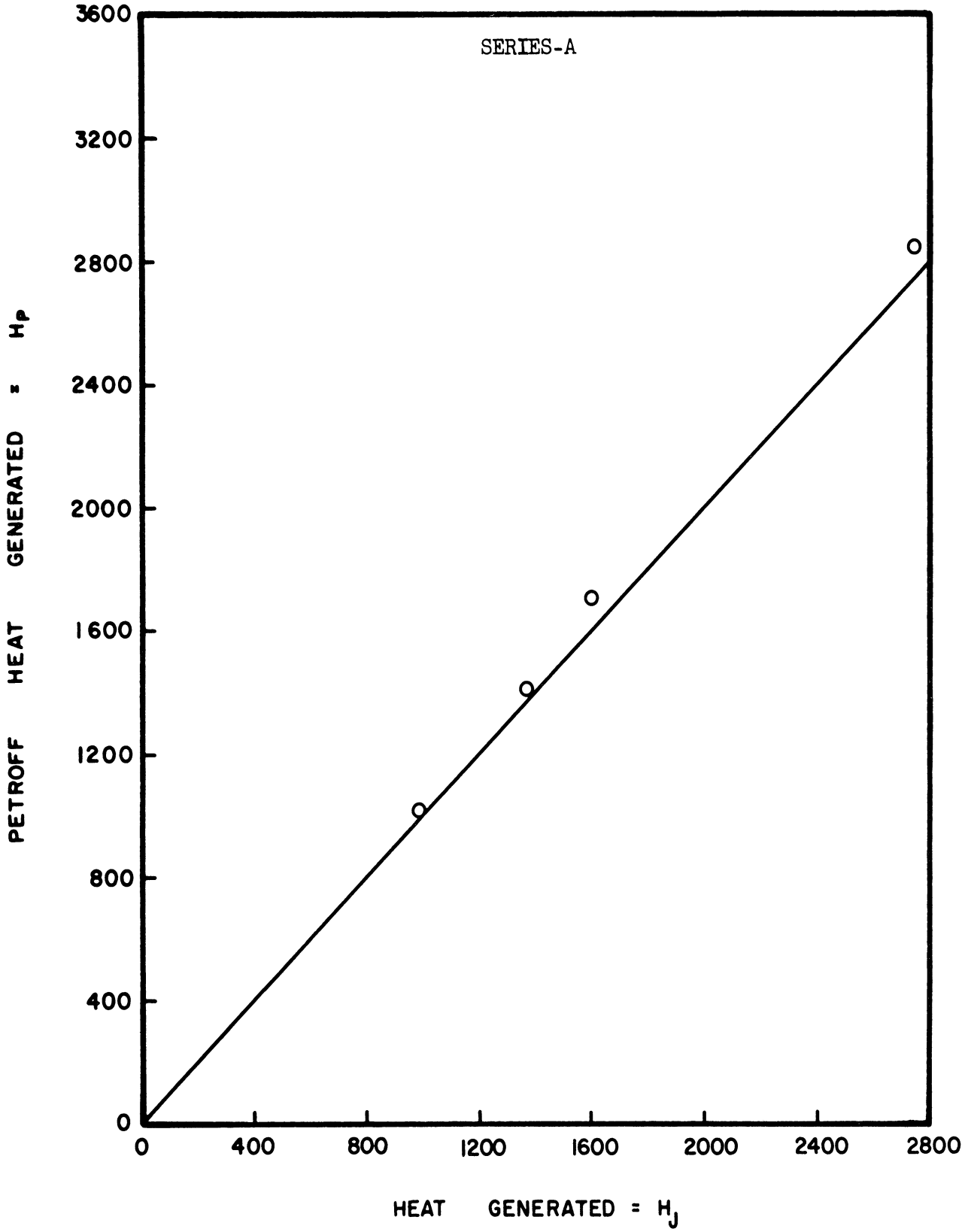

Figure 34. Heat Generated H_J vs. Petroff Heat Generated.

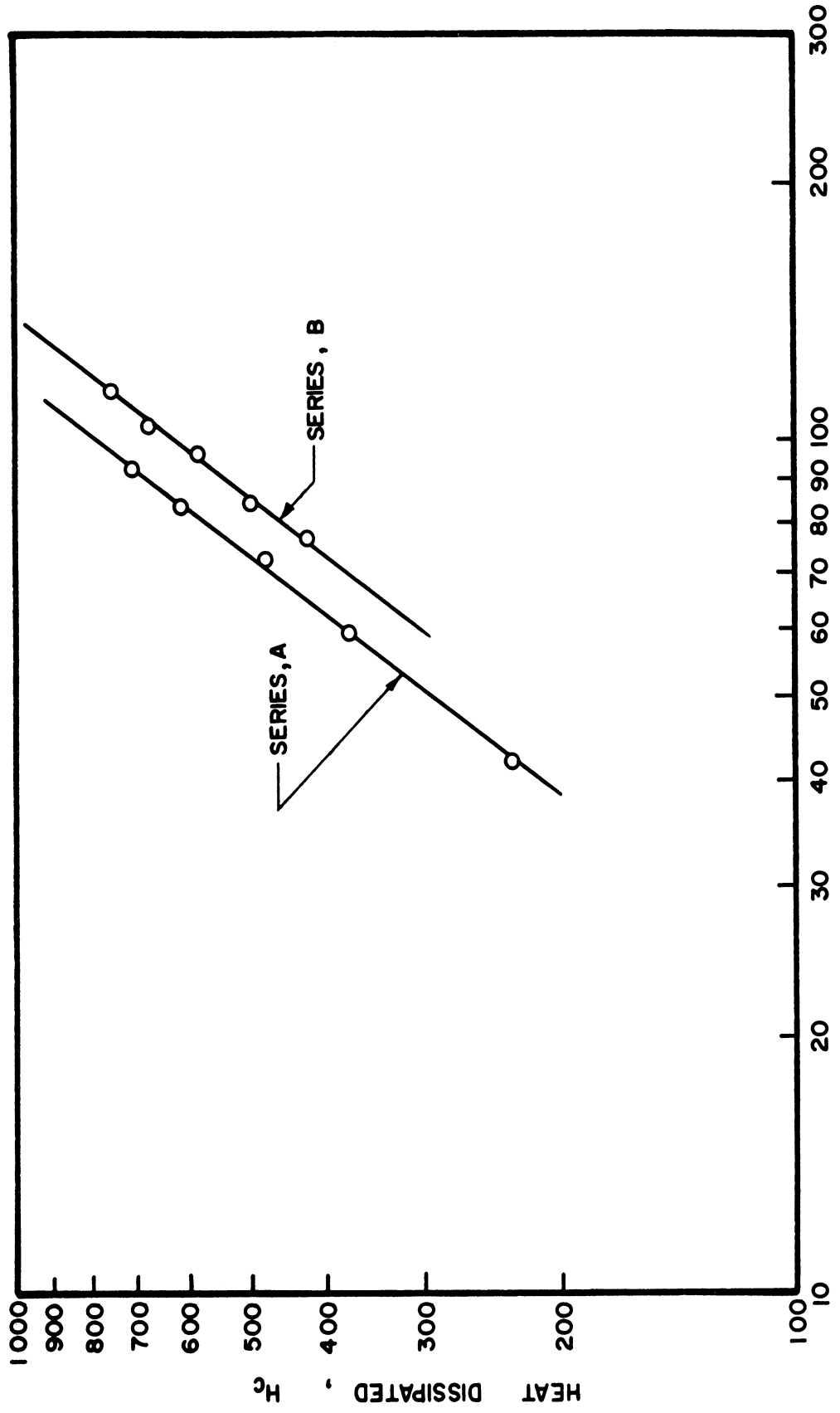

Figure 35. Heat Dissipated H_C vs. Temperature Elevation ΔT.

The effect of speed and load on the heat convected by the oil flow is indicated in Figures 36 through 38. In Figure 36, the heat convected by oil flow is plotted against the calculated eccentricity ratio n. The data are reduced to a single curve when the nondimensional heat convection parameter H_o/H_p is described as a function of the load number 1/S as shown in Figure 37. Plotting the same parameters on log paper in Figure 38, yields a straight line relationship. The correlating equation can be expressed as follows:

$$H_o/H_p = .1845\ (1/S)^{.2146} \qquad (5.3)$$

The effect of speed and load on the heat dissipated through the bearing and housing is presented in Figures 39 and 40. Figure 39 shows the heat dissipated H_c as a function of the load number 1/S at different speeds. The heat dissipated H_c was determined by the use of the empirical Equation (5.2) which is presented graphically in Figure 35. The data shown in Figure 39 are reduced to a single curve, when the nondimensional heat ratio H_c/H_p is plotted, instead of H_c, against the load number 1/S as illustrated in Figure 40.

A comparison, between the analytical heat generation ratio H_J/H_p and the total heat dissipation ratio $(H_c + H_o)/H_p$, is given in Figure 41. Equation (2.21) was used in calculating H_J/H_p. The total heat dissipation ratio $(H_c + H_o)/H_p$ was obtained by the addition of the smoothed data of H_o/H_p and H_c/H_p, presented in Figures 37 and 40 respectively.

Series B

The heat dissipation characteristics were determined using Equation (2.27). When the heat dissipated H_c was plotted against the

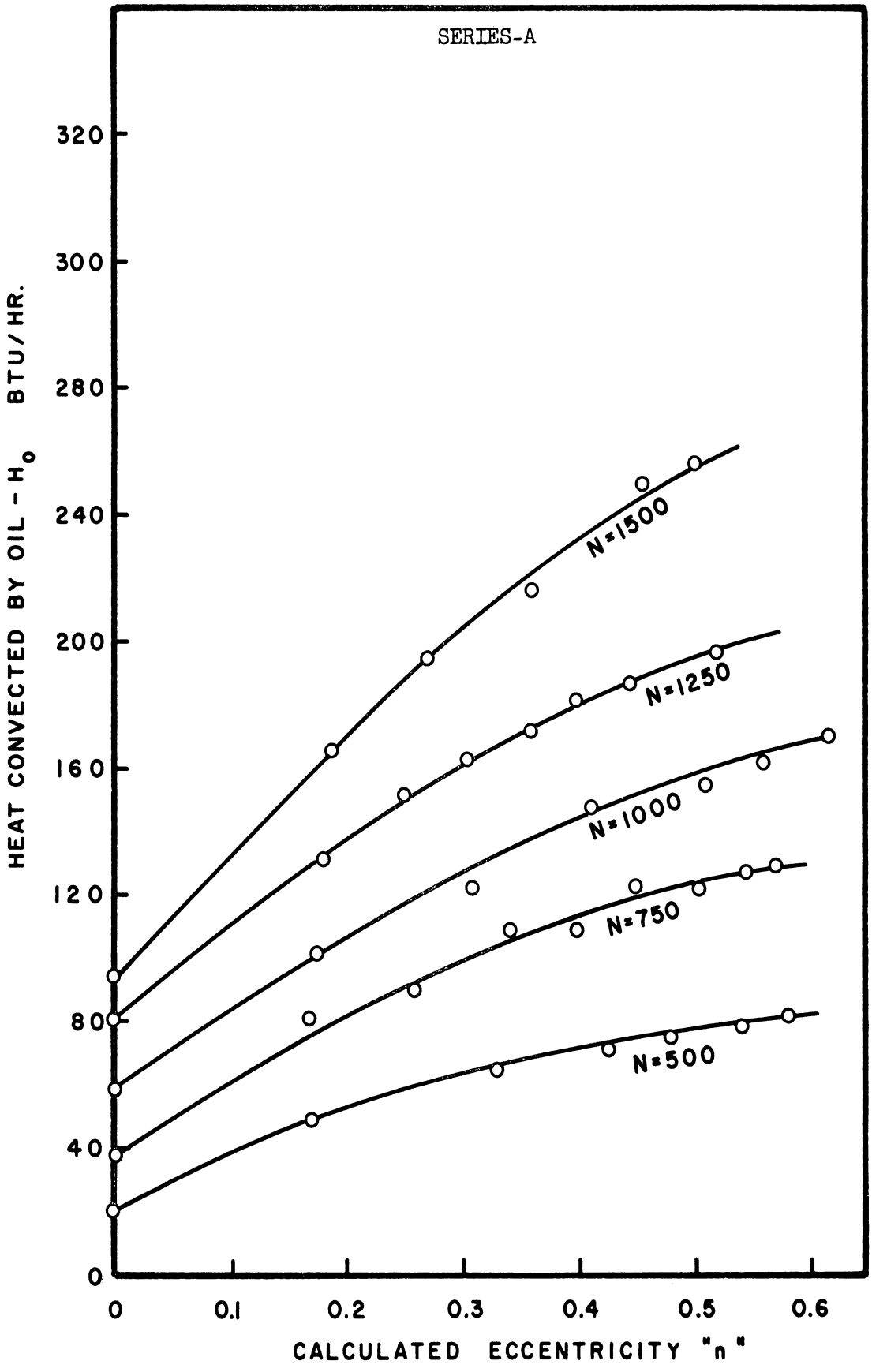

Figure 36. Heat Convected by Oil vs. Calculated Eccentricity at Different Speeds.

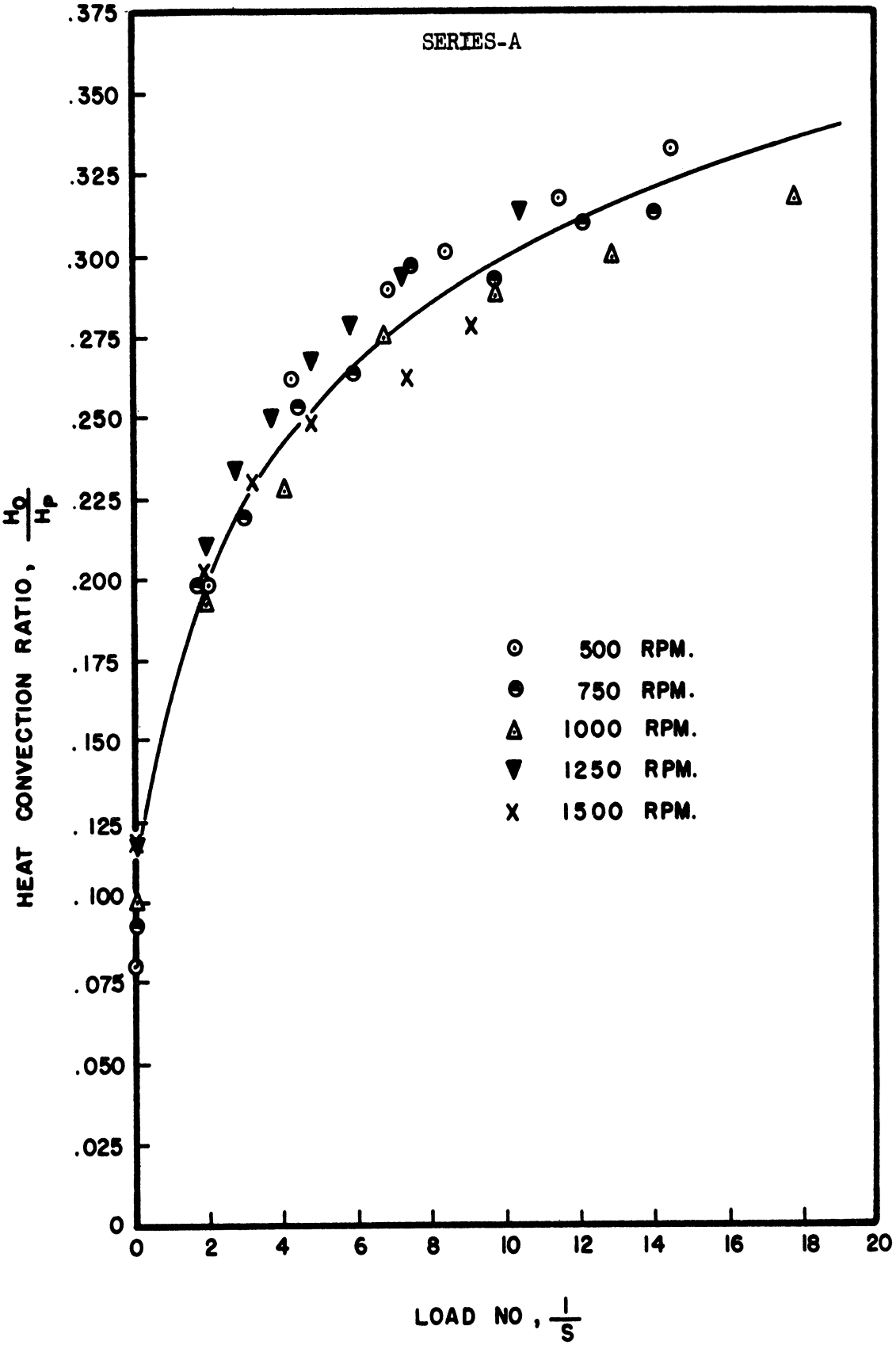

Figure 37. Nondimensional Heat Convection Ratio H_o/H_p vs. Load Number 1/S.

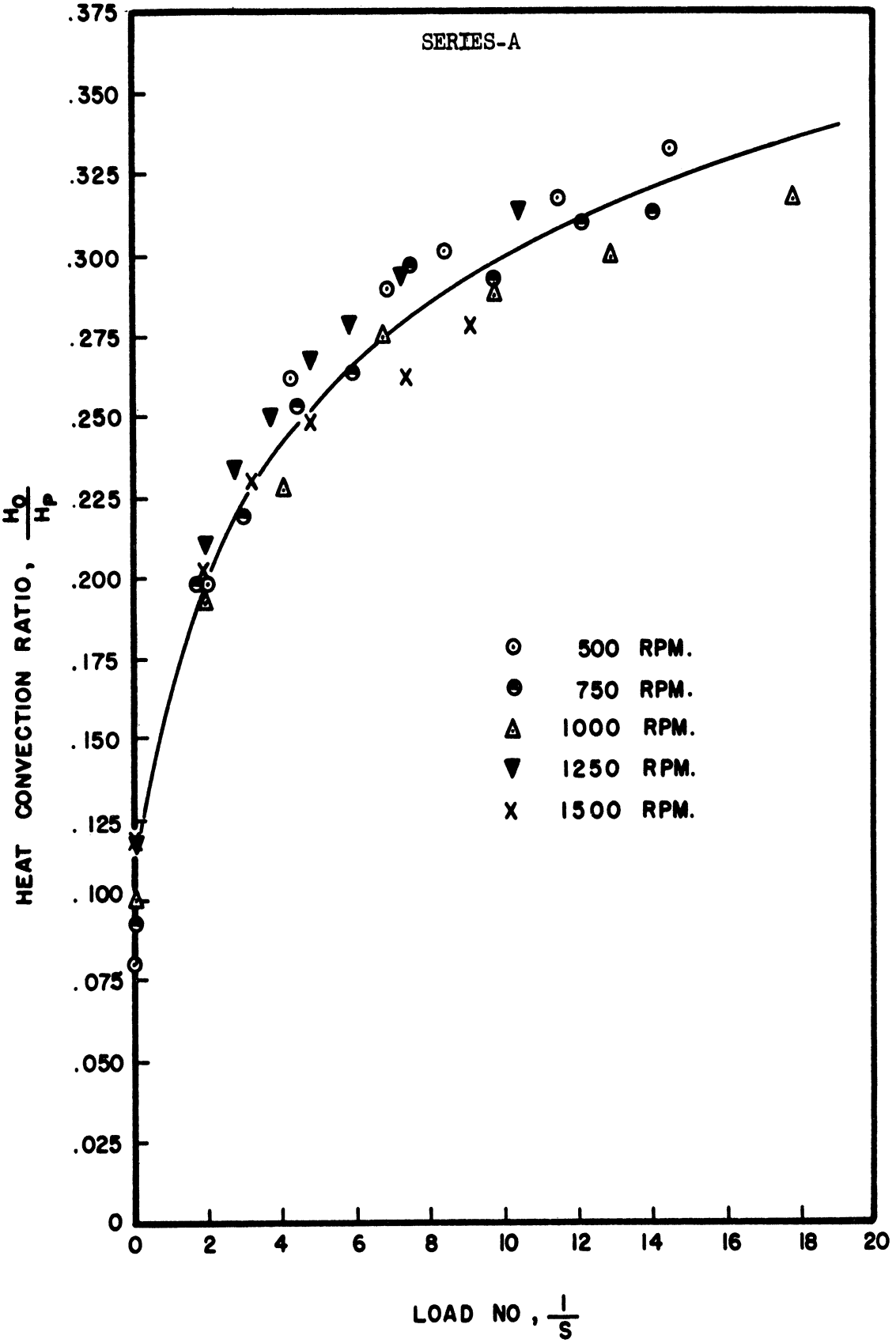

Figure 37. Nondimensional Heat Convection Ratio H_o/H_p vs. Load Number 1/S.

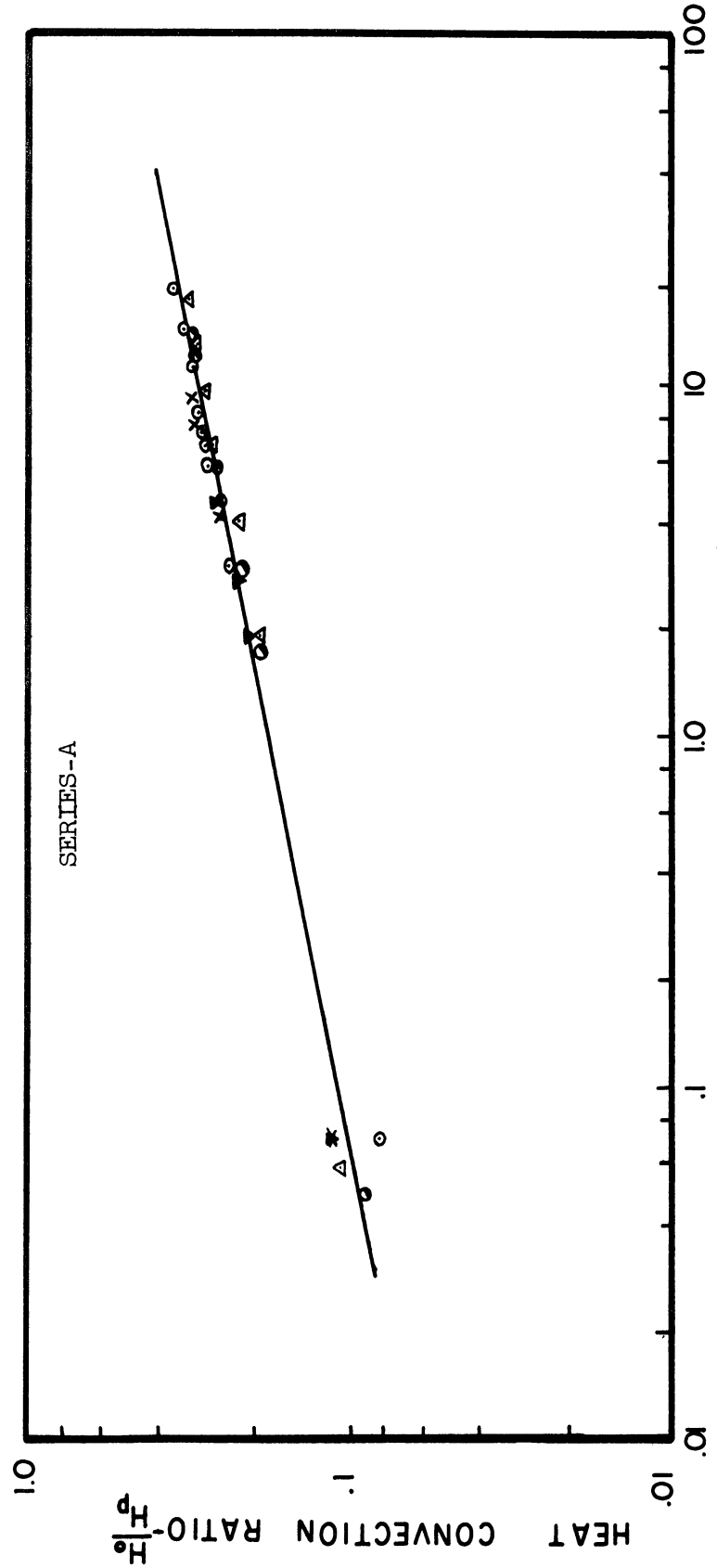

Figure 38. Nondimensional Heat Convection H_o/H_p vs. Load Number 1/S.

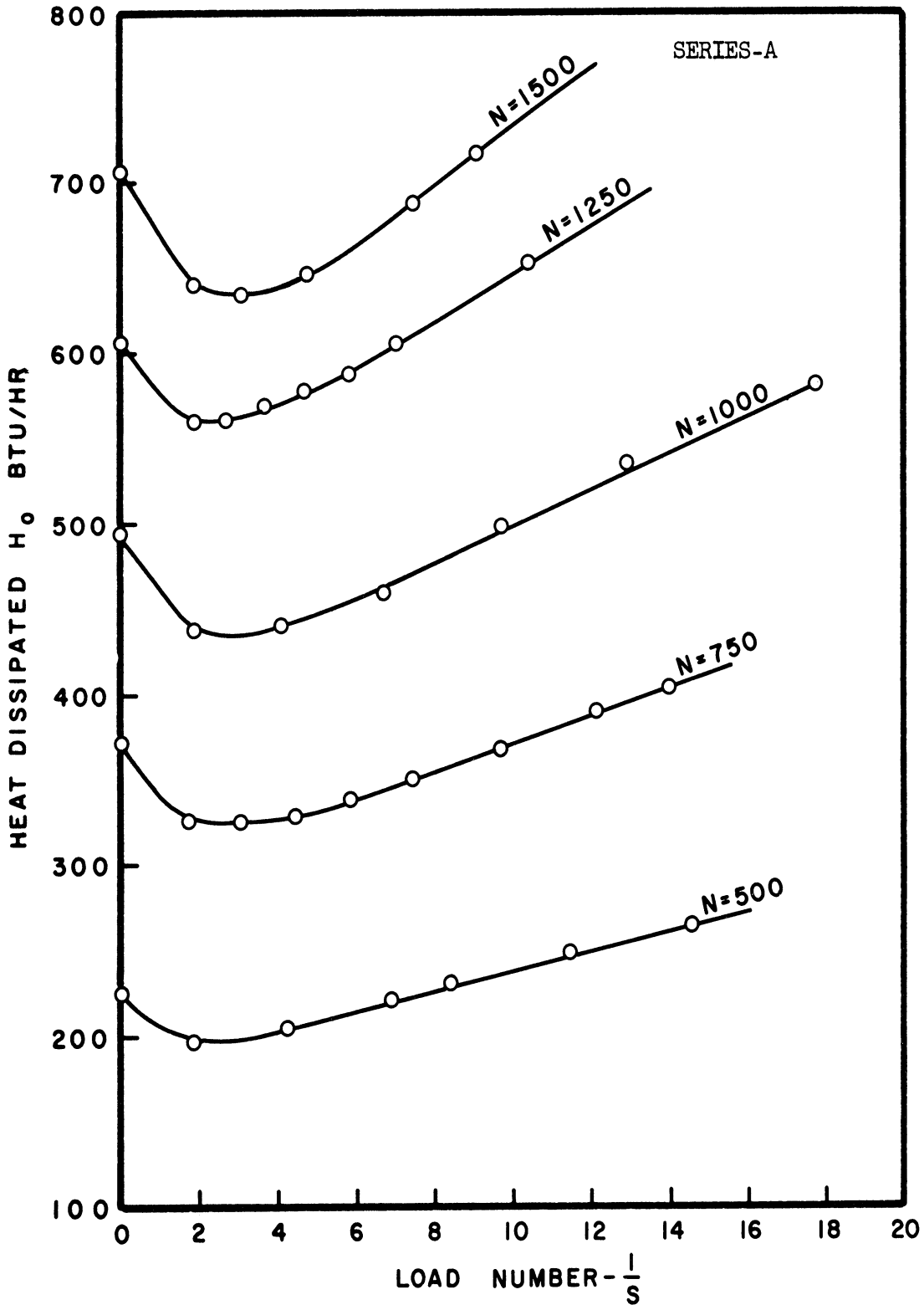

Figure 39. Heat Dissipated H_o vs. Load Number 1/S.

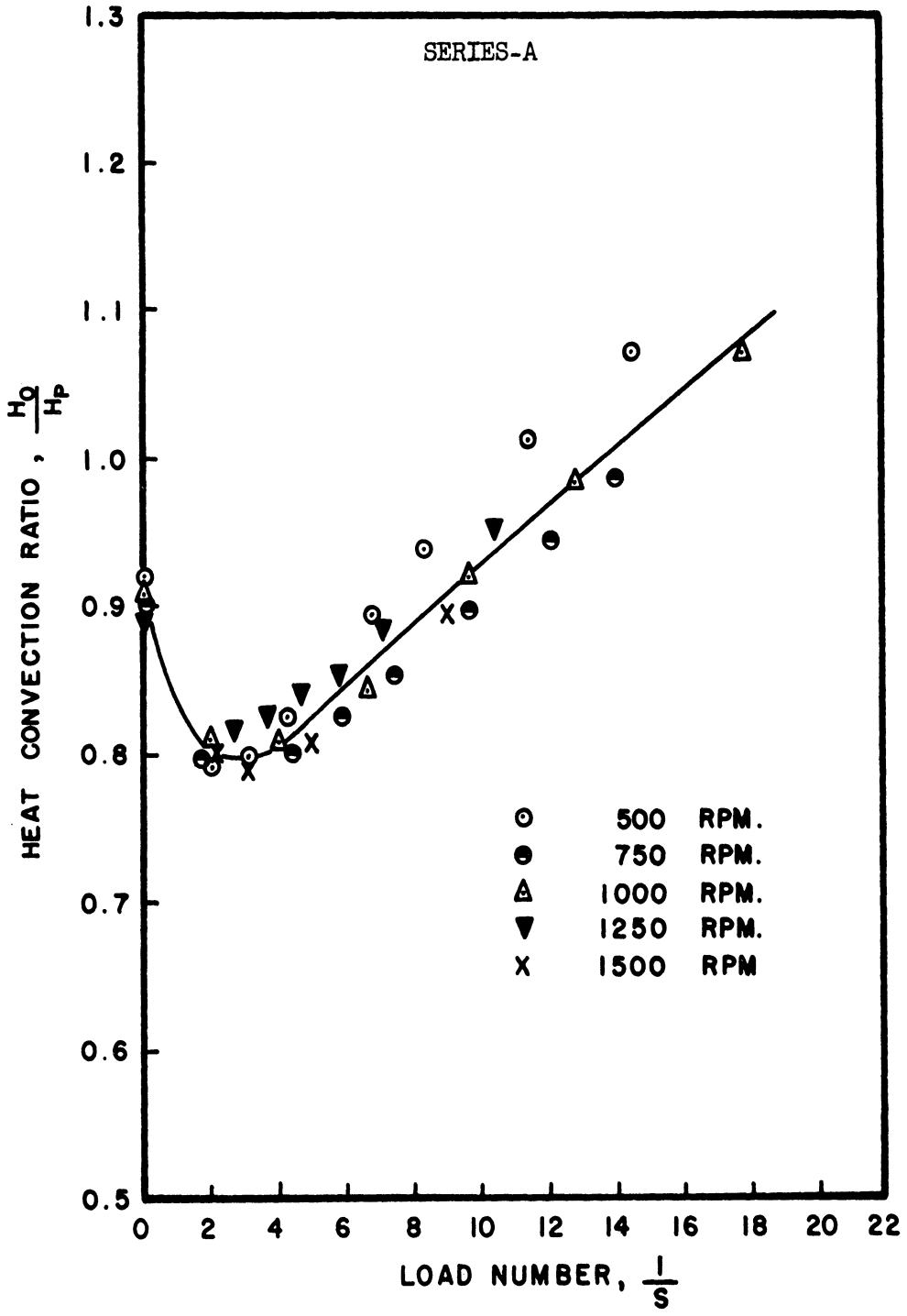

Figure 40. The Heat Dissipation Ratio H_c/H_p vs. Load Number 1/S.

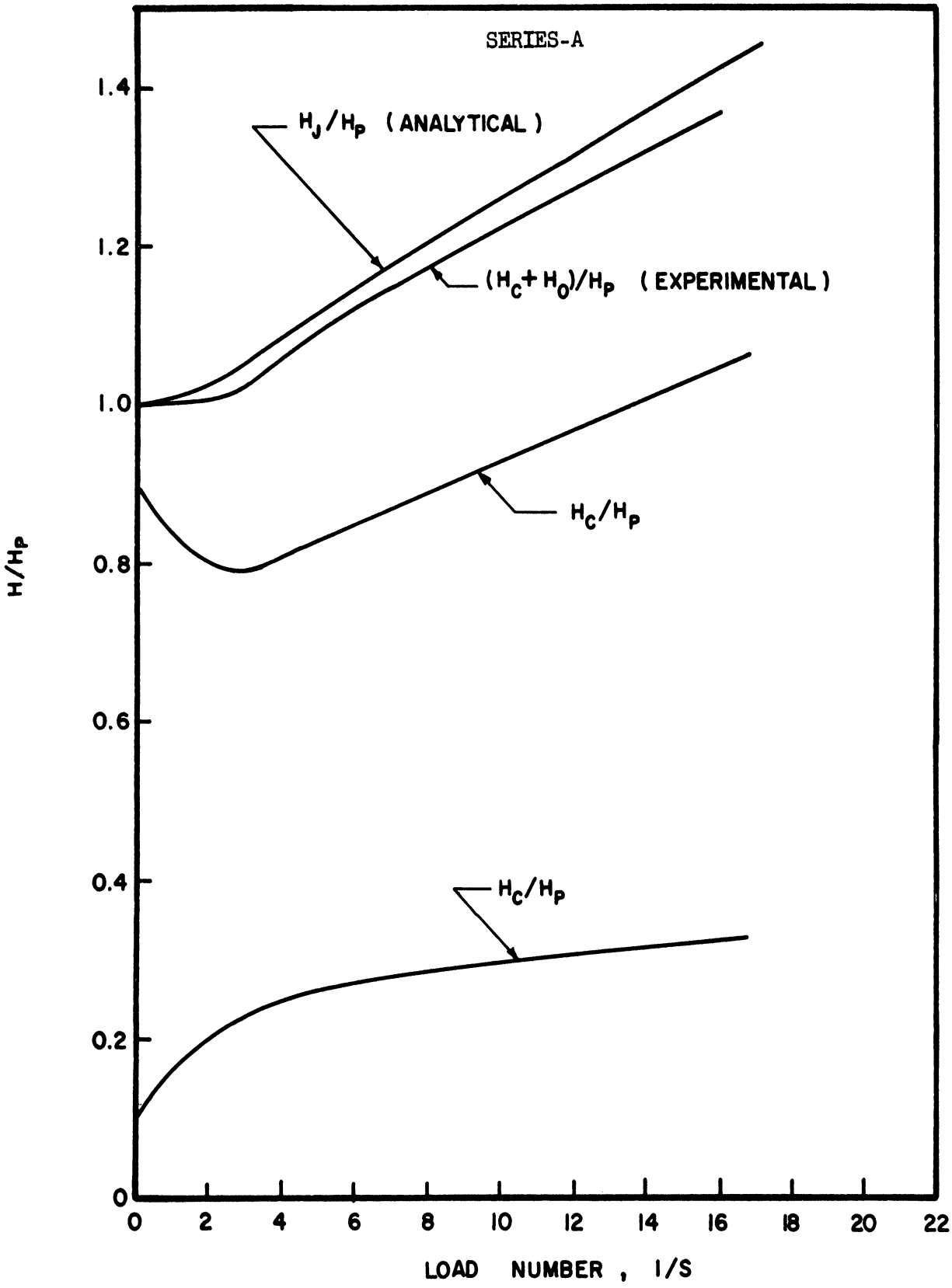

Figure 41. Heat Balance Sheet.
Total Heat Dissipation Ratio $(H_C + H_0)/H_p$ and Heat Generation Ratio H_J/H_p vs. Load Number.

temperature elevation ΔT on log paper, a straight line relationship was obtained as presented in Figure 35.

The effect of speed and load on both the heat dissipated through the bearing and housing, and the heat convected by the oil flow is shown in Figures 42 through 45.

In Figure 46 a heat balance between the analytical heat generation by friction as suggested by Barwell[1] and the total heat dissipation is made. The data is presented in a nondimensional form by expressing both quantities in terms of the heat generated at no-load.

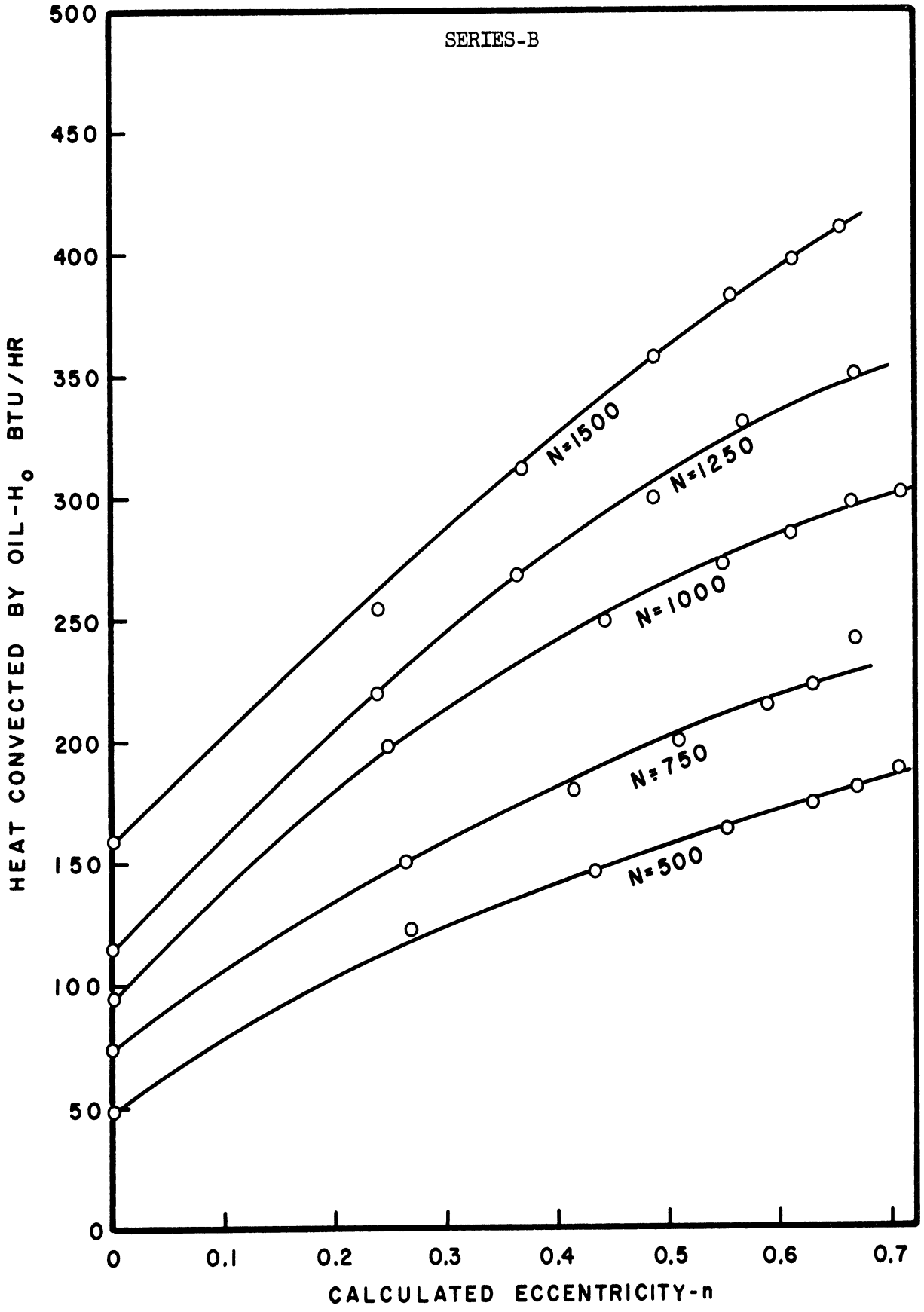

Figure 42. Heat Convected by Oil Flow vs. Calculated Eccentricity at Different Speeds.

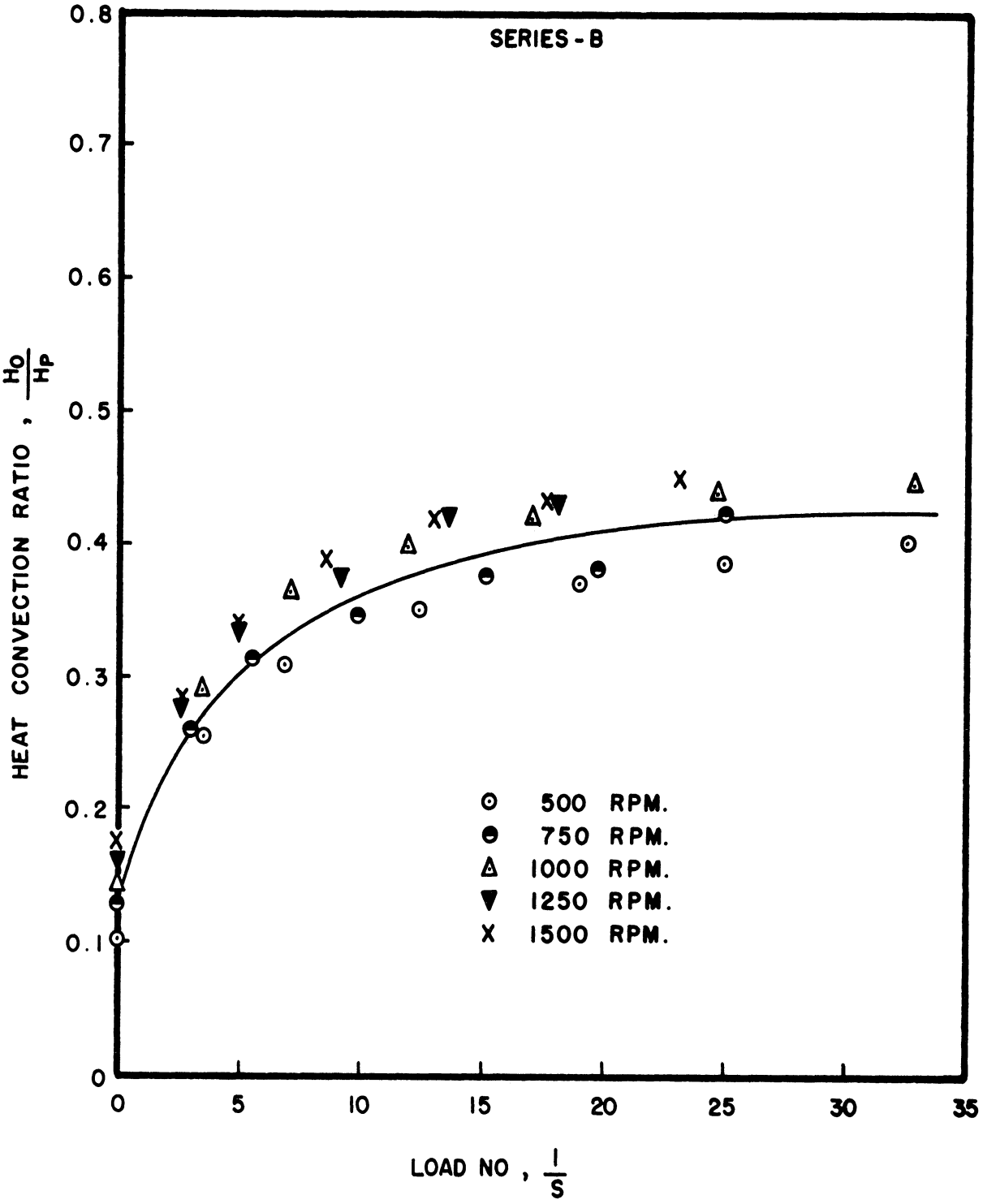

Figure 43. Heat Convection Ratio H_o/H_p vs. Load Number 1/S.

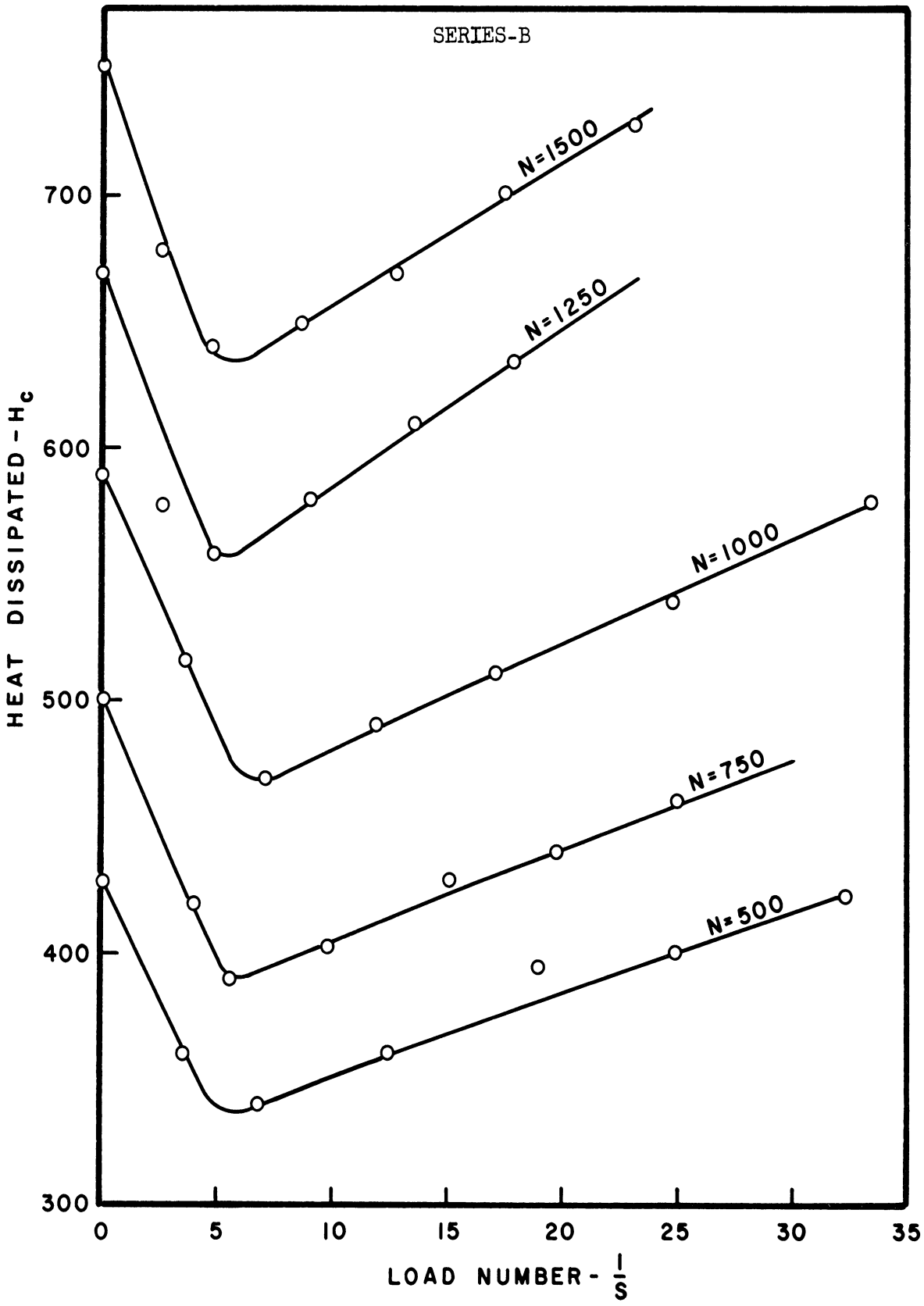

Figure 44. Heat Dissipated H_c vs. Load Number 1/S.

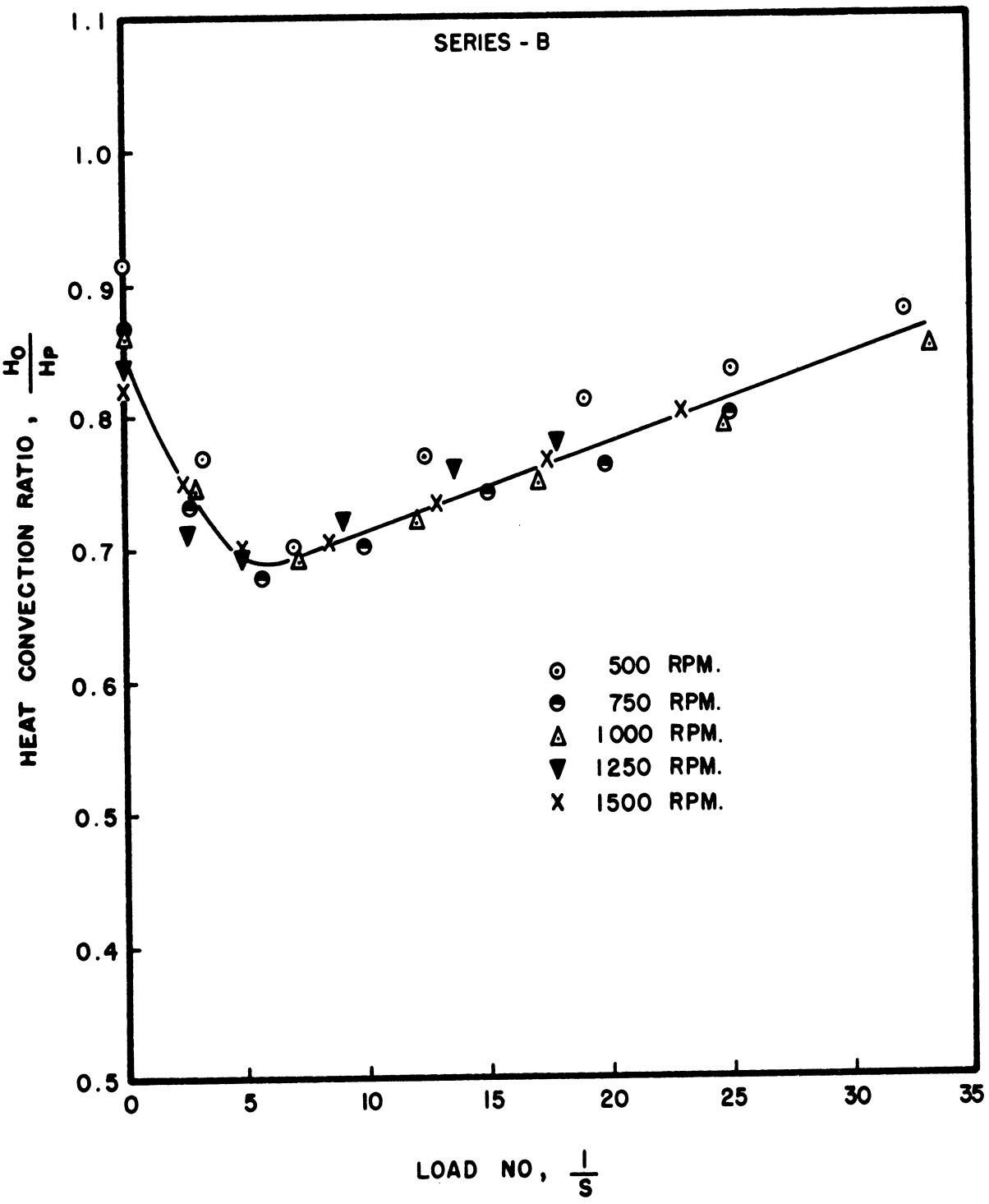

Figure 45. The Ratio H_c/H_p vs. the Load Number 1/S.

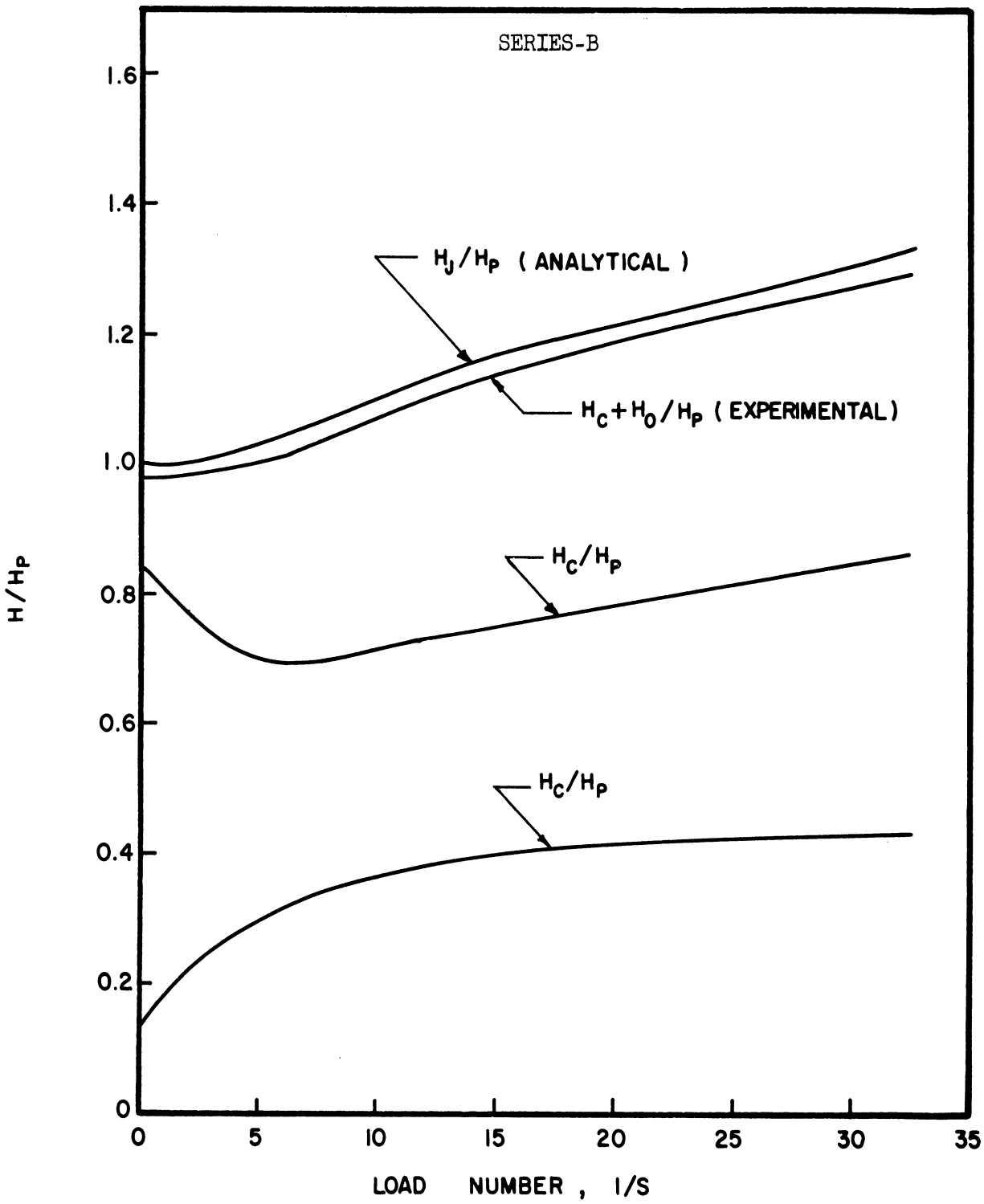

Figure 46. Heat Balance Sheet.
Ratio of Total Heat Dissipated ($H_c + H_o/H_p$ and Heat Generation Ratio H_J/H_p vs. Load Number.

VI. ANALYSIS AND DISCUSSION OF RESULTS

Effect of Load on the Average Oil Film Temperature

Due to the increase in heat generation by load application, the average oil film temperature is expected to increase correspondingly. Actually, the average oil film temperature decreases to a certain minimum and then starts to increase as shown in Figure 22 and 23.

The difference between the pressure developed in the axial direction, to support the load, and the atmospheric pressure at the ends of the bearing causes a rapid increase in the oil flow. This, in turn, increases the amount of heat carried away by the oil, causing the bearing to run at a cooler temperature.

At heavy loads, the rate of heat generation is greater than the increase in the oil flow rate. Accordingly, the temperature of the bearing starts to rise again.

This observation seems to have passed unnoticed by most of the previous investigators. This can be attributed to the following reasons:

1. The most detailed work on heat effects on journal bearings was done on unloaded or lightly loaded bearings. The technique, used in carrying out the lightly loaded bearing tests, was performed in such a way that this observation could not be detected. Muskat and Morgan[15] varied the speed while keeping the load and inlet oil pressure constant. Boyd and Robertson[3] changed the oil supply pressure and the speed while keeping the load constant.

2. In other related investigations in the field of lubrication the lack of sufficient temperature measurements of the bearing was reported. Besides, there is some doubt about the time given for the thermal equilibrium condition to be reached.

3. The use of high oil supply pressure with the adoption of the oil outlet temperature as a true representation of the bearing temperature tends to give misleading results. This is mainly due to the excess oil flow which leaves the bearing almost immediately without contributing effectively to the cooling of the bearing.

It is worthy of note that Rosenblatt and Wilcock[20], working on a different type of sleeve-bearing, were the first to report this observation in their study on oil flow.

In the external heating case, the same phenomena is noticed as shown in Figure 30. The only difference between the 2 cases is that the average oil film temperature in the case of external heating starts to increase at a greater load.

Effect of Speed on the Average Oil Film Temperature

When the bearing is running under hydrodynamic lubrication conditions, the average temperature of the oil film is influenced more by variations in speed than by variations in load. This is due to the fact that the heat generated in the film is a function of the square of the speed as can be seen from Equation (3.24). This can be illustrated by comparing the difference in the average oil film temperature due to the

variation of speed with that due to the variation of load. From Figure 22 the level of the average oil film temperature has increased by about 55°F due to the variation of speed from 500 to 1500 rpm, while the average oil film temperature has increased by about 10°F due to the variation of load from zero to 3429 pounds.

This result is also confirmed when the effect of speed and load on the average oil film temperature for the external heating case, shown in Figure 30, are compared.

From this result, it can be concluded that the speed of rotation has an important effect on the heat condition of journal bearings.

Effect of Speed on the Circumferential Temperature Distribution

As shown in Figures 24, 25, 31, and 32, for both series of tests performed, it is noticed that the variation in the circumferential temperature distribution, for the no load tests, at different speeds, can be considered negligible when compared to the corresponding variation for the loaded bearing tests.

The small temperature variation recorded is mainly due to the introduction of fresh oil supply to the bearing.

From these experimental results, the assumption that the temperature gradient $\partial T/\partial x$ is negligible, as considered in the theoretical investigation for the case of the unloaded bearing, has been justified.

Effect of Load on the Circumferential Temperature Distribution

When the load is applied to the journal, the circumferential temperature ceases to be constant, and starts to vary around the circumference. This variation becomes more pronounced when the load is increased as shown in Figures 24, 25, 31, and 32.

It is noted in all the experimental results, that the maximum temperature is located within the vicinity of the minimum film thickness, confirming the results obtained by Stephen.(22)

Effect of Speed on Oil Flow Rate

At no load, the oil flow increases with the increase in speed. Figure 26 gives a comparison between the experimental results and the theoretical flow predicted by Muskat and Morgan.(16) Their equation is written here for convenience:

$$= \frac{\Delta p \ \pi \ c_d^3}{3\mu\left[\frac{\ell}{2d} - 2 \log_e \frac{di}{d} - 4 \sum_1^\infty \frac{1}{b\left(1+e^{b\frac{\ell}{d}}\right)}\right]} \qquad (6.1)$$

where

Δp = Inlet pressure - ambient pressure psi

di = Oil inlet hole diameter inches

b = An integer with values 1, 2, 3, 4, ... ∞ .

The agreement between the theory and experiments is fairly close. The most probable reason for the discrepancy is that the clearance in Equation (6.1) is raised to the third power. Any small error in the measurement of the clearance will have a great effect on the calculated oil flow rate.

It is to be noted that the speed does not enter explicitly as a variable in the above equation, in spite of the fact that the experimental results do show a positive increase in the oil flow rate with the increase in speed. This can be explained by the following reasoning: Increasing the speed will raise the average oil film temperature level.

As the viscosity of the oil is strongly related to the oil temperature, a corresponding decrease in the viscosity will result causing an increase in the oil flow rate.

By the same reasoning, the increase in the oil flow for the external heating series, as illustrated in Figure 33, over the no heating series can be explained.

Effect of Load on Oil Flow Rate

When the load is applied on the journal, the oil flow rate increases rapidly as indicated in Figure 27. This can be attributed to the increase in the hydrodynamic oil flow with the increase in load.

The equation of the correlating line (5.1), in Figure 28, can be used in predicting the oil flow in similar bearings working under low oil feed pressure.

For the external heating case, the oil flow increases, following the same trend observed in the above case, as shown in Figure 33. It is noticed that the correlating line, for this case, is very close to the no heating case correlating line, as illustrated in Figure 28.

Although the effect of load is considered small with respect to the effect of speed on the average oil film temperature, it is interesting to note that it has a greater influence on the oil flow rate than that of speed.

Effect of Speed and Load on the Heat Convected

The increase in oil flow, with speed and particularly load, is the main reason for the increase of the amount of heat convected by the oil flow as indicated in Figures 36 and 37.

The equation of the straight line (5.3), correlated from the data plotted in Figure 38, can be used in estimating the heat convection ratio H_o/H_p as a function of the load number in similar bearings. To illustrate the effect of external heating, a comparison is made between the results obtained in Series A and Series B runs. It is noticed in Figures 37 and 43 that the heat convection ratio in the case of external heating is about seven percent greater than in the case of no heating. This is mainly due to the decrease of the oil viscosity with external heating, causing the amount of oil flow to increase. This will accordingly increase the amount of heat convected by the oil flow and the heat convection ratio H_o/H_p.

Effect of Speed and Load on the Heat Dissipated H_c

From Figures 40 and 45, for both Series A and B, it is noticed that the heat dissipated through the bearing decreases at light load and then increases with the increase in load.

The decrease in the heat dissipation is mainly attributed to the increase in the rate of heat convection due to the rapid increase in the hydrodynamic oil flow at light loads. At heavy loads, the rate of increase in the heat generation rate is much greater than that of the heat convection rate. This, correspondingly, causes the heat dissipation through the bearing and housing to rise again.

Effect of the Average Oil Film Temperature on the Heat Dissipated H_c

From Figure 35, the heat dissipation rate through the bearing and housing increases with the increase of the average oil film temperature. The empirical equation, relating the two variables is:

$$H_c = 3.26(\Delta T)^{1.43}$$

This confirms the assumption, first introduced by Lasche[11], that the heat dissipation can be described by a power of the temperature elevation of the oil film over the ambient.

The low value of the exponent gives an indication of the small role played by the radiation heat transfer.

Comparing the values of the empirical constants with those determined by the following investigators:

Lasche[11]:	a = 2.9	m = 1.30
Muskat and Morgan[15]:	a = 2.0	m = 1.35
Burwell[2] :	a = 2.9	m = 1.5
McKee[13]:	a = 3.42	m = 1.65

shows that the values obtained in this investigation lie within the range of the above results.

It is interesting to note that the heat dissipation rate for the case of external heating is less than that for the no heating case as illustrated in Figure 35. This is mainly due to the increase in the rate of heat convection by the oil flow and the decrease in the heat generation rate due to external heating.

Heat Balance

Under thermal equilibrium condition, the heat generated in the oil film balances the total heat dissipated from the bearing.

From Figures 41 and 46, it is noted that the experimental results are in agreement with the analytical, for both series of tests A and B. This confirms the validity of Barwell formula, Equation (2.21), in calculating the heat generated in loaded bearings.

VII. CONCLUSIONS AND RECOMMENDATIONS

Conclusions

The following conclusions may be drawn from the results of this investigation:

1. The consideration of the heat dissipated through the bearing and housing, and that convected by oil flow, in the analysis of the experimental results, gives a better understanding of the effect of speed, load, and external heating on the average oil film temperature and the heat balance.
2. The phenomena, that the bearing will run cooler at light loads than at no load is well established and confirmed experimentally.
3. The average oil film temperature is affected more by variations in speed than by variations in load. The level of the average oil film temperature has increased by about 55°F due to the variation of speed from 500 to 1500 rpm, while it has increased only by about 10°F due to the variation of load from zero to 3429 pounds.
4. The oil flow rate is influenced more by changes in load than by changes in speed. The oil flow rate has increased by about 350 percent due to the change in load from zero to 3429 pounds, while it has increased only by about 200 percent due to the change in speed from 500 to 1500 rpm.
5. The heat convected by the oil flow increases by external heating application.

6. The heat dissipated through the bearing and housing for the external heating case is less than that for the no heating case, when the temperature elevation of the bearing over the ambient is the same in both cases.

Recommendations

It is recommended that further investigations of the same nature be made to cover larger ranges of speeds and oil inlet pressures.

The study of the effect of the following variables,

1. the diametral clearance
2. the bearing length/diameter ratio
3. water cooling
4. oil grooves,

on the temperature and heat balance of journal bearings is also needed in order that the problem of heat removal from journal bearings can be completely solved.

APPENDIX A

JOURNAL AND BEARING DIMENSIONS

The dimensions of the journal and bearing are given in Figure 11 and 12 respectively.

The machining and grinding of the bearing and journal was made at the U.M.R.I. machine shop. The dimensions of the journal diameter was measured at three different positions. The average diameter was found to be 3.001 inches. The surface roughness was measured by means of a profilometer. Its value was 9 RMS microinch.

The bearing bore was measured along two perpendicular planes at the two ends and at the middle section. The average value was 3.0068 inches. The surface roughness was found to be 14 RMS microinch.

Summary of the Major Dimensions

The journal diameter = 3.001 inches

The journal length = 5.000 inches

The bearing bore = 3.0068 inches

The diametral clearance = .0058 inches

APPENDIX B

PROPERTIES OF GULFPRIDE NO. 30 OIL

The properties which entered the analysis of the experimental data are:

1. The Specific Heat - The specific heat was considered constant. An average value covering the range of temperature used, is chosen from Figure 47.

$$\text{The average specific heat} = 0.515 \quad \frac{\text{BTU}}{\text{lb } ^\circ\text{F}}$$

2. The Specific Gravity - As shown in Figure 48, the variation of the specific gravity, within the range of the temperature used, can be neglected. The following average value is adopted.

$$\text{The average specific heat} = 0.858$$

3. The Coefficient of Thermal Conductivity - The following formula, given by Wilcock and Booser[25], were used in estimating the coefficient of thermal conductivity.

$$k = \frac{0.812}{\rho_{60}} [1 - .0003 (T-32)] \quad \frac{\text{BTU}}{\text{hr ft}^2 \ ^\circ\text{F}} \text{ per inch}$$

where ρ_{60} = density in gm/cc

An average value covering the range of temperatures used (120°F - 200°F) was used.

$$k = .0737 \quad \frac{\text{BTU}}{\text{hr ft}^2 \ ^\circ\text{F}} \text{ ft}$$

$$= .0159 \quad \frac{\text{lb}}{\text{sec } ^\circ\text{F}}$$

4. The Kinematic Viscosity - The kinematic viscosity temperature relationship was furnished by the manufacturer, as shown in Figure 49. To check the accuracy of the curve, the encircled points in the figure were determined experimentally.

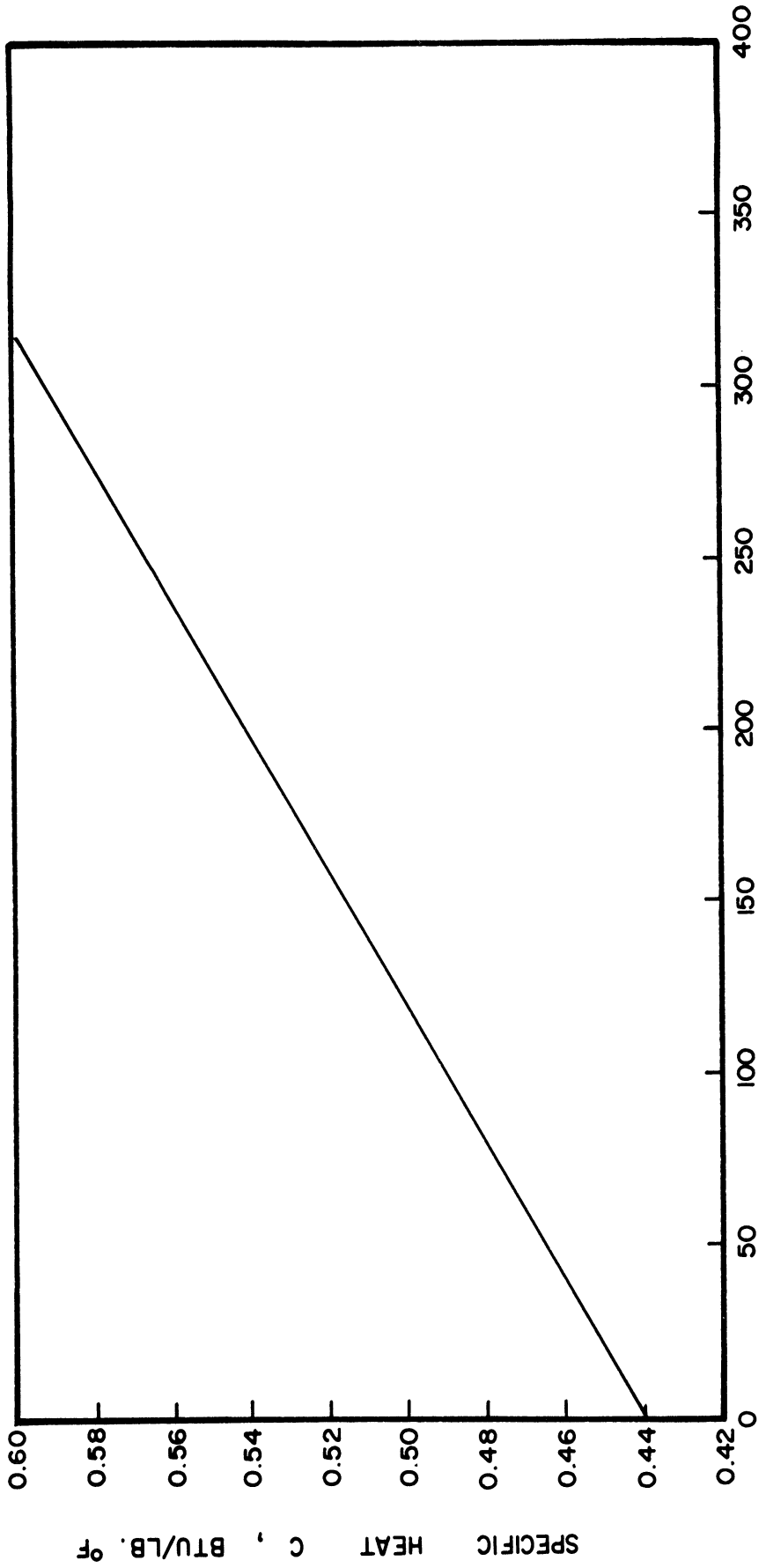

Figure 47. Variation of Specific Heat with Temperature for Gulfpride No. 30 Oil.

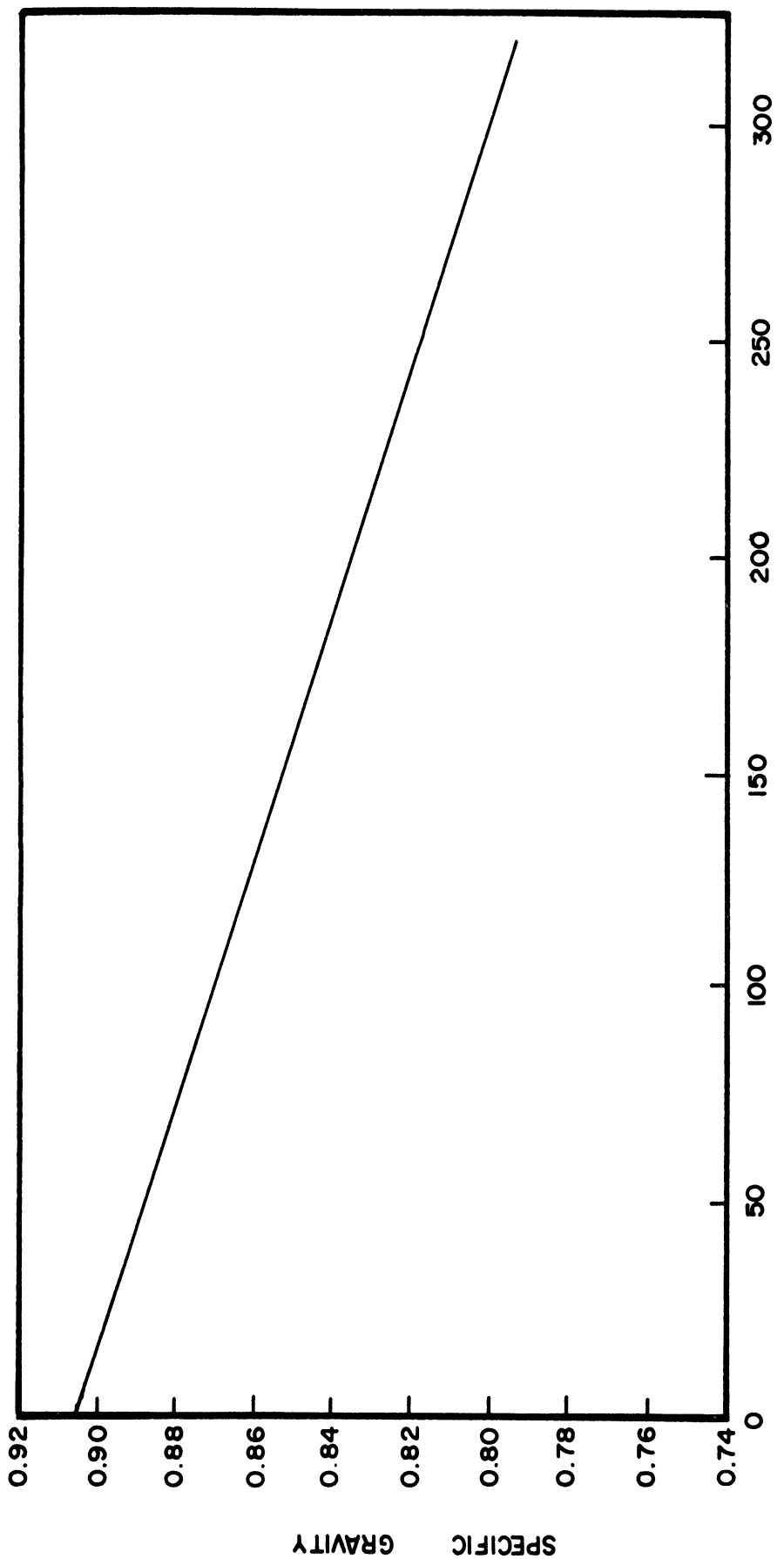

Figure 48. Variation of Specific Gravity with Temperature for Gulfpride No. 30 Oil.

APPENDIX C

LAMINAR FLOW CRITERION IN JOURNAL BEARINGS

In 1923 Taylor analyzed the problem for the liquid between two concentric cylinders, and developed a criterion for the initiation of turbulence under these circumstances. This criterion, fortunately, can also be applied to journal bearings with sufficient accuracy as has been demonstrated by Wilcock[24].

The transition between normal laminar behavior and turbulence takes place at a Reynolds number given by

$$R_e = \frac{\pi N' DC}{\nu} = 41.1 \left(\frac{D}{2C}\right)^{1/2}$$

and the transition speed can be written as:

$$N = 1.57 \times 10^3 \frac{\nu}{D^{1/2} C_D^{2/3}} \quad \text{rpm}$$

To evaluate the speed at which turbulence initiates, the following substitutions are made.

$$D = 3 \text{ inches}$$

$$C_D = .00649 \text{ inches}$$

$$\nu = \frac{\mu}{\rho} \frac{24 \times 10^{-7} \times (12)^3 \times 386}{.858 \times 62.4} = 3.0 \times 10^{-2} \quad \text{in}^2/\text{sec}$$

$$N = 1.57 \times 10^3 \times \frac{3.00 \times 10^{-2}}{1.73 \times (.00649)^{3/2}}$$

$$= 1.57 \times 10^3 \times \frac{3.00 \times 10^{-2}}{1.73 \times 5.23 \times 10^{-4}}$$

$$= 5.21 \times 10^4 \quad \text{rpm}$$

As the maximum speed used in this investigation is 1500 rpm, it can be concluded that the flow is highly laminar.

APPENDIX D

ESTIMATION OF THE AVERAGE OIL FILM TEMPERATURE

As a result of this investigation, the average oil film temperature can be estimated.

When the heat balance Equation (2.2)) is divided by the rate of heat generation at no load, one gets

$$\frac{H_J}{H_p} = \frac{H_c}{H_p} + \frac{H_o}{H_p} \qquad (D.1)$$

Substituting for the values of H_c and H_o/H_p, in Equations (5.2) and (5.3) respectively, in the above equation gives:

$$\frac{H_J}{H_p} = \frac{3.26(\Delta T)^{1.43}}{H_p} + .1845(1/S)^{.2146} \qquad (D.2)$$

To determine H_p, the average oil film temperature for the unloaded bearing must first be evaluated.

For the unloaded bearing Equation (6.2) reduces to:

$$1 = \frac{3.26(\Delta T)^{1.43}}{H_p} + .1845(1/S)^{.2146} \qquad (D.3)$$

The above equation contains two unknown; the viscosity of the oil μ which is included in the H_p and $1/S$ terms; and the temperature elevation ΔT. If a suitable viscosity-temperature relationship or an A.S.T.M. viscosity-temperature chart is used, the value of the temperature elevation ΔT can be evaluated graphically.

After determining H_p, the average oil film temperature for the loaded bearing can then be estimated.

Substituting for the value of H_J in Equation (2.21) in Equation (6.3) one gets:

$$\frac{300}{H_p}\left[\frac{8\pi^3 r^3 \ell \mu N'^2}{J\, c(1-n^2)^{1/2}} + \left(\frac{W\, e \sin\gamma}{2\, J}\right) 2\,\pi\, N'\right] = \frac{3.26(\Delta T)^{1.43}}{H_p} + .1845(1/S)^{.2146} \qquad (D.4)$$

Making use of Ocvirk and DuBois results[17], the value of n and α can be obtained. The temperature elevation ΔT can then be determined, when the same procedure used in its evaluation for the unloaded bearing case is followed.

APPENDIX E

THE JOURNAL FRICTIONAL HEAT GENERATION

From equilibrium conditions, the bearing frictional torque is less than the journal frictional torque. This can be shown when moments are taken about the center of the bearing O in Figure 50.

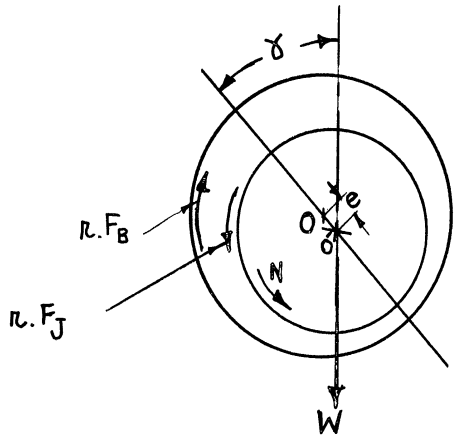

Figure 50. Forces Tending to Cause Rotation of the Oil Film in a Full Journal Bearing.

$$r F_J - r F_B = W e \sin \gamma$$

where F_J = Frictional force on journal surface, lbs.

F_B = Frictional force on bearing surface, lbs.

The eccentricity of the journal is thus seen to be the source of the difference in the frictional torque between the journal and the bearing.

The short bearing approximation theory does not indicate a difference between the journal and bearing frictional torques because of the assumption that the velocity distribution across the oil film is linear.

To estimate the journal frictional torque Ocvirk and DuBois[17] gave the following equation

$$M_J = \frac{4\pi^2 r^3 \ell \mu N'}{c (1-n^2)^{1/2}} + W e \sin \gamma .$$

The second term is the frictional torque obtained, using the short bearing approximation theory. The third term is the load couple caused by the eccentricity of the journal.

Barwell[1] suggested the following modified form of Ocvirk's equation

$$M_J = \frac{4\pi^2 r^3 \ell \mu N'}{c (1-n^2)^{1/2}} + \frac{W}{2} e \sin \gamma .$$

He based his equation on the assumption that the short bearing approximation theory, while underestimating the journal frictional torque, it overestimates the bearing frictional torque. It can, then, be considered as an average value between the journal and bearing frictional torques. As a closer approximation to the true journal frictional torque, he added one half of the load couple to the frictional torque derived, using the short bearing approximation theory.

Barwell's equation was derived analytically by Mack and Shaw[21] without the use of the short bearing approximation theory. For this reason his equation was used in the prediction of the journal heat generation. Multiplying the journal frictional torque by $2\pi N'$, and using appropriate conversion factors, the journal frictional heat generation can be expressed as

$$H_J = 300 \left[\frac{8\pi r \ell}{J c} \frac{\mu N'}{(1-n^2)^{1/2}} + \left(\frac{W e \sin \gamma}{2 J}\right) 2\pi N'\right] \qquad (2.21)$$

Sample Calculations for Run Number 5

The journal frictional heat generation

$$= 300 \left[\frac{8\pi^3 r^3 \ell}{J c} \frac{\mu N'}{(1-n^2)^{1/2}} + \left(\frac{W e \sin \gamma}{2 J}\right) 2\pi N'\right] . \qquad (2.21)$$

The short bearing approximation theory was used to calculate the eccentricity ratio n and the attitude angle γ. Ocvirk and DuBois[17] derived the following equation which expresses the attitude angle γ as a function of the eccentricity ratio n

$$\tan \gamma = \frac{\pi}{} \frac{(1-n^2)^{1/2}}{}$$

This equation was used in estimating the attitude angle γ.

For Run 5:

$r = 1.5$ inches

$\ell = 5.00$ inches

$c = .00306$ inches

$N' = 8.34$ rps

$n = .48$

$\mu = 66.3 \times 10^{-7}$ Reyns.

$W = 1727$ lbs.

$\tan \gamma = 1.434$

$\sin \gamma = .82$

Substituting the above values in Equation (2.21) yields

$$H_J = 208 + 21 = 301 \text{ BTU/hr} .$$

Similar calculations were made for the other runs as shown in Table VI.

APPENDIX F

THERMAL EXPANSION EFFECT ON CLEARANCE

As the journal and the bearing were made of dissimilar metals, the effect of the change of bearing clearance with temperature was taken into consideration. The method used by Von Gersdorfer[23] was adopted.

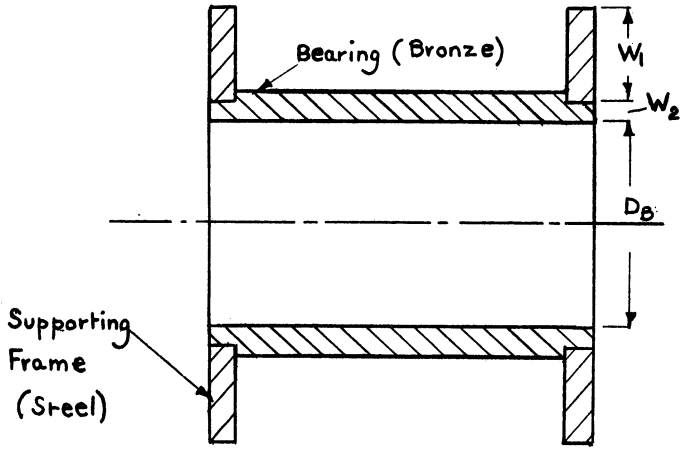

Figure 51. Bearing Construction.

The Effect of Thermal Expansion on the Journal

The following equation will be used to determine the change in the journal diameter:

$$\Delta D_J = D_J \times \alpha_J \times \Delta T_J \ .$$

where

ΔD_J = The increase in the diameter of the journal due to ΔT_J.

D_J = Journal diameter at room temperature inches

α_J = Coefficient of thermal expansion of journal material

= 6.2×10^{-6} $1/°F$

ΔT_J = Temperature elevation of the journal over the ambient.

The Effect of Thermal Expansion on the Bearing

According to the way the bearing unit is constructed, the bearing mid-section is free to expand, while the ends are constrained by the supporting frame as illustrated in the above figure.

Expansion at the mid-section =

$$\Delta D_{B1} = D_B \times \alpha_B \quad \Delta T_B = \Delta D_{B1}$$

Expansion at the ends of the bearing =

$$\Delta D_{B2} = D_B \frac{W_1 E_1 \alpha_1 \Delta T_1 + W_2 E_B \alpha_B \Delta T_B}{W_1 E_1 + W_2 E_2}$$

where

W_1 = Radial thickness of the supporting frame = 2".

E_1 = Youngs Modulus of elasticity of the support material = 30×10^6 lb/in^2 .

E_B = Youngs Modulus of elasticity of the bearing material = 15.9×10^6 lb/in^2 .

ΔT_1 = Temperature elevation of support over ambient.

ΔT_B = Temperature elevation of bearing over ambient.

α_B = Coefficient of thermal expansion of the bearing material = 12.2×10^{-6} 1/°F .

W_2 = Thickness of the bearing at the end.

Sample Calculation at 1500 rpm: From Table I

$\Delta T_B = 93.2$ °F

$\Delta T_1 = 148-88 = 60$°F .

Bearing expansion at the mid-section =

$$\Delta B_1 = 3.0068 \times 12.2 \times 10^{-6} \times 93.2 = 3.4188 \times 10^{-3} \text{ inches} .$$

Bearing expansion at the ends =

$$\Delta B_2 = 3.0068 \times \frac{2 \times 30 \times 10^6 \times 6.2 \times 10^{-6} \times 60 + .625 \times 15.9 \times 10^6 \times 12.2 \times 10^{-6} \times 93.2}{2 \times 30 \times 10^6 + .625 \times 15.9 \times 10^6}$$

$$= 1.4477 \times 10^{-3} \quad \text{inches}$$

The increase in the bearing diameter was taken as the average of the increase of the mid-section and that at the ends.

Average bearing increase in diameter =

$$\Delta D = \frac{(\Delta D_{B1} + \Delta D_{B2})}{2}$$

$$= \frac{3.4188 + 1.4477}{2} \times 10^{-3}$$

$$= 2.4332 \times 10^{-3} \quad \text{inches}$$

The change in journal diameter =

$$\Delta D_J = D_J \times \alpha_J \times \Delta T_J$$

$$= 3.001 \times 6.2 \times 10^{-6} \times 93.2$$

$$= 1.73409 \times 10^{-3} \quad \text{inches}$$

The change in diametral clearance =

$$\Delta D_{Bm} - \Delta D_j = (2.43320 - 1.73409)\ 10^{-3} = .69911 \times 10^{-3}$$

The new diametral clearance =

$$c_d + (\Delta D_{Bm} - \Delta D_J) = .00580 + .00069911 = .006499 \quad \text{inches}$$

Following the same method of calculation, the change in diametral clearance with temperature can be evaluated.

As the average oil film temperature was influenced more by the variation in speed than by the variation in load, the value of the

diametral clearance at constant speed under no-load condition was substituted for the diametral clearance at the corresponding speed for any load.

The result of the calculations is given in Table I and presented graphically in Figure 29.

TABLE I

THERMAL EXPANSION EFFECT ON CLEARANCE

1	2	3	4	5	6	7	8	9	10	11	12	13	14	15	16	17	18	19	20
ΔT_J	D_J Inches	$\alpha \times 10^{-6}$	ΔD_J Inches	D_B Inches	$\alpha_{B_1} \times 10^{-6}$ /°F	ΔT_1	$W_1E_1 \times 10^6$	$W_1E_1\alpha_1\Delta T_1 \times 10^3$	$W_BE_B \times 10^5$	$W_BE_B\alpha_B\Delta T_J \times 10^3$	9 + 11 $\times 10^3$	8 + 10 $\times 10^6$	12/13 $\times 10^{-3}$	ΔD_{B1} 10^{-3} Inches	ΔD_{B2} $\times 10^{-3}$ Inches	ΔD_{Bm} $\times 10^{-3}$ Inches	C_D $\times 10^{-3}$ Inches	C Inches	N rpm
42.2	3.001	6.2	.78518	3.0068	12.2	30.2	60	11.2344	9.9375	5.1162	16.3506	69.9375	.23378	1.54808	.7029	1.12545	6.13030	3.065	500
59.9	3.001	6.2	1.1145	3.0068	12.2	40	60	14.880	9.9375	7.2621	22.142	69.9375	.3166	2.197309	.95195	1.5744	6.2599	3.1299	750
73	3.001	6.2	1.35825	3.0068	12.2	50.5	60	18.7860	9.9375	8.8503	27.636	69.9375	.39515	2.67785	1.1881	1.9329	6.36465	3.1823	1000
84.2	3.001	6.2	1.56292	3.0068	12.2	55	60	20.460	9.9375	10.1839	30.6439	69.9375	.43816	3.081368	1.31746	2.1994	6.4365	3.2182	1250
93.2	3.001	6.2	1.73409	3.0068	12.2	60	60	22.320	9.9375	11.2993	33.6193	69.9375	.48070	3.4188	1.4477	2.4332	6.4991	3.2490	1500

APPENDIX G

DETERMINATION OF THE THEORETICAL JOURNAL TEMPERATURE

Equation (2.12) was used in the calculation of the theoretical journal temperature,

$$\Theta = \frac{1}{\beta'} \ln [\beta' \, Pr.E.(Y - \frac{Y^2}{2}) + 1] \qquad (2.12)$$

multiplying the above equation by $T_J - T_B$ and substituting for Y by 1, gives

$$T_J - T_B = \frac{1}{\beta} \ln [\frac{\beta \mu_B U^2}{2 k} + 1]$$

The details of the calculations are presented in Table II.

TABLE II

COMPARISON BETWEEN THE EXPERIMENTAL AND THEORETICAL (JOURNAL TEMPERATURE-BEARING TEMPERATURE)

T_{av}	Speed N rpm	T_B °F	μ_B x 10^{-7} Reyns.	k $\frac{lb}{sec\,°F}$	U in/sec	U^2 x 10^4	$1 + \frac{\beta \mu_B U^2}{2 k}$	ΔT Calc. °F	ΔT Exp. °F
128	500	127.2	69.6	.0159	78.5	.6162	1.0237	1.21	1.6
143.5	750	142.2	51	.0159	117.8	1.385	1.039	2.23	2.7
157.5	1000	155.77	39.8	.0159	157	2.46	1.054	3.00	3.6
169.1	1250	166.7	32.4	.0159	196.3	3.85	1.069	3.8	4.5
181.7	1500	178.5	26.15	.0159	235.7	5.54	1.080	4.38	5.40

APPENDIX H

EXPERIMENTAL DATA AND CALCULATIONS

This appendix contains all the original data for all the experiments. The data and the results of the calculations are given in the following tables:

Table III - Temperature Data

Table IV - Oil Flow Data

Table V - Calculation of the Sommerfeld Number, the Load Number, and the Eccentricity Ratio

Table VI - Summary of Correlation Calculations

Figure 52 describes the positions of the bearing thermocouples given in Table III,

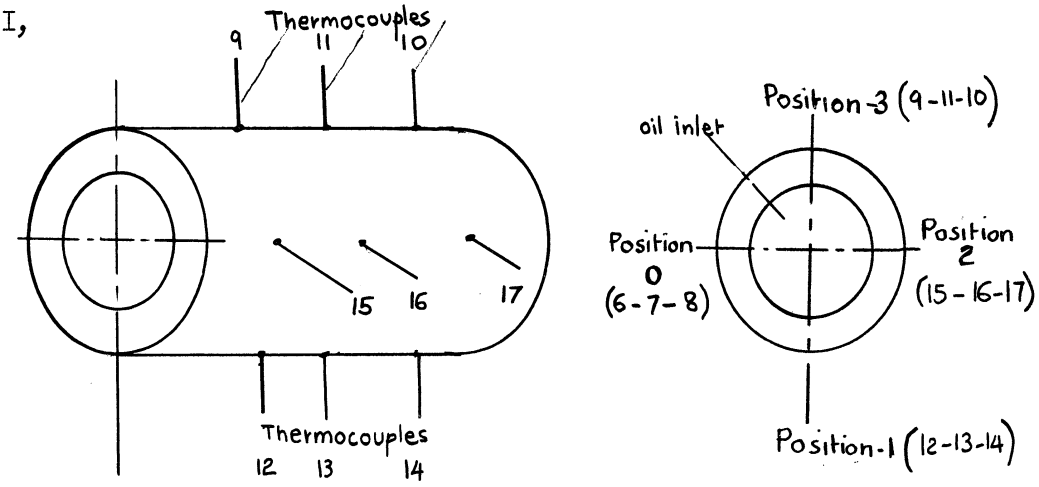

Figure 52. Bearing Thermocouple Positions.

while Figure 53 was used in evaluating the eccentricity ratio-n from the load number 1/S.

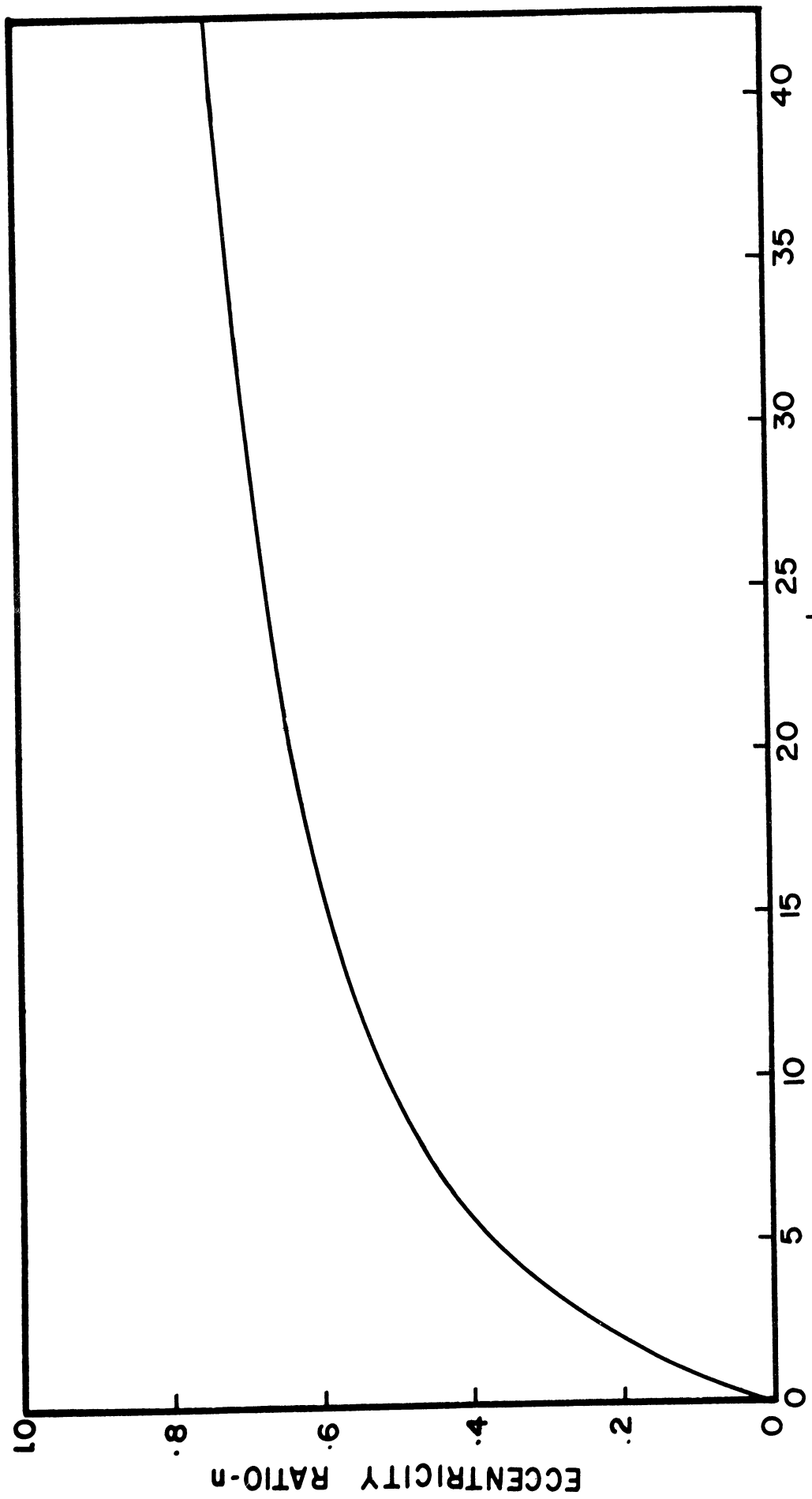

Figure 53. Eccentricity Ratio vs. Load Number 1/S (After DuBois and Ocvirk).

TABLE III

TEMPERATURE DATA: SERIES A

Run No	Speed N rpm	Ambient Temp. °F	Calibrating Thermocouple m.v.	°F	Correction °F	Journal Thermocouple Readings 1 m.v.	2 m.v.	3 m.v.	4 m.v.	Average Temperature T_J m.v.	°F	Corrected Temp. T_J °F	Bearing Thermocouple Readings - m.v. Position - 0 6	7	8	Position - 3 9	10	11	Position - 1 12	13	Position - 2 14	15	16	17	Average T_B	T_{av}	Housing Temp. m.v.	Load lbs.
1	500	85.8	1.55	86	.2	2.812	2.729	2.785	2.834	2.79	129	128.2	2.718	2.732	2.722	2.752	2.722	2.767	2.718	2.752	2.704	2.722	2.762	2.733	127.2	128	2.417	0
2	500	86.9	1.575	87.5	.6	2.801	2.714	2.727	2.786	2.757	127.9	127.3	2.622	2.612	2.618	2.656	2.622	2.662	2.668	2.693	2.665	2.655	2.704	2.700	124.5	125.8	2.369	427
3	500	86.9	1.575	87.5	.6	2.811	2.743	2.774	2.796	2.781	128.7	128.1	2.638	2.631	2.637	2.663	2.632	2.672	2.712	2.738	2.713	2.679	2.739	2.732	125.4	126.25	2.382	927
4	500	87.1	1.581	87.7	.6	2.835	2.814	2.825	2.830	2.826	130.3	129.7	2.685	2.682	2.686	2.705	2.673	2.713	2.769	2.800	2.782	2.729	2.791	2.790	127.1	128.4	2.419	1427
5	500	86.9	1.572	87.4	.5	2.884	2.865	2.879	2.880	2.877	131.9	131.4	2.707	2.712	2.716	2.729	2.698	2.739	2.798	2.832	2.814	2.755	2.822	2.815	128	129.7	2.432	1727
6	500	89.7	1.653	90.1	.4	3.120	2.960	2.989	3.050	3.030	137	136.6	2.840	2.863	2.846	2.847	2.810	2.862	2.992	3.009	2.972	2.892	2.963	2.952	132.9	134.4	2.538	2127
7	500	88.3	1.614	88.8	.5	3.150	2.964	3.020	3.080	3.051	137.7	137.2	2.851	2.879	2.866	2.860	2.828	2.875	2.989	3.021	2.996	2.912	2.981	2.967	133.3	135.3	2.550	2627
8	750	83.6	1.483	84.1	.5	3.348	3.223	3.242	3.275	3.272	145.4	144.9	3.153	3.159	3.165	3.203	3.159	3.221	3.154	3.202	3.148	3.161	3.218	3.179	142.2	143.5	2.632	0
9	750	84	1.501	84.7	.7	3.184	3.110	3.128	3.150	3.143	141.1	140.4	2.967	2.917	2.972	2.993	2.978	3.040	3.041	3.063	3.085	3.031	3.110	3.098	136.8	138.6	2.588	427
10	750	84.8	1.519	85.3	.5	3.218	3.121	3.138	3.179	3.164	141.8	141.3	2.976	2.912	2.958	3.012	2.985	3.029	3.057	3.083	3.063	3.044	3.110	3.107	137	139.2	2.597	727
11	750	85.2	1.537	85.9	.7	3.224	3.189	3.199	3.200	3.203	143.1	142.4	2.976	2.922	2.978	3.023	2.988	3.034	3.088	3.120	3.102	3.072	3.138	3.130	137.7	140	2.614	1029
12	750	85.6	1.540	86	.4	3.265	3.207	3.220	3.288	3.245	144.5	144.1	2.993	2.951	3.008	3.045	3.009	3.057	3.470	3.162	3.148	3.108	3.172	3.160	138.8	141.45	2.640	1330
13	750	85.6	1.540	86	.4	3.298	3.238	3.286	3.318	3.285	145.6	145.2	3.026	2.997	3.049	3.076	3.043	3.091	3.173	3.217	3.202	3.158	3.218	3.196	140.3	142.7	2.672	1630
14	750	85.7	1.549	86.3	.6	3.371	3.289	3.343	3.409	3.353	148.1	147.5	3.082	3.066	3.121	3.134	3.100	3.150	3.241	3.290	3.278	3.224	3.284	3.259	142.6	145	2.720	2030
15	750	86	1.558	86.6	.6	3.423	3.347	3.410	3.472	3.413	150.1	149.5	3.163	3.121	3.185	3.206	3.152	3.212	3.333	3.368	3.350	3.266	3.355	3.353	144.8	147.1	2.754	2429
16	750	85.1	1.531	85.7	.6	3.487	3.388	3.439	3.482	3.449	151.3	150.7	3.198	3.160	3.227	3.238	3.168	3.245	3.370	3.414	3.414	3.312	3.405	3.398	146.2	148.4	2.768	2780
17	1000	84.5	1.516	85.2	.7	3.742	3.663	3.701	3.734	3.710	160	159.3	3.554	3.549	3.577	3.622	3.566	3.641	3.549	3.604	3.547	3.565	3.632	3.588	155.7	157.5	2.977	0
18	1000	88.7	1.629	89.3	.6	3.714	3.657	3.688	3.673	3.683	159.1	158.5	3.490	3.428	3.428	3.510	3.502	3.548	3.502	3.540	3.500	3.518	3.600	3.593	153.4	155.7	2.938	427
19	1000	87	1.581	87.7	.7	3.701	3.629	3.628	3.656	3.656	158.2	157.5	3.345	3.283	3.341	3.411	3.362	3.426	3.465	3.498	3.482	3.455	3.540	3.538	150.7	154.1	2.888	927
20	1000	88.5	1.629	89.3	.8	3.811	3.764	3.773	3.796	3.786	162.55	161.75	3.374	3.362	3.412	3.453	3.400	3.470	3.557	3.610	3.591	3.538	3.621	3.600	152.8	157.6	2.941	1427
21	1000	86	1.567	86.9	.9	3.864	3.829	3.842	3.861	3.849	164.65	163.75	3.462	3.350	3.476	3.526	3.461	3.528	3.648	3.678	3.693	3.583	3.682	3.703	155.3	159.6	2.998	2027
22	1000	83.9	1.498	84.6	.7	3.885	3.844	3.862	3.873	3.866	165.2	164.5	3.489	3.369	3.522	3.563	3.503	3.566	3.698	3.732	3.758	3.650	3.737	3.752	156.8	160.9	3.048	2631
23	1000	83.9	1.501	84.7	.8	4.024	3.987	4.001	4.004	4.004	169.8	169	3.608	3.457	3.639	3.669	3.605	3.669	3.833	3.852	3.882	3.763	3.850	3.868	160.4	165.2	3.137	3329
24	1250	84.9	1.522	85.4	.5	4.084	4.045	4.057	4.070	4.064	171.8	171.3	3.87	3.862	3.903	3.953	3.879	3.974	3.876	3.947	3.890	3.891	3.977	3.928	166.9	169.1	3.1[illegible]	0
25	1250	85.9	1.558	86.6	.7	3.949	3.916	3.930	3.945	3.935	167.5	166.8	3.750	3.700	3.717	3.808	3.759	3.834	3.816	3.861	3.820	3.817	3.926	3.915	163.2	165	3.071	427
26	1250	86.2	1.56	87	.8	4.022	4.007	4.009	4.014	4.013	170.1	169.3	3.767	3.773	3.747	3.810	3.763	3.850	3.874	3.950	3.904	3.853	3.981	3.959	164.7	166	3.082	625
27	1250	87	1.587	87.9	.9	4.053	4.012	4.028	4.043	4.034	170.8	169.9	3.750	3.777	3.753	3.810	3.750	3.846	3.908	3.983	3.942	3.872	4.00	3.977	165.1	167.5	3.098	826
28	1250	87	1.584	87.8	.8	4.076	4.034	4.048	4.068	4.056	171.4	170.6	3.768	3.811	3.790	3.832	3.770	3.867	3.960	4.042	3.998	3.919	4.045	4.012	166.4	168.5	3.127	1027
29	1250	87.8	1.611	88.7	.9	4.134	4.098	4.107	4.109	4.112	173.4	172.5	3.785	3.843	3.822	3.854	3.791	3.890	4.002	4.088	4.042	3.955	4.080	4.040	167.5	170	3.150	1227
30	1250	88.8	1.641	89.7	.9	4.286	4.248	4.264	4.266	4.266	178.4	177.5	3.805	3.868	3.849	3.875	3.811	3.908	4.040	4.129	4.084	3.992	4.112	4.064	168.5	173	3.168	1427
31	1250	88.2	1.617	88.9	.7	4.453	4.398	4.399	4.414	4.391	182.7	182	3.850	3.920	3.900	3.921	3.855	3.953	4.112	4.198	4.156	4.056	4.172	4.115	170.40	176	3.210	1929
32	1500	88	1.614	88.8	.8	4.488	4.442	4.462	4.472	4.466	185.2	184.4	4.227	4.223	4.287	4.330	4.242	4.352	4.242	4.323	4.273	4.249	4.345	4.297	179	181.7	3.343	0
33	1500	88.3	1.629	89.3	1.0	4.318	4.299	4.304	4.307	4.307	179.9	178.9	4.037	3.885	3.963	4.106	4.058	4.129	4.085	4.078	4.061	4.100	4.182	4.191	172.3	175.6	3.262	427
34	1500	86.9	1.59	88	1.1	4.307	4.276	4.282	4.297	4.289	179.3	178.2	3.905	3.754	3.888	4.023	3.941	4.023	4.049	4.019	4.039	4.049	4.136	4.162	169.6	173.9	3.222	726
35	1500	89	1.65	90	1.0	4.389	4.358	4.372	4.385	4.376	182.2	181.2	3.948	3.890	3.978	4.078	3.990	4.090	4.158	4.185	4.183	4.150	4.265	4.261	172.8	177	3.280	1028
36	1500	89.1	1.656	90.2	1.1	4.535	4.514	4.519	4.525	4.523	187.1	186	4.012	4.013	4.062	4.133	4.050	4.157	4.263	4.331	4.313	4.250	4.372	4.345	176	181	3.333	1529
37	1500	90.7	1.704	91.8	1.1	4.883	4.841	4.860	4.864	4.862	188.4	187.3	4.230	4.282	4.268	4.282	4.148	4.300	4.640	4.677	4.613	4.400	4.587	4.570	182.7	185	3.384	1749

TABLE III (CONT'D)

TEMPERATURE DATA: SERIES B

Run No.	Speed N rpm	Ambient Temp. °F	Calibrating Thermocouple m.v.	°F	Correction °F	Journal Thermocouple Readings 1 m.v.	2 m.v.	3 m.v.	4 m.v.	Average Temperature T_J m.v.	°F	Corrected Temp. °F T_J	Bearing Thermocouple Readings - m.v. Position - 0 6	7	8	Position - 3 9	10	11	Position -1 12	13	14	Position - 2 15	16	17	Average T_B	T_{av}	Housing Temp. m.v.	Load lbs.
38	500	84.2	1.488	84.2	0	3.886	3.746	3.754	3.842	3.807	163.2	163.2	3.664	3.718	3.722	3.790	3.668	3.782	3.664	3.759	3.692	3.673	3.782	3.752	160.4	161.8	3.081	0
39	500	84.8	1.510	85	0.2	3.557	3.622	3.582	3.584	3.586	155.9	155.7	3.362	3.260	3.361	3.438	3.357	3.432	3.453	3.518	3.517	3.431	3.536	3.5 7	150.9	153.4	2.898	427
40	500	84.4	1.501	84.7	0.3	3.524	3.509	3.501	3.514	3.512	153.4	153.1	3.241	3.224	3.243	3.284	3.256	3.276	3.402	3.426	3.420	3.398	3.417	3.406	147.4	150.25	2.922	835
41	500	85.8	1.552	86.4	0.6	3.637	3.626	3.620	3.624	3.6267	157.2	156.6	3.372	3.288	3.400	3.458	3.382	3.456	3.508	3.580	3.582	3.482	3.590	3.608	152	154.3	2.968	1436
42	500	86.6	1.564	86.8	0.2	3.761	3.767	3.754	3.763	3.761	161.7	161.5	3.440	3.379	3.471	3.523	3.448	3.528	3.578	3.659	3.657	3.549	3.667	3.679	154.8	158.1	2.997	2036
43	500	86.4	1.555	86.5	0.1	3.790	3.794	3.788	3.792	3.791	162.7	162.6	3.459	3.408	3.506	3.539	3.472	3.547	3.631	3.715	3.715	3.608	3.712	3.708	155.8	159.2	3.002	2640
44	500	86.4	1.558	86.6	0.2	3.882	3.870	3.829	3.907	3.871	165.4	165.2	3.604	3.588	3.596	3.636	3.586	3.656	3.728	3.822	3.814	3.703	3.823	3.766	159.4	162.3	3.012	3237
45	750	86.2	1.548	86.2	0	4.173	4.179	4.164	4.170	4.171	175	175	3.922	3.950	3.985	4.059	3.933	4.055	3.919	4.010	3.944	3.938	4.050	4.018	169	172	3.263	0
46	750	86.6	1.56	87	0.4	3.922	3.903	3.872	3.863	3.890	166	165.6	3.621	3.582	3.585	3.847	3.790	3.866	3.800	3.870	3.829	3.594	3.633	3.679	160.2	163	3.174	427
47	750	87.4	1.584	87.8	.4	3.855	3.821	3.792	3.804	3.818	163.6	163.2	3.516	3.330	3.517	3.630	3.450	3.600	3.652	3.682	3.698	3.632	3.729	3.779	156.6	160	3.042	835
48	750	87.4	1.584	87.8	.4	3.906	3.900	3.88	3.86	3.886	165.9	165.5	3.516	3.33	3.537	3.634	3.533	3.613	3.712	3.741	3.763	3.669	3.770	3.820	157.5	161.5	3.058	1436
49	750	88	1.596	88.2	0.2	4.019	4.029	3.952	3.942	3.985	169.2	169	3.640	3.413	3.675	3.739	3.650	3.714	3.882	3.899	3.938	3.822	3.906	3.950	162	165.5	3.177	2036
50	750	87.8	1.591	88.05	0.25	4.029	4.026	3.974	3.968	3.999	169.35	169.1	3.703	3.470	3.727	3.761	3.681	3.748	3.948	3.962	4.008	3.868	3.963	4.00	163.7	166.4	3.182	2640
51	750	88.0	1.593	88.10	0.10	4.142	4.161	3.984	3.956	4.060	171.7	171.6	3.717	3.677	3.764	3.803	3.692	3.805	4.014	4.064	4.064	3.885	4.042	4.059	165.8	168.7	3.203	3237
52	1000	87.7	1.587	87.9	.2	4.572	4.570	4.562	4.568	4.568	188.6	188.4	4.279	4.307	4.347	4.422	4.288	4.426	4.271	4.364	4.297	4.292	4.410	4.368	181	184.7	3.492	0
53	1000	89.3	1.644	89.8	.5	4.393	4.332	4.342	4.338	4.351	181.4	180.9	4.025	3.850	3.968	4.114	4.048	4.118	4.048	4.081	4.075	4.072	4.174	4.205	171.8	176.3	3.344	427
54	1000	88	1.59	88	0	4.186	4.164	4.154	4.107	4.152	174.4	174.4	3.79	3.543	3.780	3.919	3.840	3.907	3.947	3.938	3.979	3.952	4.033	4.082	166.3	170.3	3.268	927
55	1000	90.5	1.665	90.5	0	4.378	4.353	4.342	4.365	4.359	181.6	181.6	3.850	3.613	3.879	3.999	3.929	3.992	4.086	4.096	4.147	4.093	4.163	4.197	169.6	175.6	3.413	1427
56	1000	88.6	1.62	89	.4	4.399	4.379	4.389	4.384	4.387	182.6	182.2	3.883	3.55	3.883	4.005	3.919	3.980	4.140	4.139	4.196	4.090	4.176	4.192	170	176.1	3.40	2025
57	1000	88.6	1.632	89.4	.8	4.503	4.494	4.501	4.490	4.497	186	185.2	3.948	3.605	3.969	4.068	3.968	4.040	4.253	4.238	4.306	4.165	4.258	4.319	172.8	179	3.450	2726
58	1000	88.7	1.632	89.4	.7	4.638	4.621	4.619	4.640	4.629	190.6	189.9	4.171	3.809	4.200	4.260	4.171	4.241	4.482	4.482	4.561	4.386	4.482	4.535	180	184.9	3.620	3429
59	1250	87	1.56	87	0	4.882	4.878	4.796	4.819	4.828	197.2	197.2	4.489	4.458	4.521	4.616	4.505	4.622	4.486	4.551	4.480	4.506	4.600	4.557	187.4	192.3	3.713	0
60	1250	87	1.572	87.4	.4	4.540	4.538	4.529	4.519	4.531	187.4	187	4.187	3.930	4.127	4.268	4.235	4.278	4.233	4.208	4.253	4.278	4.34	4.372	177.2	182.1	3.569	427
61	1250	86.2	1.566	87.2	1.0	4.508	4.480	4.473	4.498	4.489	186	185	3.978	3.692	3.980	4.118	4.068	4.113	4.168	4.122	4.205	4.192	4.248	4.290	173	179	3.511	835
62	1250	88.3	1.629	89.3	1.0	4.603	4.609	4.607	4.605	4.606	189.9	188.9	4.090	3.892	4.138	4.256	4.200	4.267	4.346	4.369	4.422	4.382	4.452	4.447	178.7	183.8	3.698	1436
63	1250	89	1.656	90.2	1.2	4.738	4.760	4.754	4.776	4.757	194.8	193.6	4.181	4.012	4.242	4.328	4.234	4.296	4.507	4.557	4.588	4.512	4.580	4.550	182.4	188	3.890	2036
64	1250	86.9	1.587	87.9	1.0	4.828	4.679	4.759	4.878	4.811	196.7	195.7	4.261	4.064	4.327	4.358	4.317	4.372	4.614	4.618	4.661	4.600	4.623	4.598	184.7	189.2	4.003	2640
65	1500	87.9	1.592	88	0.1	5.131	5.210	5.150	5.184	5.168	208.6	208.5	4.767	4.725	4.801	4.901	4.780	4.908	4.769	4.831	4.760	4.787	4.882	4.837	196.7	202.6	3.872	0
66	1500	88.3	1.632	89.4	1.1	4.897	4.943	4.905	4.955	4.925	200.5	199.4	4.397	4.269	4.498	4.574	5.558	4.566	4.514	4.548	4.552	4.587	4.688	4.636	187.4	193.4	3.614	427
67	1500	88.8	1.638	89.6	0.8	4.847	4.891	4.881	4.889	4.877	198.9	198.1	4.213	4.187	4.224	4.420	4.402	4.426	4.471	4.480	4.483	4.542	4.585	4.568	183.5	190.8	3.498	835
68	1500	89.5	1.659	90.3	.8	4.903	4.910	4.919	4.932	4.916	200.2	199.4	4.241	4.203	4.261	4.432	4.419	4.439	4.559	4.564	4.572	4.627	4.658	4.635	185.2	192.3	3.522	1436
69	1500	89.8	1.674	90.8	1.0	5.001	4.997	5.008	5.018	5.006	203.2	202.2	4.314	4.245	4.326	4.578	4.561	4.583	4.684	4.695	4.712	4.784	4.821	4.792	189.3	195.8	3.589	2036
70	1500	89.9	1.671	90.7	0.8	5.110	5.108	5.112	5.126	5.114	206.8	206	4.417	4.325	4.476	4.614	4.588	4.628	4.767	4.774	4.793	4.872	4.921	4.883	192	199	3.677	2640
71	1500	91.2	1.713	92.1	0.9	5.257	5.245	5.278	5.288	5.267	211.9	211	4.499	4.388	4.583	4.676	4.620	4.714	5.002	5.041	5.047	5.069	5.122	5.079	197	204	3.722	3237

TEMPERATURE DATA: SERIES C

Run No.	Speed N rpm	Ambient Temp. °F	Thermocouple m.v.	°F	Correction °F	Journal Thermocouple Readings 1 m.v.	2 m.v.	3 m.v.	4 m.v.	Average Temperature T_J m.v.	°F	Corrected Temp. °F T_J	Bearing Thermocouple Readings - m.v. Position - 0 6	7	8	Position - 3 9	10	11	Position - 1 12	13	14	15	16	17	Average T_B m.v.	°F	T_{av}	Housing Temp. m.v.
72	750	75	1.232	75.4	.4	2.124	2.065	2.107	2.112	2.102	105.4	105	2.051	2.040	2.040	2.110	2.090	2.130	1.974	2.01	1.902	2.020	2.050	1.980	2.033	103	104	1.675
73	1000	75.6	1.256	76.2	.6	2.407	2.377	2.394	2.402	2.395	115.5	114.9	2.328	2.295	2.302	2.395	2.377	2.417	2.22	2.261	2.129	2.281	2.310	2.230	2.295	112.1	113.5	1.860
74	1250	76.6	1.289	77.3	.7	2.703	2.671	2.691	2.699	2.691	125.7	125	2.651	2.604	2.621	2.729	2.709	2.752	2.520	2.570	2.433	2.592	2.633	2.543	2.613	123	124	2.113
75	1500	77.5	1.300	78.5	1.0	2.593	2.562	2.577	2.588	2.580	122	121	2.445	2.372	2.410	2.395	2.407	2.430	2.410	2.427	2.190	2.388	2.362	2.375	2.384	115	118	1.468

TABLE IV

OIL FLOW DATA: SERIES A

Run No.	Speed N rpm	Oil Outlet Thermocouple Readings m.v.	m.v.	Avg. Outlet Oil Temp. m.v.	°F	Inlet Oil Thermocouple Reading m.v.	Inlet Oil Temp. °F	Oil Flow Rate lb/hr.
1	500	2.474	2.478	2.476	118.2	1.534	85.8	1.2
2	500	2.454	2.492	2.473	118.1	1.546	86.2	2.95
3	500	2.489	2.517	2.503	119.1	1.549	86.3	3.80
4	500	2.502	2.522	2.512	119.4	1.558	86.6	4.2
5	500	2.512	2.528	2.52	120	1.564	86.8	4.35
6	500	2.518	2.546	2.532	120.4	1.561	86.7	4.50
7	500	2.531	2.569	2.550	121.0	1.564	86.8	4.65
8	750	2.797	2.843	2.820	130	1.468	83.6	1.59
9	750	2.782	2.828	2.805	129.5	1.495	84.5	3.5
10	750	2.789	2.809	2.799	129.3	1.516	85.2	3.96
11	750	2.792	2.818	2.805	129.5	1.528	85.6	4.6
12	750	2.741	2.779	2.76	128	1.537	85.9	4.98
13	750	2.788	2.816	2.802	129.4	1.546	86.2	5.48
14	750	2.794	2.840	2.817	129.9	1.549	86.3	5.4
15	750	2.832	2.868	2.850	131	1.560	87	5.61
16	750	2.820	2.850	2.835	130.5	1.546	86.2	5.64
17	1000	3.174	3.226	3.200	143	1.495	84.5	1.95
18	1000	3.015	3.081	3.048	137.6	1.522	85.4	3.8
19	1000	2.989	3.019	3.004	136.1	1.513	85.1	4.65
20	1000	3.021	3.087	3.054	137.8	1.522	85.4	5.49
21	1000	3.024	3.066	3.045	137.5	1.510	85	5.75
22	1000	3.011	3.031	3.021	136.7	1.477	83.9	5.97
23	1000	3.030	3.072	3.051	137.7	1.495	84.5	6.22
24	1250	3.401	3.425	3.413	150.2	1.507	84.9	2.325
25	1250	3.321	3.367	3.344	147.8	1.510	85	4.05
26	1250	3.318	3.322	3.320	147	1.534	85.8	4.80
27	1250	3.219	3.241	3.230	144	1.531	85.7	5.40
28	1250	3.244	3.294	3.269	145.3	1.540	86	5.60
29	1250	3.272	3.296	3.284	145.8	1.540	86	5.88
30	1250	3.291	3.331	3.311	146.7	1.552	86.4	6.0
31	1250	3.199	3.211	3.205	146.5	1.540	86	6.3
32	1500	3.641	3.689	3.665	158.5	1.590	88	2.64
33	1500	3.521	3.665	3.593	156.1	1.593	88.1	4.72
34	1500	3.520	3.528	3.524	153.8	1.546	86.2	5.60
35	1500	3.574	3.660	3.617	156.9	1.563	87.1	6.0
36	1500	3.644	3.710	3.677	158.9	1.596	88.2	6.85
37	1500	3.670	3.714	3.692	159.4	1.602	88.4	7.0

TABLE IV (CONT'D)

OIL FLOW DATA: SERIES B

Run No.	Speed N rpm	Oil Outlet Thermocouple Readings m.v.	m.v.	Avg. Outlet Oil Temp. m.v.	°F	Inlet Oil Thermocouple Reading m.v.	Inlet Oil Temp. °F	Oil Flow Rate lb/hr
38	500	3.295	3.405	3.35	148	1.486	84.2	1.48
39	500	3.224	3.362	3.293	146.1	1.486	84.2	3.75
40	500	3.198	3.220	3.209	143.3	1.480	84	4.75
41	500	3.214	3.330	3.272	145.4	1.501	84.7	5.25
42	500	3.327	3.403	3.365	148.5	1.510	85	5.30
43	500	3.400	3.438	3.419	150.3	1.519	85.3	5.40
44	500	3.425	3.509	3.467	151.9	1.516	85.2	5.50
45	750	3.597	3.607	3.602	156.4	1.546	86.2	2.05
46	750	3.449	3.533	3.491	152.7	1.549	86.3	4.4
47	750	3.451	3.477	3.464	151.8	1.561	86.7	5.4
48	750	3.498	3.526	3.512	153.4	1.561	86.7	5.83
49	750	3.548	3.596	3.572	155.4	1.564	86.8	6.1
50	750	3.602	3.644	3.623	157.1	1.561	86.7	6.25
51	750	3.619	3.645	3.632	157.4	1.552	86.4	6.65
52	1000	3.866	3.914	3.890	166	1.552	86.4	2.33
53	1000	3.744	3.790	3.767	161.9	1.567	86.9	5.15
54	1000	3.858	3.898	3.878	165.6	1.558	86.6	6.15
55	1000	3.908	3.950	3.929	167.3	1.587	87.9	6.65
56	1000	3.933	3.979	3.956	168.2	1.566	87.2	6.85
57	1000	3.964	4.014	3.989	169.3	1.563	87.1	7.05
58	1000	4.002	4.024	4.013	170.1	1.563	87.1	7.25
59	1250	4.008	4.192	4.100	173	1.560	87	2.92
60	1250	3.829	3.879	3.854	164.8	1.563	87.1	5.50
61	1250	3.767	3.815	3.791	162.7	1.560	87	6.90
62	1250	3.859	3.909	3.884	165.8	1.566	87.2	7.40
63	1250	3.941	3.995	3.958	168.6	1.578	87.6	8.1
64	1250	3.962	3.998	3.980	169	1.560	87	8.3
65	1500	4.237	4.287	4.262	178.4	1.599	88.3	3.44
66	1500	3.974	4.016	3.995	169.5	1.605	88.5	6.10
67	1500	4.010	4.046	4.028	170.6	1.608	88.6	7.35
68	1500	4.101	4.153	4.127	173.9	1.617	88.9	8.15
69	1500	4.149	4.249	4.199	176.3	1.617	88.9	8.5
70	1500	4.201	4.245	4.223	177.1	1.62	89	8.75
71	1500	4.304	4.346	4.325	180.5	1.65	90	8.8

OIL FLOW AND WATER FLOW DATA

SERIES C

Run No.	Speed N rpm	Oil Flow Rate lb/hr	Outlet Oil Thermocouple Readings m.v.	m.v.	Outlet Oil Temp. m.v.	°F	Inlet Oil Temp. m.v.	°F	Water Flow Rate lb/hr	Outlet Water Temp. m.v.	°F	Inlet Water Temp. m.v.	°F
72	750	1.09	1.700	1.688	1.694	91.5	1.175	73.5	29.1	1.80	95	.838	61.6
73	1000	1.50	1.915	1.878	1.896	98.5	1.193	74.1	29.2	2.147	106.9	.805	60.5
75	1250	1.80	2.191	2.163	2.177	108.2	1.262	76.4	29.2	2.417	116.2	.838	62
75	1500	1.94	1.97	1.94	1.955	100.5	1.235	76.5	133.2	1.136	72.2	.581	52.7

TABLE V

CALCULATION OF THE SOMMERFELD NUMBER,
THE LOAD NUMBER, AND THE ECCENTRICITY RATIO

SERIES - A

Run No.	N rpm	N' rps	T_{av} °F	μ C.S.	$\mu \times 10^{-7}$ Reyn.	W lbs.	p lbs/in^2	$c_d \times 10^{-3}$ in.	$\frac{d}{cd} \times 10^2$	$(\frac{d}{cd})^2_{10^5}$	S	1/S	n
1	500	8.34	128	54	67.2	12.83	.855	6.13	4.98	2.48	16.25	.0616	0
2	500	8.34	125.5	59	73.4	427	28.5	6.13	4.98	2.48	.533	1.878	.17
3	500	8.34	126.3	57	70.9	927	61.8	6.13	4.98	2.48	.237	4.22	.33
4	500	8.34	128.4	54	67.2	1427	95	6.13	4.98	2.48	.1462	6.84	.425
5	500	8.34	129.7	53.3	66.3	1727	115	6.13	4.98	2.48	.1192	8.4	.48
6	500	8.34	134.7	48	59.8	2127	141.8	6.13	4.98	2.48	.0873	11.47	.54
7	500	8.34	135.3	47	58.5	2627	175	6.13	4.98	2.48	.0691	14.5	.58
8	750	12.5	143.5	40	51	12.83	.855	6.26	4.80	2.30	20.10	.0498	0
9	750	12.5	138.6	45	56	427	28.5	6.26	4.80	2.30	.565	1.77	.170
10	750	12.5	139.2	44	54.8	727	48.5	6.26	4.80	2.30	.325	3.08	.26
11	750	12.5	140	43	53.55	1029	68.65	6.26	4.80	2.30	.224	4.46	.34
12	750	12.5	141.45	42	52.1	1330	88.6	6.26	4.80	2.30	.169	5.92	.40
13	750	12.5	142.7	41	51	1630	108.75	6.26	4.8	2.3	.1348	7.42	.45
14	750	12.5	145	39	48.6	2030	135.2	6.26	4.8	2.3	.1031	9.7	.505
15	750	12.5	147.1	37.5	46.64	2429	162	6.26	4.8	2.3	.0827	12.1	.545
16	750	12.5	148.4	37	46	2780	185	6.26	4.8	2.3	.0714	14	.57
17	1000	16.67	157.5	31	38.6	12.83	.855	6.36	4.72	2.225	16.74	.0598	0
18	1000	16.67	155.7	32	39.8	427	28.5	6.36	4.72	2.225	.516	1.94	.175
19	1000	16.67	154.1	32.8	40.8	927	61.8	6.36	4.72	2.225	.2447	4.09	.31
20	1000	16.67	157.6	31	38.6	1427	95	6.36	4.72	2.225	.1505	6.65	.41
21	1000	16.67	159.6	30	37.35	2027	135	6.36	4.72	2.225	.1025	9.75	.51
22	1000	16.67	160.9	29.4	36.6	2631	175.5	6.36	4.72	2.225	.0774	12.92	.56
23	1000	16.67	165.2	27	33.6	3329	222	6.36	4.72	2.225	.0561	17.81	.615
24	1250	20.81	169.1	25	31.1	12.83	.855	6.436	4.665	2.175	16.5	.0606	0
25	1250	20.81	165	27	33.6	427	28.5	6.436	4.665	2.175	.526	1.90	.18
26	1250	20.81	166	26.5	33	625	41.6	6.436	4.665	2.175	.359	2.785	.25
27	1250	20.81	167.5	26	32.4	826	55.1	6.436	4.665	2.175	.266	3.76	.305
28	1250	20.81	168.5	25.5	31.75	1027	68.5	6.436	4.665	2.175	.210	4.76	.36
29	1250	20.81	170	25	31.1	1227	81.8	6.436	4.665	2.175	.172	5.81	.397
30	1250	20.81	173	23.5	29.25	1427	95	6.436	4.665	2.175	.1392	7.17	.445
31	1250	20.81	176	22	27.35	1929	128.3	6.436	4.665	2.175	.0965	10.4	.520
32	1500	25	181.7	20.5	25.5	12.83	.855	6.498	4.62	2.13	15.9	.0629	0
33	1500	25	175.6	22.5	28	427	28.5	6.498	4.62	2.13	.524	1.91	.187
34	1500	25	173.9	23.5	29.25	726	48.4	6.498	4.62	2.13	.322	3.108	.27
35	1500	25	177	21.5	26.75	1028	68.55	6.498	4.62	2.13	.208	4.81	.36
36	1500	25	181	20.5	25.5	1529	102	6.498	4.62	2.13	.1332	7.50	.455
37	1500	25	185	19.3	24	1749	116.2	6.498	4.62	2.13	.110	9.10	.50

TABLE V (CONT'D)

CALCULATION OF THE SOMMERFELD NUMBER,
THE LOAD NUMBER, AND THE ECCENTRICITY RATIO

SERIES - B

Run No.	N rpm	N' rps	T_{av} °F	μ C.S.	$\mu \times 10^{-7}$ Reyn.	W lbs.	p lbs/in^2	$c_d \times 10^{-3}$ in.	$\frac{d}{cd} \times 10^2$	$(\frac{d}{cd})^2 10^5$	S	1/S	n
38	500	8.34	161.8	28.85	35.9	12.83	.855	6.335	4.745	2.25	7.9	.127	0
39	500	8.34	153.4	34	42.3	427	28.5	6.335	4.745	2.25	.2785	3.59	.27
40	500	8.34	150.25	35	43.6	835	55.7	6.335	4.745	2.25	.147	6.8	.435
41	500	8.34	154.3	33	41.1	1436	95.6	6.335	4.745	2.25	.0806	12.4	.555
42	500	8.34	158.1	30.6	38.1	2036	135.7	6.335	4.745	2.25	.0528	19.0	6.3
43	500	8.34	159.2	30	37.4	2640	176	6.335	4.745	2.25	.0398	25.1	6.7
44	500	8.34	162.3	28.5	35.5	3237	215	6.335	4.745	2.25	.031	32.3	7.09
45	750	12.5	172	24	29.8	12.83	.855	6.44	4.66	2.17	9.44	.106	0
46	750	12.5	163	27.5	34.2	427	28.5	6.44	4.66	2.17	.326	3.076	.266
47	750	12.5	160	29.5	36.7	835	55.7	6.44	4.66	2.17	.1783	5.64	.392
48	750	12.5	161.5	28.5	35.45	1436	95.6	6.44	4.66	2.17	.1005	9.95	.51
49	750	12.5	165.5	26.5	33	2036	135.6	6.44	4.66	2.17	.066	15.15	.59
50	750	12.5	166.4	26.3	32.7	2640	176	6.44	4.66	2.17	.0504	19.87	.632
51	750	12.5	168.7	25.5	31.74	3237	215	6.44	4.66	2.17	.040	25	.67
52	1000	16.67	183.75	19.8	24.6	12.83	.855	6.55	4.58	2.1	10	0.10	0
53	1000	16.67	176.3	22.5	28	427	28.5	6.55	4.58	2.1	.276	3.62	.3
54	1000	16.67	170.3	24.7	30.8	927	61.8	6.55	4.58	2.1	.14	7.15	.445
55	1000	16.67	175.6	22.7	28.25	1427	95	6.55	4.58	2.1	.0835	12	.55
56	1000	16.67	176.1	22.5	28	2025	135	6.55	4.58	2.1	.0583	17.15	.612
57	1000	16.67	179	21	26.15	2726	181.8	6.55	4.58	2.1	.0404	24.75	.668
58	1000	16.67	184.9	19.6	24.4	3429	228.5	6.55	4.58	2.1	.03	33.3	.713
59	1250	20.81	192.3	17.5	21.8	12.82	.855	6.55	4.56	2.079	11.04	.0905	0
60	1250	20.81	182.1	20	24.9	427	28.5	6.55	4.56	2.079	.3786	2.64	.24
61	1250	20.81	179	21	26.1	835	55.7	6.55	4.56	2.079	.203	4.938	.365
62	1250	20.81	183.8	19.5	24.25	1436	95.6	6.55	4.56	2.079	.11	9.1	.492
63	1250	20.81	188	18.5	23	2036	135.7	6.55	4.56	2.079	.0735	13.62	.570
64	1250	20.81	189.2	18.2	22.75	2640	176	6.55	4.56	2.079	.056	17.88	.62
65	1500	25	202.6	15	18.65	12.83	.855	6.66	4.5	2.03	11.08	.093	0
66	1500	25	193.4	17.1	21.3	427	28.5	6.66	4.5	2.03	.379	2.64	.24
67	1500	25	190.8	18	22.4	835	55.7	6.66	4.5	2.03	.204	4.9	.37
68	1500	25	192.3	17.5	21.78	1436	95.6	6.66	4.5	2.03	.1146	8.65	.49
69	1500	25	195.8	16.75	20.82	2036	135.7	6.66	4.5	2.03	.0781	12.8	.56
70	1500	25	199	15.9	19.8	2640	176	6.66	4.5	2.03	.0571	17.5	.615
71	1500	25	204	14.7	18.3	3237	215	6.66	4.5	2.03	.0433	23.1	.656

TABLE VI

SUMMARY OF CORRELATION CALCULATIONS

SERIES A

Run No.	Speed N rpm	ΔT °F	S	1/S	n	H_o BTU/hr	H_c BTU/hr	H_p BTU/hr	H_o/H_p	H_c/H_p	$\frac{H_o+H_c}{H_p}$	H_J	H_J/H_p	$\frac{\mu Q}{c^3 p}\sqrt{\frac{N}{500}}$
1	500	42.2	16.25	0.0616	0	20	226	246	.081	.918	.999	246	1	2.96
2	500	38.6	.533	1.878	.17	48.5	195	246	.197	.792	.989	251.7	1.021	.238
3	500	39.35	.237	4.22	.33	64.2	203	246	.262	.825	1.087	268.65	1.091	.1363
4	500	41.3	.1462	6.84	.425	71.0	220	246	.289	.895	1.184	288.1	1.170	.093
5	500	42.8	.1192	8.4	.48	74.4	231	246	.303	.938	1.241	301	1.222	.0786
6	500	45	.0873	11.47	.54	78.0	249.5	246	.317	1.012	1.329	320.5	1.300	.0596
7	500	47	.0691	14.5	.58	82.0	264.3	246	.333	1.0715	1.404	336.8	1.370	.0487
8	750	59.9	20.1	.0498	0	38	372	410	.0926	.907	.999	410	1	3.06
9	750	54.5	.565	1.77	.17	81	327	410	.1975	.7965	.994	419.42	1.021	.2478
10	750	54.4	.325	3.08	.26	90	326	410	.2194	.795	1.014	432.64	1.053	.1622
11	750	54.8	.224	4.46	.34	104	328	410	.2536	.80	1.053	451.45	1.100	.130
12	750	55.85	.169	5.92	.4	108	338	410	.2634	.825	1.088	469.4	1.144	.106
13	750	57.1	.1348	7.42	.45	122	350	410	.2978	.854	1.151	489.8	1.191	.093
14	750	59.3	.1031	9.7	.505	121	368	410	.295	.8965	1.191	514.65	1.252	.0704
15	750	61.1	.0827	12.1	.545	127	388	410	.310	.946	1.256	537.5	1.308	.0584
16	750	63.3	.0714	14	.57	128.5	404	410	.314	.985	1.299	556.2	1.355	.0506
17	1000	73	16.74	.0598	0	58.7	484.3	543	.109	.910	1.019	543	1	3.10
18	1000	67	.516	1.94	.175	102	439	543	.1915	.8075	.999	551.68	1.012	.21
19	1000	67.1	.2447	4.09	.31	122	440	543	.227	.81	1.037	583.05	1.072	.121
20	1000	69.1	.1505	6.65	.41	148	459.6	543	.275	.845	1.120	621.6	1.141	.0876
21	1000	73.6	.1025	9.75	.51	155	500	543	.288	.920	1.208	678.9	1.249	.0628
22	1000	77	.0774	12.92	.56	162	535.7	543	.301	.984	1.285	721.75	1.328	.0491
23	1000	81.3	.0561	17.81	.615	170	581.5	543	.316	1.070	1.386	775.5	1.427	.0372
24	1250	84.2	16.5	.0606	0	81	606	687	.1179	.882	1.00	687	1.00	3.22
25	1250	79.1	.526	1.90	.18	131	559	687	.211	.814	1.025	704.1	1.025	.2032
26	1250	79.8	.359	2.785	.25	151	561	687	.233	.815	1.048	721.05	1.049	.162
27	1250	80.5	.266	3.76	.305	162	568	687	.25	.826	1.076	739.97	1.077	.1352
28	1250	81.5	.210	4.76	.36	171	578	687	.2675	.841	1.108	761.95	1.108	.1108
29	1250	82.2	.172	5.81	.397	181	589	687	.279	.856	1.135	780.75	1.136	.095
30	1250	84.2	.1392	7.17	.445	186	607.5	687	.294	.884	1.178	809.55	1.179	.0788
31	1250	88.8	.0965	10.4	.520	196	653	687	.313	.950	1.263	868.15	1.212	.0570
32	1500	93.7	15.9	.0629	0	94	707	801	.1174	.883	1.00	801	1.00	2.06
33	1500	87.3	.524	1.91	.187	165	640	801	.206	.799	1.005	821.63	1.025	.210
34	1500	87	.322	3.108	.27	195	634	801	.2436	.790	1.033	848.2	1.06	.153
35	1500	87	.208	4.81	.36	216	647	801	.27	.807	1.077	889.7	1.110	.106
36	1500	91.9	.1332	7.50	.455	249	688	801	.311	.859	1.170	956.5	1.193	.0775
37	1500	94.3	.110	9.1	.50	256	718	801	.3198	.895	1.214	994.3	1.24	.0654

TABLE VI (CONT'D)

SUMMARY OF CORRELATION CALCULATIONS

SERIES B

Run No.	Speed N rpm	ΔT °F	S	1/S	n	H_o BTU/hr	H_c BTU/hr	H_p BTU/hr	H_o/H_p	H_c/H_p	$\frac{H_o+H_c}{H_p}$	H_J	H_J/H_p	$\frac{\mu Q}{c\beta_p}\sqrt{\frac{N}{500}}$
38	500	77.6	7.9	.127	0	48.6	420	468.6	.1037	.9133	1.0170	468.6	1	1.76
39	500	68.6	.2785	3.59	.27	119.4	360	468.6	.255	.7682	1.0232	476.7	1.018	.157
40	500	65.85	.147	6.8	.435	145	340	468.6	.31	.7255	1.0355	492.3	1.05	.105
41	500	68.5	.0806	12.4	.555	164	360	468.6	.350	.7682	1.1182	513.4	1.094	.0637
42	500	71.5	.0528	19.0	.63	173.3	382	468.6	.370	.8151	1.1851	533.6	1.138	.0422
43	500	72.8	.0398	25	.67	180.4	390	468.6	.386	.8322	1.2182	550.4	1.173	.0325
44	500	75.9	.031	32.3	.709	188	412	468.6	.401	.8792	1.2802	566.9	1.210	.0256
45	750	85.8	9.44	.106	0	74.2	501	575.2	.1289	.8692	.9981	575.2	1	2.35
46	750	76.4	.326	3.076	.266	150	420	575.2	.2607	.7301	.9908	590	1.025	.1732
47	750	72.6	.1783	5.64	.392	181	390	575.2	.3146	.6780	0.9926	609.4	1.058	.117
48	750	74.1	.1005	9.95	.510	200	403	575.2	.3477	.7006	1.0483	642.1	1.114	.071
49	750	77.5	.066	15.15	.59	215	428	575.2	.3737	.7440	1.1177	672.9	1.168	.0489
50	750	78.4	.0504	19.87	.632	220.4	438	575.2	.383	.7614	1.1444	700.5	1.218	.03815
51	750	81	.040	25	.670	243	460	575.2	.4224	.7997	1.2221	719.6	1.25	.0323
52	1000	96	10	10	0	96.6	582.6	679.2	.1422	.8686	1.0108	679.2	1	2.42
53	1000	87	.276	3.62	.30	198.6	507	679.2	.2924	.7464	1.0388	703	1.033	.182
54	1000	82.3	.140	7.15	.445	248	470	679.2	.3651	.6919	1.0570	736.2	1.082	.1105
55	1000	85.1	.0835	12.0	.55	272	490	679.2	.400	.7214	1.1214	776.4	1.142	.0715
56	1000	87.5	.0583	17.15	.612	286	510	679.2	.421	.7508	1.1718	813.4	1.198	.0514
57	1000	90.4	.0404	24.75	.668	299	538	679.2	.44	.7921	1.2321	855.2	1.258	.03665
58	1000	96.2	.03	33.3	.713	302	580	679.2	.444	.8539	1.2979	895.2	1.318	.0279
59	1250	105.3	11.04	.0905	0	129	676.2	805.2	.160	.8320	.9920	805.2	1	3.02
60	1250	95.1	.378	2.64	.24	220	577	805.2	.273	.7165	.9895	827.3	1.028	.1898
61	1250	92.8	.203	4.938	.365	269	558	805.2	.334	.6929	1.0269	865.8	1.073	.1275
62	1250	95.5	.110	9.1	.492	300	580	805.2	.3725	.7203	1.0928	922.8	1.145	.0737
63	1250	99.0	.0735	13.62	.570	338	610	805.2	.420	.7575	1.1775	977.7	1.212	.0544
64	1250	102.3	.056	17.88	.620	350	635	805.2	.435	.7886	1.2236	1031.3	1.28	.0424
65	1500	114.7	11.08	.093	0	159.8	752.4	912.2	.175	.8243	0.9993	912.2	1	3.17
66	1500	105.1	.379	2.64	.24	254	680	912.2	.2785	.7454	1.0239	939	1.028	.191
67	1500	102	.204	4.9	.37	312	640	912.2	.342	.7016	1.0436	982.9	1.076	.124
68	1500	102.8	.1146	8.65	.49	357	645	912.2	.391	.7070	1.098	1052.8	1.152	.0780
69	1500	106	.0781	12.8	.56	383	670	912.2	.420	.7344	1.1544	1117.2	1.222	.0547
70	1500	109.1	.0571	17.5	.615	397	702	912.2	.4355	.7695	1.2050	1180.4	1.292	.0412
71	1500	112.8	.0433	23.10	.656	410	730	912.2	.450	.8002	1.2502	1239.4	1.358	.0332

SERIES C

Run No.	Speed N rpm	H_w BTU/hr	H_o BTU/hr	H_w+H_o BTU/hr	H_p BTU/hr	Percentage Error
72	750	973	10	983	1027	4.28
73	1000	1355	18.8	1373.8	1410	2.54
74	1250	1582	31.2	1613.2	1710	5.68
75	1500	2730	25	2755	2850	3.34

APPENDIX I

EXACT SOLUTION OF EQUATION (2.6) FOR THE NO HEATING CASE

$$e^{\beta'\Theta} \frac{d^2\Theta}{dY^2} = - \text{Pr. E.} \tag{2.6}$$

Let $$\text{Pr. E.} = \frac{1}{2} \eta^2 \beta' .$$

$\therefore$ $$\frac{d^2\Theta}{dY^2} = - \frac{1}{2} \eta^2 \beta' e^{-\beta'\Theta}$$

Multiplying both sides of the above equation by $2 \frac{d\Theta}{dY} dY$ one gets:

$$2 \frac{d\Theta}{dY} \frac{d^2\Theta}{dY^2} dY = - \eta^2 \beta' e^{-\beta'\Theta} \frac{d\Theta}{dY} \tag{I.1}$$

Integrating both sides yields:

$$\left(\frac{d\Theta}{dY}\right)^2 = \eta^2 e^{-\beta'\Theta} - \xi^2 .$$

$$\frac{d\Theta}{dY} = \pm \sqrt{\eta^2 e^{-\beta'\Theta} - \xi^2} \tag{I-2}$$

where ξ is a constant of integration.

Separating the variables and multiplying both sides of the above equation by $\eta \frac{\beta'}{2}$ one gets:

$$\frac{\eta \frac{\beta'}{2} e^{\beta'\Theta/2} d\Theta}{\pm \sqrt{\eta^2 - \xi^2 e^{\beta'\Theta}}} = \eta \frac{\beta'}{2} dY \tag{I-3}$$

Integrating one gets:

$$\sin^{-1} \frac{\xi e^{\beta'\Theta/2}}{\eta} = \eta \frac{\beta'}{2} Y + \delta ,$$

where δ is a constant of integration.

$\therefore$ $$\frac{\xi e^{\beta'\Theta/2}}{\eta} = \sin \left(\eta \frac{\beta'}{2} Y + \delta\right),$$

and $$\Theta = \frac{2}{\beta'} \ell n \frac{\eta}{\xi} \sin (\eta \frac{\beta'}{2} Y + \delta) \qquad (I.4)$$

This is the general solution of Equation (2.6).

Boundary Conditions

1) at $Y = 0$ $\quad \Theta = 0$

2) at $Y = 1$ $\quad \frac{d\Theta}{dY} = 0$, $\Theta = 1$

Applying the first boundary condition on Equation (I-4) one gets:

$$\sin \delta = \frac{\xi}{\eta} \qquad (I.5)$$

Applying the second boundary condition gives:

$$\left.\frac{d\Theta}{dY}\right|_{Y=1} = \frac{2}{\beta'} \frac{\eta \frac{\beta'}{2} \cos (\eta \frac{\beta'}{2} + \delta)}{\sin (\eta \frac{\beta'}{2} + \delta)} = \eta \cot(\eta \frac{\beta'}{2} + \delta) = 0 ,$$

which has $\eta \frac{\beta'}{2} + \delta = \frac{\pi}{2}$ as a solution.

$$\therefore \quad \delta = \frac{\pi}{2} - \eta \frac{\beta'}{2}$$

and $$\cos \eta \frac{\beta'}{2} = \sin \delta = \frac{\xi}{\eta} \qquad (I.6)$$

From Equation (I-6), the values of δ and $\frac{\eta}{\xi}$ can be determined for different values of the nondimensional number $\eta \frac{\beta'}{2}$. The result of the calculations is shown in Table VII.

To determine the temperature difference between the journal and bearing surfaces, the following substitution is made in Equation (I-4)

$$\Theta = 1 \quad \text{at } Y = 1$$

$$1 = \frac{2}{\beta'} \ell n \frac{\eta}{\xi} \sin (\eta \frac{\beta'}{2} + \delta)$$

But $$\beta' = \beta(T_J - T_B)$$

$$T_J - T_B = \frac{2}{\beta} \ell n \frac{\eta}{\xi} \sin (\eta \frac{\beta'}{2} + \delta) \qquad (I.7)$$

The above equation was used in the determination of the temperature difference between the journal and the bearing surface. The result of the calculations is given in Table VII. It is noted that the results obtained, using the exact solution, are higher than those from the approximate theory represented in Chapter II. The maximum relative difference is about 13 percent. This is due to the neglect of the higher order term in the linearization process of Equation (2.6).

Comparison Between the Theoretical and Experimental Temperature Difference $(T_J - T_B)$

From Table VII, it is seen that the maximum experimental temperature difference is higher than the theoretical by about 20 percent. This discrepancy can be attributed to the following:

1. The introduction of simplified assumptions, such as the neglect of the end leakage and the adoption of a linear velocity distribution, in carrying out the mathematical analysis.
2. The assumption that the clearance space is completely filled with oil is doubtful, especially when the oil is fed through a single hole in the bearing under low pressure. This explains the reason for the high values of the temperature difference $(T_J - T_B)$ obtained experimentally.

TABLE VII

CALCULATION OF THE TEMPERATURE DIFFERENCE ($T_J - T_B$)

N rpm 1	δ 2	η/ξ 3	$T_J - T_B$ Theoretical 4	$T_J - T_B$ Exp. 5	$T_J - T_B$ Approx. 6	Percent Difference (5-4)/4
500	1.416	1.012	1.340	1.60	1.21	19.4
750	1.373	1.021	2.28	2.70	2.23	19.5
1000	1.338	1.03	3.37	3.6	3.00	6.84
1250	1.307	1.037	4.10	4.5	3.80	9.75
1500	1.287	1.042	4.67	5.4	4.38	15

BIBLIOGRAPHY

1. Barwell, F. T., Trans. A.S.M.E., 77, 1178 (1955).

2. Burwell, J. T., "Effect of Diametrical Clearance on the Load Capacity of a Journal Bearing," Trans. A.S.M.E., 64, 458, 1942.

3. Boyd, J. and Robertson, B. P., "Oil Flow and Temperature Relations in Lightly Loaded Journal Bearing," Trans. A.S.M.E., 70, 257-262, 1948.

4. Cameron, A., "Heat Transfer in Journal Bearings: A Preliminary Investigation," Proc. General Discussion on Heat Transfer, arranged by I.M.E. and A.S.M.E., 194-197, 1951.

5. Christopherson, D. G., "A New Mathematical Method for the Solution of Film Lubrication Problems," Proc. I.M.E., 146, 126, 1941.

6. Clayton, D., and Wilkie, M. J., "Temperature Distribution in the Bush of a Journal Bearing," Engineering, 166, 49, 1948.

7. Cope, W. F., "The Hydrodynamical Theory of Film Lubrication," Proc. Royal Society of London, Series A, 197, 201, 1949.

8. Cordullo, F. E., "Some Practical Deductions from Theory of Lubrication of Short Cylindrical Bearings," Trans. A.S.M.E., MSP-52-12, 52, 143-153, 1930.

9. Dizioglu, B., "Temperatur-, Zahigkeits-und Reibungsverhaltnisse in raschlaufenden Gleitlagern," 50 Jahre Grenzschichtforschung, F. Viewey and Sohn, 241, 1954.

10. Hagg, A. C., "Heating Effects in Lubricating Films," J. Applied Mechanics, 11, A72-A76, 1944.

11. Lasche, O., "Die Reibungsverhaltnisse in Lagern mit Hoher Umfangsgeschwindigkeit," Forschungsh. Ver. dtsh. Ing., 46, 1881-1890, 1932-1938, and 1961-1971, 1902.

12. Leeds and Northrup, Conversion Tables for Thermocouple, Issue 2.

13. McKee, S. A., "Friction and Temperature as Criteria for Safe Operation of Journal Bearings," Nat. Bur. Stds. J. Res., 24, 491, 1940.

14. Michell, A. G. M., "Progress in Fluid-Film Lubrication," Trans. A.S.M.E., MSP-51-21, 51, 153-163, 1929.

15. Muskat, M., and Morgan, F., "Temperature Behaviour of Journal Bearing Systems," J. Applied Mechanics, 10, A131-A138, 1943.

BIBLIOGRAPHY (CONT'D)

16. Muskat, M., and Morgan, F., "The Theory of Thick Film Lubrication of a Complete Journal Bearing, of Finite Length with Arbitrary Positions of the Lubricant Source," J. Applied Physics, 10, 51 and 60, 1939.

17. Ocvirk, F. W., and DuBois, G. B., "Experimental Investigation of Eccentricity Ratio, Friction, and Oil Flow of Long and Short Journal Bearings with Load-Number Charts," N.A.C.A., T.N. 3491, 1955.

18. Pinkus, O., and Sternlicht, B., "The Maximum Temperature Profile in Journal Bearings," Trans. A.S.M.E., 79, 337-342, 1957.

19. Purvis, M. B., Meyer, W. E., and Benton, T. C., "Temperature Distribution in the Journal Bearing Lubricant Film," Trans. A.S.M.E., 79, 343-350, 1957.

20. Rosenblatt, M., and Wilcock, D. F., "Oil Flow, Key Factor in Sleeve-Bearing Performance," Trans. A.S.M.E., 74, 849-866, 1952.

21. Shaw, C. M., and Macks, F., "Analysis and Lubrication of Bearings," 1st Ed., New York: McGraw-Hill Book Co., 177,206,258, 1949.

22. Stephan, H., "Temperatur und Verdagerung von Zylindrischen Gleitlagern bei hoher Drehzahl," Forschungsh. Ver. dtsch. Ing., 439, 1953.

23. Von Gersdorfer, O., "Das Gleitlager. Wirkungsweise, Konstruktion, Baustoffe und Berechnung," Industrie-und Fachverlag, S.89, 1954.

24. Wilcock, D. F., "Turbulence in High Speed Journal Bearings," Trans. A.S.M.E., 72, 825-834, 1950.

25. Wilcock, D. F., and Booser, E. R., Bearing Design and Application, 1st Ed., New York: McGraw-Hill Book Co., 410, 1957.